

8-9-2019 11:00 AM

The Reactivity of Ditetrelenes Towards Organophosphorus Oxides

Maissa Belcina, *The University of Western Ontario*

Supervisor: Baines, Kim M., *The University of Western Ontario*

A thesis submitted in partial fulfillment of the requirements for the Master of Science degree in Chemistry

© Maissa Belcina 2019

Follow this and additional works at: <https://ir.lib.uwo.ca/etd>

 Part of the [Inorganic Chemistry Commons](#)

Recommended Citation

Belcina, Maissa, "The Reactivity of Ditetrelenes Towards Organophosphorus Oxides" (2019). *Electronic Thesis and Dissertation Repository*. 6522.
<https://ir.lib.uwo.ca/etd/6522>

This Dissertation/Thesis is brought to you for free and open access by Scholarship@Western. It has been accepted for inclusion in Electronic Thesis and Dissertation Repository by an authorized administrator of Scholarship@Western. For more information, please contact wlsadmin@uwo.ca.

Abstract

The reactivity of tetramesityldisilene **4** and tetramesityldigermene **5** towards organophosphorus oxides was explored in this thesis. The reaction of dialkyl and diarylphosphine oxides and phosphites with ditetrelenes **4** and **5** resulted in a 1,3-addition to form diorganodisilyl and digermyl phosphinites **27**, **28**, **31**, **32** and disilyl phosphites **35** and **36**. The 1,3-addition resulted in a mild two electron reduction of the P(V) centre of the phosphine oxide and phosphite to a P(III) centre in the products, without the use of heat or a catalyst. The reaction of organophosphorus oxides provides another example of a main group oxide that can be activated by ditetrelenes **4** and **5** in addition to nitro and sulfonyl containing compounds, CO and CO₂.

The mechanism for the reaction of diorganophosphorus oxides and phosphites with ditetrelenes **4** and **5** was investigated through deuterium labelling studies and KIE experiments. The mechanism for the formation of disilyl and digermyl phosphinites and phosphites was determined to proceed through a nucleophilic addition. An exchange phenomenon between the OP(pentyl)₂ moiety of **32** and an OPPh₂ group from diphenylphosphine oxide was discovered and the mechanism of this exchange was investigated.

Keywords: Group 14, silicon, germanium, disilene, digermene, organophosphorus oxides, phosphine oxides, phosphites, nucleophilic addition

Summary for Lay Audience

Just as houses can only be utilized after first laying down a stable foundation, understanding the fundamental chemistry of compounds is important for the future development of applications of the chemistry. In this thesis, reactions with compounds containing silicon and germanium are explored. These compounds are of interest because of their ability to easily react with numerous reagents to form new compounds that are not easily synthesized in any other way. The addition of phosphorus oxides to the silicon or germanium species was investigated. The new compounds formed were identified using state-of-the-art analytical techniques and the pathways to these compounds were elucidated using physical inorganic methodology. The chemistry reported is simple to perform and, with the mechanistic insights provided, it is hoped that the chemistry can be utilized in applications such as the organic functionalization of semiconductor surfaces.

Acknowledgements

First and foremost, I'd like to thank my supervisor, Dr. Kim Baines for giving me the opportunity to complete my Masters in her research group. She has provided helpful advice and guidance that allowed me to overcome many obstacles in my research. The time she took to edit and proofread my thesis has enhanced my writing skills and improved my ability to explain concepts clearly in my thesis. It has been pleasure working in her group for the past three years.

I would also like to thank all the members of the Baines group that have helped me throughout my 4491 thesis and my Masters. I would like to give a special thanks to Andrew. He was always there for me in the most stressful times and gave continuous support throughout my time in the lab, especially near the end of my thesis.

I wouldn't have been able to finish this degree without the support of all the friends that I have made throughout my undergraduate and Masters degrees. Thank you to my friends in the Blacquiere, FLL, Ding and Corrigan groups for always having time to talk about research and for all the pasta lunches on Thursdays. Jonathan, Curtis and Karan would always help me take my mind off all the stress outside of school with all their savage comments that lead to non-stop laughter.

I'd like to extend my thanks to the staff at Western that keep this department running. I'd like to thank Mat Willans, Doug Hairsine and Paul Boyle for their expertise in NMR, MS and X-ray crystallography, respectively. Without them, the characterization of my compounds would not be complete.

Lastly, I would like to thank my family and friends back home in Windsor. I am grateful for their constant support and encouragement to achieve my goals.

Table of Contents

Abstract	ii
Summary for Lay Audience	iii
Acknowledgements	iv
Table of Contents	v
List of Tables	viii
List of Figures	ix
List of Schemes	xi
List of Appendices	xiv
List of Abbreviations	xvi
1 Stable Doubly Bonded Si and Ge Compounds	1
1.1 Introduction	1
1.2 Structure and Bonding in Ditetrelenes	3
1.3 Reactivity of Ditetrelenes	5
1.4 Reactions with Organic Main Group Oxides Including CO ₂ and CO	8
1.5 Reactions with Organophosphorus Oxides	11
1.6 References	14
2 Synthesis and Characterization of Disilyl and Digermyl Phosphinites and Phosphites	17
2.1 The Addition of Organophosphorus Oxides to Ditetrelenes	17
2.2 Characterization of Disilyl and Digermyl Phosphinites and Phosphites	21
2.3 Reactivity of Disilyl and Digermyl Phosphinites and Phosphites	25

2.4	Discussion	28
2.5	Summary	34
2.6	Experimental	35
2.6.1	General Experimental Details	35
2.6.2	Addition of Diphenylphosphine Oxide to Tetramesityldisilene 4	36
2.6.3	Addition of Diphenylphosphine Oxide to Tetramesityldigermene 5	37
2.6.4	Addition of Dipentylphosphine Oxide to Tetramesityldisilene 4	37
2.6.5	Addition of Dipentylphosphine Oxide to Tetramesityldigermene 5	38
2.6.6	Addition of Dimethyl Phosphite to Tetramesityldisilene 4	39
2.6.7	Direct Hydrolysis of 35	40
2.6.8	Addition of Diphenyl Phosphite to Tetramesityldisilene 4	41
2.6.9	Addition of Diethylphosphinic Acid to Tetramesityldisilene 4	41
2.7	References	43
3	Mechanistic Studies and Competition Experiments	45
3.1	Introduction	45
3.2	Deuterium Labelling Experiment	47
3.3	Kinetic Isotope Effect	48
3.4	Relative Rate Studies and Exchange Reactivity on the Addition of Phosphine Oxides to Tetramesityldigermene 5	51
3.5	Summary	58
3.6	Experimental	59
3.6.1	General Experimental Details	59
3.6.2	Addition of Diphenylphosphine Oxide- <i>d</i> ₁ to Tetramesityldigermene 5	60

3.6.3	Competition Kinetic Isotope Effect	60
3.6.4	Addition of Dipentyl- and Diphenylphosphine Oxide to Tetramesityl- digermene 5	60
3.6.5	Addition of Diphenylphosphine Oxide to Dipentyldigermyl Phosphinite 32	61
3.6.6	Addition of Dipentylphosphine Oxide to Dipenyldigermyl Phosphinite 28	61
3.6.7	Addition of Diphenylphosphine Oxide to Dimethyldisilyl Phosphite 35	61
3.6.8	Addition of Diphenyl Phosphite to Dimethyldisilyl Phosphite 35	61
3.6.9	The Addition of Diphenylphosphine Oxide- <i>d</i> ₁ to Dipentyldigermyl Phosphinite 32	62
3.7	References	63
4	Conclusions and Future Work	64
4.1	Summary and Conclusions.....	64
4.2	Future Work	66
4.3	References	69
	Appendices.....	70

List of Tables

Table 1. <i>Trans</i> -bending angle (θ) and twist angle (τ) of selected disilenes and digermenes.....	5
Table 2. ^{31}P chemical shifts of P(V) reagents, disilyl/ digermyl phosphinites and phosphites. ...	22
Table 3. The ^{29}Si chemical shifts and coupling constants of disilyl phosphinites and phosphites.	23

List of Figures

Figure 1. The structures of a Si/Ge(100) 2x1 surface and tetramesityldisilene and -digermene....	2
Figure 2. Structural deformations of the M=M bond.....	3
Figure 3. Definition for the <i>trans</i> -bent angle (θ) at M and the twist angle (τ) about the M=M bond.	4
Figure 4. MO model representing (a) the classical covalent interaction, (b) the non-classical donor-acceptor interaction (M = Si, Ge) and (c) the donor-acceptor double bond. ¹⁰	4
Figure 5. π - and σ^* -orbital interactions of the M=M bond in ditetrelenes. ¹⁰	5
Figure 6. Structure of organophosphorus oxides.	12
Figure 7. Displacement ellipsoid plot of 34 . Ellipsoids are at the 50% probability level and hydrogen atoms are omitted for clarity except the hydrogen on Si2. Selected bond lengths (Å) and angles (deg): Si1-O1 = 1.6830(17), Si1-Si2 = 2.3742(10), P1-O1 = 1.5802(17), P1-O2 = 1.4711(18), O1-Si1-Si2 = 105.63(7), Si1-Si2-H2 = 100.6(10), P1-O1-Si1 = 150.79(12).	19
Figure 8. The reaction of 4 with diethylphosphinic acid monitored by $^{31}\text{P}\{^1\text{H}\}$ NMR spectroscopy (C_6D_6 , 162 MHz).	20
Figure 9. The ^1H - ^{29}Si gHMBC spectrum of 35 showing the correlations to the signal at 5.67 ppm in the ^1H dimension.....	23
Figure 10. Displacement ellipsoid plot of 35 . Ellipsoids are at the 50% probability level and hydrogen atoms are omitted for clarity except the hydrogen on Si2. Selected bond lengths (Å) and angles (deg): Si1-O1 = 1.6685(11), Si1-Si2 = 2.3806(7), P1-O1 = 1.6043(11), O1-Si1-Si2 = 108.52(4), Si1-Si2-H2 = 100.0(7), P1-O1-Si1 = 141.92(7).	24
Figure 11. IR spectrum of compound 36	25
Figure 12. Compounds isolated from the preparative TLC plate.	28
Figure 13. General structures of disilyl and digermyl phosphinites and phosphites.	34

Figure 14. Consumption of protonated and deuterated diphenylphosphine oxide in the reaction with digermene 5	49
Figure 15. $^{31}\text{P}\{^1\text{H}\}$ NMR (C_6D_6 , 162 MHz) spectra of the competition reaction between dipentyl- and diphenylphosphine oxide with digermene 5	52
Figure 16. $^{31}\text{P}\{^1\text{H}\}$ NMR (C_6D_6 , 162 MHz) spectra of the addition of diphenyl phosphine oxide to dipentyl digermyl phosphinite 32	53
Figure 17. $^{31}\text{P}\{^1\text{H}\}$ NMR (C_6D_6 , 162 MHz) spectra of the addition of diphenylphosphine oxide- d_1 to 32 . (a) Shows all signals present in the spectra. (b) Expansion shows the zoomed region containing the signals for protonated and deuterated dipentylphosphine oxide.	55

List of Schemes

Scheme 1. The synthesis of a mixed inorganic-organic material 3 by copolymerization of 1 and 2	1
Scheme 2. The addition of acrylonitrile to (a) the Ge(100) 2x1 surface and (b) tetramesityldigermene 5	2
Scheme 3. Common modes of reactivity for ditetrelenes.	6
Scheme 4. The [2+2] cycloaddition of acetonitrile to tetramesityldigermene 5	6
Scheme 5. The addition of benzil to disilene 4	7
Scheme 6. General cycle for the catalytic functionalization of small molecules.	7
Scheme 7. Activation of (a) NH ₃ and (b) H ₂ by iminodisilene 11	8
Scheme 8. The activation of CO ₂ by 11 to yield oxadisilacyclobutanone 14	8
Scheme 9. Partial reduction of CO by cyclotrisilene 15	9
Scheme 10. The addition of aldehydes and ketones to tetramesityldisilene 4	9
Scheme 11. The addition of methyl furoate to 4	10
Scheme 12. The 1,2-addition of carboxylic acids to digermene 5	10
Scheme 13. The addition of nitromethane to ditetrelenes 4 and 5	11
Scheme 14. The reduction of arylsulfonyl chlorides by ditetrelenes 4 and 5	11
Scheme 15. The reactivity of diphenylphosphine oxide with germylene 25	12
Scheme 16. The addition of phosphine oxides and phosphites to 4 and 5	13
Scheme 17. The addition of diphenyl- and dipentylphosphine oxide to 4 and 5	17
Scheme 18. The addition of 95% diethylphosphine oxide to 4	18
Scheme 19. The synthesis of diethylphosphine oxide.	20
Scheme 20. The addition of dimethyl and diphenyl phosphite to 4	21

Scheme 21. The secondary reactivity observed for (a) disilyl phosphinite 31 and (b) digermyl phosphinite 32 .	26
Scheme 22. The oxidation of the Si-H moiety of 35 .	26
Scheme 23. The formation of 41 following preparative TLC.	26
Scheme 24. The direct hydrolysis of dimethyldisilyl phosphite 35 .	27
Scheme 25. The hydrolysis of trimethyl phosphite with ^{17}O -labelled water. ⁹	27
Scheme 26. The addition of organophosphorus oxides to 4 and 5 .	29
Scheme 27. Reduction of diphenylphosphine oxide by a borinic acid precatalyst.	29
Scheme 28. Reaction of diorganophosphine oxides and phosphites with chlorosilanes in the presence of amines.	30
Scheme 29. The synthesis of (a) germyl phosphinite 48 and (b) germyl phosphite 49 through a salt metathesis reaction.	30
Scheme 30. (a) <i>Anti</i> -Markovnikov addition of diphenylphosphine oxide to 1-decene. (b) Hydrophosphorylation of an alkene with dialkyl phosphites.	31
Scheme 31. The Ni-catalyzed hydrophosphinylation of 1-octene.	32
Scheme 32. Proposed mechanism for the hydrophosphinylation of 1-octene. ¹⁹	32
Scheme 33. The Pd-catalyzed hydrophosphinylation of 54 .	33
Scheme 34. Proposed mechanism for the Pd-catalyzed hydrophosphinylation of 1,3-dienes.	33
Scheme 35. Plausible reaction mechanisms for the addition of organophosphorus oxides to 4 and 5 .	46
Scheme 36. The synthesis of diphenylphosphine oxide- <i>d</i> ₁ .	47
Scheme 37. The addition of diphenylphosphine oxide- <i>d</i> ₁ to 5 .	47
Scheme 38. The addition of ethanol to transient disilene 56 .	49

Scheme 39. The (a) nucleophilic addition and (b) electrophilic addition of phenols to disilene 4	50
Scheme 40. The addition of (a) diphenyl phosphite and (b) diphenylphosphine oxide to 35	54
Scheme 41. The addition of diphenylphosphine oxide- <i>d</i> ₁ to 32	54
Scheme 42. Proposed reaction mechanisms for the addition of diphenylphosphine oxide- <i>d</i> ₁ to 32	57
Scheme 43. Plausible mechanisms for the nucleophilic addition of diphenylphosphine oxide to 5	58
Scheme 44. The addition of diphenylphosphine oxide to 32 to yield diphenyldigermyl phosphinite 28	59
Scheme 45. The addition of organophosphorus oxides to ditetrelenes 4 and 5	64
Scheme 46. Plausible mechanisms for the addition of organophosphorus oxides to 4 and 5	65
Scheme 47. The addition of diphenylphosphine oxide to 32	66
Scheme 48. Plausible mechanism for the exchange phenomenon between 32 and diphenylphosphine oxide.	66
Scheme 49. The addition of diphenylphosphine oxide to cyclic digermene 58	67

List of Appendices

Appendix A: NMR Data	70
Figure A1: ^1H NMR spectrum (C_6D_6 , 600 MHz) of 27	70
Figure A2: $^{31}\text{P}\{^1\text{H}\}$ NMR spectrum (C_6D_6 , 243 MHz) of 27	71
Figure A3: $^{13}\text{C}\{^1\text{H}\}$ NMR spectrum (C_6D_6 , 151 MHz) of 27 . The region of the spectrum from 30 to 120 ppm has been omitted.	71
Figure A4: ^1H - ^{29}Si gHMBC NMR spectrum (C_6D_6) of 27	72
Figure A5: ATR-IR spectrum of 27	72
Figure A6: ^1H NMR spectrum (C_6D_6 , 600 MHz) of 28	73
Figure A7: $^{31}\text{P}\{^1\text{H}\}$ NMR spectrum (C_6D_6 , 243 MHz) of 28	73
Figure A8: $^{13}\text{C}\{^1\text{H}\}$ NMR spectrum (C_6D_6 , 151 MHz) of 28 . The region of the spectrum from 40 to 115 ppm has been omitted.	74
Figure A9: ^1H NMR spectrum (C_6D_6 , 600 MHz) of 31	74
Figure A10: $^{31}\text{P}\{^1\text{H}\}$ NMR spectrum (C_6D_6 , 162 MHz) of 31	75
Figure A11: $^{13}\text{C}\{^1\text{H}\}$ NMR spectrum (C_6D_6 , 151MHz) of 31 . The region of the spectrum from 60 to 120 ppm has been omitted.	75
Figure A12: ^1H - ^{29}Si gHMBC NMR spectrum (C_6D_6) of 31	76
Figure A13: ^1H NMR spectrum (C_6D_6 , 600 MHz) of 32	76
Figure A14: $^{31}\text{P}\{^1\text{H}\}$ NMR spectrum (C_6D_6 , 162 MHz) of 32	77
Figure A15: $^{13}\text{C}\{^1\text{H}\}$ NMR spectrum (C_6D_6 , 151 MHz) of 32	77
Figure A16: ^1H NMR spectrum (C_6D_6 , 400 MHz) of 34	78
Figure A17: $^{31}\text{P}\{^1\text{H}\}$ NMR spectrum (C_6D_6 , 162 MHz) of 34	78

Figure A18: $^{13}\text{C}\{^1\text{H}\}$ NMR spectrum (C_6D_6 , 101 MHz) of 34 . The region of the spectrum from 35 to 110 ppm has been omitted.	79
Figure A19: ^1H - ^{29}Si gHMBC NMR spectrum (C_6D_6) of 34	79
Figure A20: ^1H NMR spectrum (C_6D_6 , 600 MHz) of 35	80
Figure A21: $^{31}\text{P}\{^1\text{H}\}$ NMR spectrum (C_6D_6 , 162 MHz) of 35	80
Figure A22: $^{13}\text{C}\{^1\text{H}\}$ NMR spectrum (C_6D_6 , 101 MHz) of 35 . The region of the spectrum from 50 to 120 ppm has been omitted.	81
Figure A23: ^1H - ^{29}Si gHMBC NMR spectrum (C_6D_6) of 35	81
Figure A24: ATR-IR spectrum of 35	82
Figure A25: ^1H NMR spectrum (C_6D_6 , 600 MHz) of 36	82
Figure A26: $^{31}\text{P}\{^1\text{H}\}$ NMR spectrum (C_6D_6 , 243 MHz) of 36	83
Figure A27: $^{13}\text{C}\{^1\text{H}\}$ NMR spectrum (C_6D_6 , 151 MHz) of 36 . The region of the spectrum from 30 to 115 ppm has been omitted.	83
Figure A28: ^1H - ^{29}Si gHMBC NMR spectrum (C_6D_6) of 36	84
Figure A29: ATR-IR spectrum of 36	84
Figure A30: ^1H NMR spectrum (C_6D_6 , 600 MHz) of 41	85
Figure A31: ^{31}P NMR spectrum (C_6D_6 , 243 MHz) of 41	85
Figure A32: $^{13}\text{C}\{^1\text{H}\}$ NMR spectrum (C_6D_6 , 151 MHz) of 41 . The region of the spectrum from 55 to 115 ppm has been omitted.	86
Figure A33: ^1H - ^{29}Si gHMBC NMR spectrum (C_6D_6) of 41	86
Appendix B: X-ray Crystallography Data	87
Appendix B1: X-ray crystallography data for 34	87
Appendix B2: X-ray crystallography data for disilyl phosphites 35	90

List of Abbreviations

Å	Angstrom
ATR	Attenuated Total Reflectance
Bu	Butyl
DCM	Dichloromethane
d (NMR)	Doublet
ΔE_{elast}	Quasiclassical Electrostatic Interaction Energy
ΔE_{int}	Instantaneous Interaction Energy
ESI	Electrospray Ionization
EPA	Energy Partitioning Analysis
ΔE_{orb}	Orbital Interaction Energy
ΔE_{Pauli}	Repulsive Pauli Term
Et	Ethyl
FTIR	Fourier Transform Infrared
gHMBC	Gradient Heteronuclear Multiple Bond Correlation
IR	Infrared
KIE	Kinetic Isotope Effect
MS	Mass Spectrometry
Mes	Mesityl (2,4,6-trimethylphenyl)
m (IR)	Medium
m (NMR)	Multiplet
MO	Molecular Orbital
NBO	Natural Bond Order
NRT	Natural Resonance Theory
NMR	Nuclear Magnetic Resonance
ppm	Parts per million

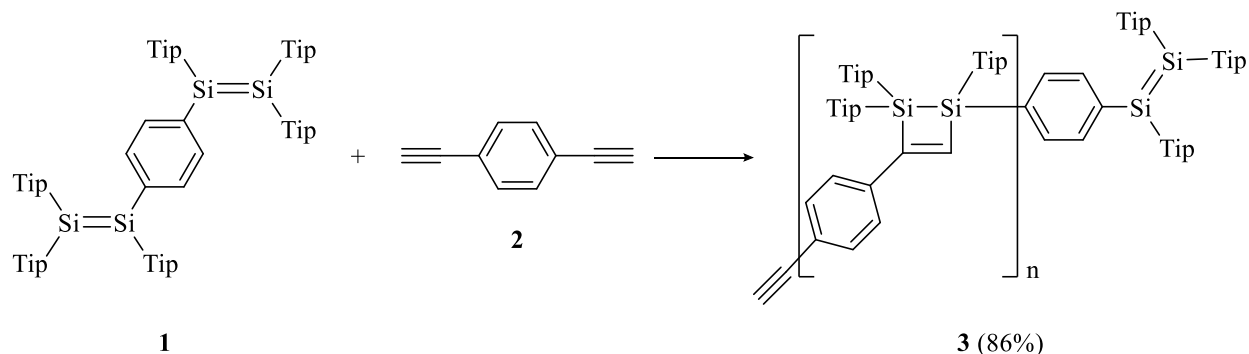
Ph	Phenyl
rds	Rate Determining Step
RT	Room Temperature
STM	Scanning Tunnelling Microscopy
s (NMR)	Singlet
s (IR)	Strong
Tip	2,4,6-triisopropylphenyl
THF	Tetrahydrofuran
TLC	Thin Layer Chromatography
Tol	Tolyl
XPS	X-ray Photoelectron Spectroscopy

Chapter 1

1 Stable Doubly Bonded Si and Ge Compounds

1.1 Introduction

The chemistry of ditetrelenes, the heavy atom analog of alkenes, has been explored for the last 40 years,¹ and the acquired knowledge is now being utilized in many interesting applications. For example, Scheschkewitz and Manners reported the atom-economic and catalyst free method for synthesis of a σ - π conjugated organosilicon polymer under mild reaction conditions.² Comonomers tetrasiladiene **1** and 1,4-diethynylbenzene **2** were reacted at room temperature in benzene to form an air stable polymer **3** in 86% yield (Scheme 1). The key reaction in the polymerization takes advantage of the well-known [2+2] cycloaddition of alkynes with disilenes.^{1b}



Tip = 2,4,6-triisopropylphenyl

Scheme 1. The synthesis of a mixed inorganic-organic material **3** by copolymerization of **1** and **2**.

As a second example, tetramesityldisilene **4** and -digermene **5** (Mes = mesityl = 2,4,6-trimethylphenyl) have been used as molecular models to understand the chemistry of the Si(100) 2x1 and Ge(100) 2x1 reconstructed surfaces (Figure 1). The elucidation of an unambiguous structure of surface adducts is difficult because surface characterization methods are limited. Such methods include Fourier Transform Infrared Spectroscopy (FTIR), X-ray Photoelectron Spectroscopy (XPS) and Scanning Tunnelling Microscopy (STM)³ which provide information on functional groups, elemental composition and oxidation states, and electronic states, respectively. The use of surface analytical techniques is often complemented by computational studies to ensure the accuracy of the proposed structures of surface adducts. In contrast, the structure of molecular species may be unequivocally determined using characterization techniques such as Nuclear

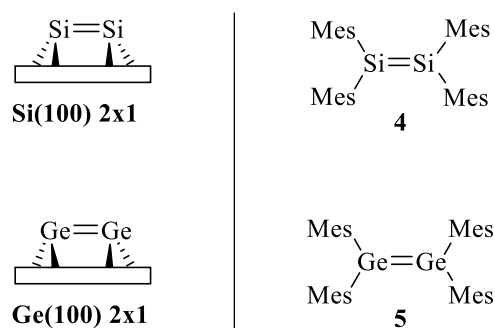
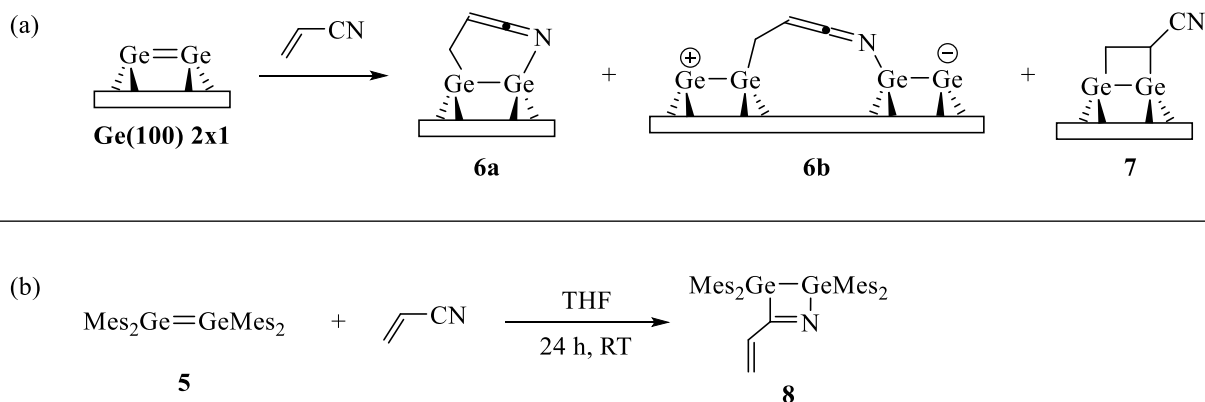


Figure 1. The structures of a Si/Ge(100) 2x1 surface and tetramesityldisilene and -digermene.

Magnetic Resonance (NMR) Spectroscopy, Mass Spectrometry (MS) and X-ray Crystallography. For this reason, comparisons between the structures derived from reactions of molecular and surface disilenes and digermenes are frequently made. For example, the addition of nitriles to **5** was compared to the reactivity between nitriles and the Ge(100) 2x1 surface.⁴ On the basis of theoretical and experimental evidence, the addition of acrylonitrile to the Ge(100) 2x1 surface was proposed to form two types of adducts: ketenimines (a cyclic single-dimer adduct **6a** and an interdimer adduct **6b**), and a cycloadduct between the surface dimer and the C=C bond of acrylonitrile, digermetane **7** (Scheme 2a).^{5,6} The addition of acrylonitrile to molecular digermene **5**, on the other hand, resulted in the formation of 1,2,3-azadigermetene **8** at room temperature (Scheme 2b).⁴ The lack of formation of the six-membered cyclic ketenimine **6a** in the molecular system suggests that ketenimine **6b** is the more likely ketenimine formed on the surface, and not **6a**. Furthermore, the surface chemistry suggests that azadigermetene **8** may be the kinetic product, and under equilibrium conditions, a molecular analog of digermetane **7** may be formed.



Scheme 2. The addition of acrylonitrile to (a) the Ge(100) 2x1 surface and (b) tetramesityldigermene **5**.

For the continued development of applications using ditetrelene chemistry, it is important to continue to study fundamental chemistry of ditetrelenes. In order to understand the chemistry, the structure, bonding and reactivity of ditetrelenes will be briefly reviewed.

1.2 Structure and Bonding in Ditetrelenes

The increased reactivity of ditetrelenes compared to alkenes, can be understood in terms of the nature of the π -bond between the heavier Group 14 elements, which is significantly weaker than the π -bond in alkenes (estimated π -bond strengths (kcal/mol) for $\text{H}_2\text{M}=\text{MH}_2$: M = C: 65, M = Si: 25, M = Ge: 25).⁷ The weak π -bond in non-polar molecules has been studied computationally by Frenking *et al.* using energy-partitioning analysis (EPA).⁸ EPA focuses on the instantaneous interaction energy (ΔE_{int}) of the bond, which is defined as the energy difference between the molecule and its fragments in a specified geometry. The interaction energy can be divided into three terms: the quasiclassical electrostatic interaction energy (ΔE_{elstat}), the repulsive Pauli term (ΔE_{Pauli}) and the orbital interaction energy (ΔE_{orb}). The interaction energies for $\text{H}_3\text{M}-\text{MH}_3$ single bonds (M = C to Pb) were calculated and shown to decrease down the group, resulting in a weaker σ -bond. While the bonding in ditetrelenes was not investigated, analogous compounds containing multiple bonds between first-row main group elements were analyzed, including diazene ($\text{HN}=\text{NH}$). The Pauli repulsion contribution significantly increases from diazene ($\Delta E_{\text{Pauli}} = 599.4$ kcal/mol) compared to ethylene ($\Delta E_{\text{Pauli}} = 281.9$ kcal/mol), which results in a smaller interaction energy, and therefore, a weaker π -bond. Similar to diazene, ditetrelenes are expected to have a strong Pauli repulsion contribution, explaining the inherently weak π -bond and increased reactivity compared to alkenes.

In contrast to planar alkenes, most ditetrelenes exhibit a *trans*-bent geometry at the silicon and germanium centre and twisting about the M=M bond (Figure 2). The bend angle (θ) is the



Figure 2. Structural deformations of the M=M bond.

angle between the M=M bond axis and the R-M-R plane, whereas, the twist angle (τ) is defined as the dihedral angle between two R-M-R planes (Figure 3).⁹

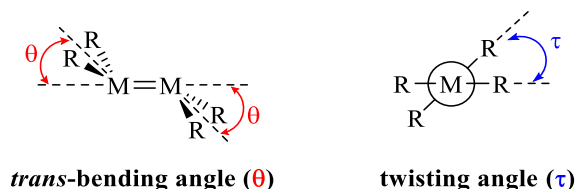


Figure 3. Definition for the *trans*-bent angle (θ) at M and the twist angle (τ) about the M=M bond.

The *trans*-bent geometry observed in ditetrelenes can be understood using two molecular orbital (MO) models. The first model rationalizes the formation of the double bond in alkenes as the covalent interaction between singly occupied MOs of two monomeric, ground state triplet carbenes, resulting in a classical planar C=C bond (Figure 4a). The heavy analogues of carbenes (silylenes and germylenes) are ground state singlets. Consequently, the covalent interaction of singlet silylenes and germylenes would result in Pauli repulsion between the doubly occupied *n*-orbitals (Figure 4b). To form a classical planar M=M bond, a significant amount of energy would be required to overcome the singlet-triplet energy gap (ΔE_{ST}) to promote an electron from *n*- to *p*-level. Alternatively, the heavy carbene analogues prefer to interact through two equivalent donor-acceptor interactions to form the non-classical M=M bond, featuring *trans*-bending at the M centres (Figure 4c).¹⁰

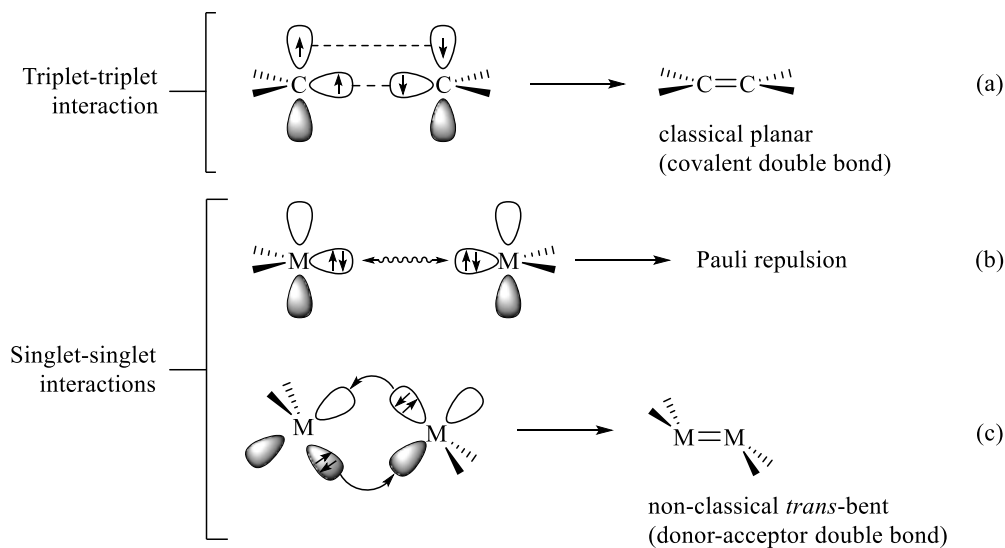


Figure 4. MO model representing (a) the classical covalent interaction, (b) the non-classical donor-acceptor interaction (M = Si, Ge) and (c) the donor-acceptor double bond.¹⁰

In an alternative MO model, *trans*-bending in ditetrelenes is rationalized by the mixing of $M=M$ π - and σ^* -orbitals, which is possible through bending at the M centres (Figure 5). The π - σ^* interaction is dependant on the π - σ^* energy gap; the mixing of π - σ^* orbitals increases as the

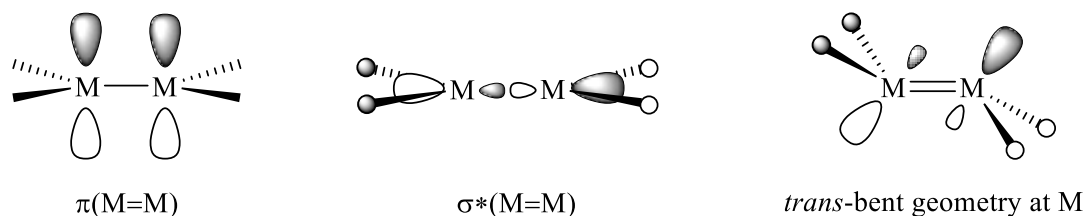


Figure 5. π - and σ^* -orbital interactions of the $M=M$ bond in ditetrelenes.¹⁰

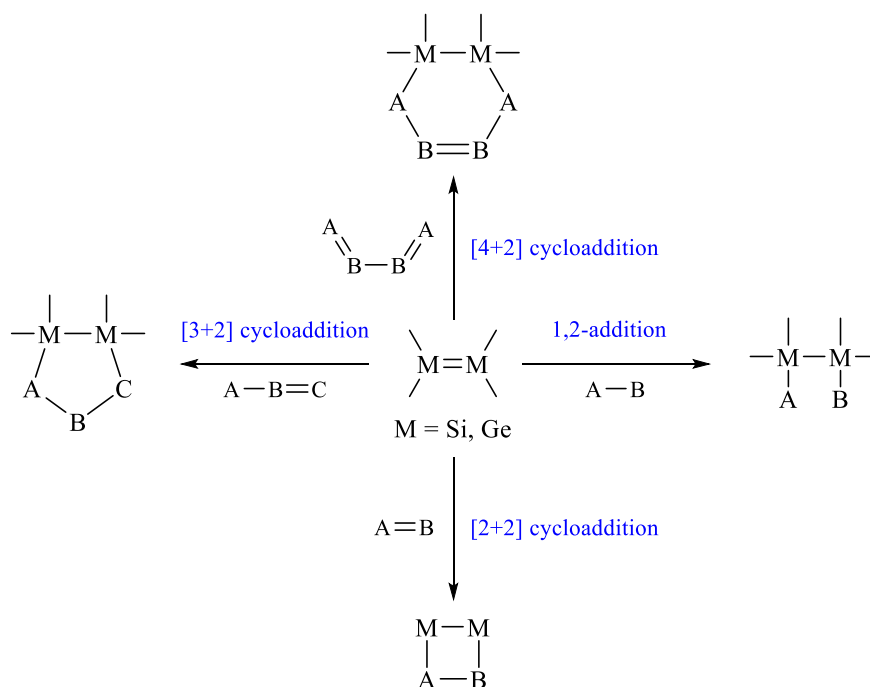
energy gap decreases, which results in a larger *trans*-bent angle. In the planar $H_2M=MH_2$ ($M = C$ to Pb), the magnitude of the π - σ^* energy separation decreases going down Group 14, thereby increasing π - σ^* mixing and the *trans*-bent angle for the heavier elements. Another factor which influences the degree of *trans*-bending in ditetrelenes is the electronegativity of the substituents on the $M=M$ bond: electronegative substituents (i.e. substituents containing O or N) lead to increased *trans*-bending, while electropositive substituents (i.e. substituents featuring Si) produce smaller bending deformations at the M centres. These trends are evident in the examples given in Table 1.

Table 1. *Trans*-bending angle (θ) and twist angle (τ) of selected disilenes and digermenes.

Compound	θ (deg)	τ (deg)	Ref.
$Mes_2Si=SiMes_2$ Mes = 2,4,6-trimethylphenyl	12, 14	3	11
$(Mes_2P)_2Si=Si(PMes_2)_2$	41	46	12
$Mes_2Ge=GeMes_2$	33	3	13
$(^iPr_3Si)_2Ge=Ge(Si^iPr_3)_2$	16	0	14

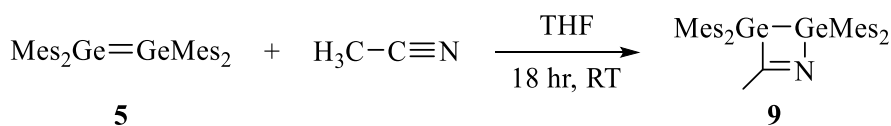
1.3 Reactivity of Ditetrelenes

The most common modes of reactivity for ditetrelenes are 1,2-additions and cycloadditions (Scheme 3).¹ Typical reagents that react with ditetrelenes via 1,2-addition reaction include polar,



Scheme 3. Common modes of reactivity for ditetrelenes.

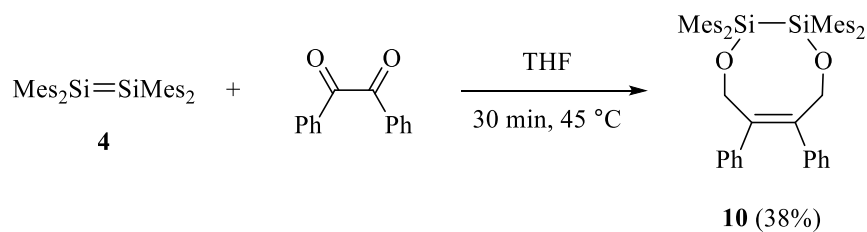
σ -bonded compounds such as water and alcohols.^{1d,e,f} Ditetrelenes also react with reagents containing π -bonds, most often in cycloaddition reactions. The most common mode of cycloaddition for ditetrelenes is the [2+2] cycloaddition. Ketones, aldehydes, alkynes and nitriles are typical reagents used in the formation of four-membered heterocyclic rings containing Si-Si/Ge-Ge fragments.^{1b, 4, 15} For example, the addition of acetonitrile to tetramesityldigermene, **5**, resulted in the formation of 1,2,3-azadigermene **9** (Scheme 4).⁴ The addition of acetonitrile to **5**



Scheme 4. The [2+2] cycloaddition of acetonitrile to tetramesityldigermene **5**.

occurs at room temperature, in stark contrast to the [2+2] cycloadditions of alkenes, which are forbidden under thermal conditions. Reactions to form larger heterocyclic rings through [3+2] and [4+2] cycloadditions have been reported; however, these examples are less common. While Diels-Alder reactions are common in alkene chemistry, stable ditetrelenes typically do not undergo [4+2] cycloadditions to form Diels-Alder adducts with conjugated dienes. Diels-Alder reactivity is only known for transient disilenes and digermenes.¹⁶ However, other examples of [4+2] cycloadditions

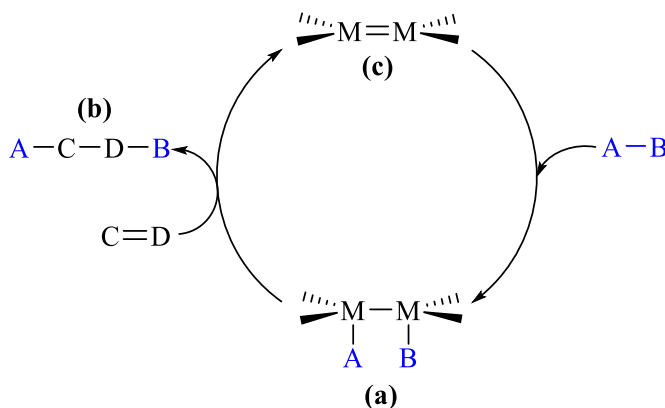
exist in ditetrelene chemistry. Boudjouk *et al.* reported the addition of benzil to disilene **4** to yield a six-membered heterocyclic ring **10** (Scheme 5).¹⁷



Scheme 5. The addition of benzil to disilene **4**.

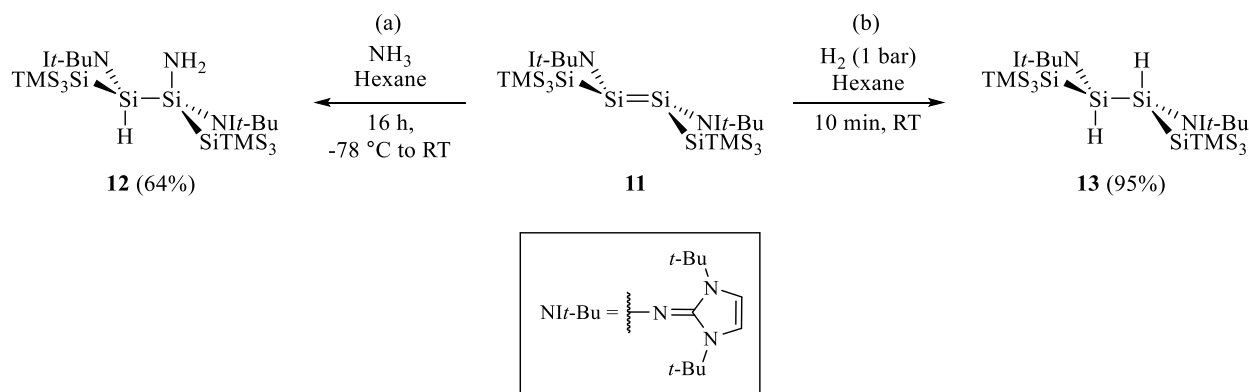
While the reactivity of ditetrelenes has focused on reactions with the π -bond, recent research has explored the synthesis of functionalized disilenes.^{1a} These functional disilenes include disilenides, containing a Li substituent, and phosphinodisilenes, containing a PR_2 substituent bound to the Si centre. By incorporating this functionality into the ditetrelene, reactivity can be explored that focuses on the reaction of the σ -bonded substituents on the ditetrelene instead of the π -bond.

Recently, the focus of reactivity studies in ditetrelene chemistry has shifted towards small molecule activation.¹⁸ Small molecules such as H_2 , NH_3 and CO_2 can be used as synthons for value added chemicals; however, these stable compounds must be activated for further functionalization. The most efficient method to achieve functionalization of these small molecules is through catalytic processes which requires activation of a small molecule (Scheme 6a), and then elimination of the functionalized product (Scheme 6b) with regeneration of the catalyst (Scheme 6c).



Scheme 6. General cycle for the catalytic functionalization of small molecules.

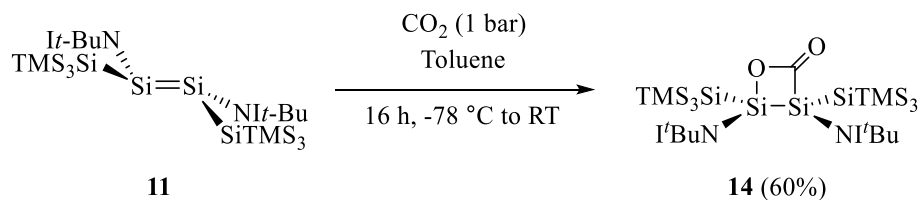
While the activation of small molecules is a new field in ditetrelene chemistry and there have been no reports of catalysis to date, there have been recent reports of small molecule activation. Inoue and co-workers synthesized the (*Z*)-diiminodisilyldisilene **11**, featuring a highly twisted ($\tau = 23^\circ$) and *trans*-bent ($\theta = 38^\circ, 39^\circ$) geometry about the Si=Si bond, leading to a weaker π -bond in comparison to other disilenes.¹⁹ When iminodisilene **11** was allowed to react with NH₃ at -78 °C, 1-aminodisilane **12** was formed as the only product in 64% yield (Scheme 7a).²⁰ Most notably, **11** was the first multiply bonded silicon compound to activate H₂, forming disilane **13** in excellent yield (Scheme 7b).¹⁹



Scheme 7. Activation of (a) NH₃ and (b) H₂ by iminodisilene **11**.

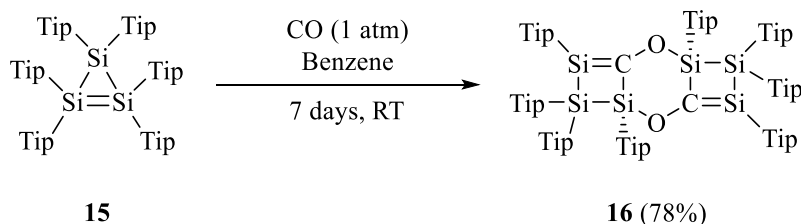
1.4 Reactions with Organic Main Group Oxides Including CO₂ and CO

Although the reactivity of ditetrelenes has been extensively explored, studies of the addition of organic main group oxides are few. Following the shift in interest towards the activation of small molecules, reactions of CO₂ and CO with ditetrelenes have been explored. In addition to NH₃ and H₂, the reaction of iminodisilene **11** with CO₂ selectively formed oxadisilacyclobutanone **14** in 60% yield (Scheme 8).²⁰ The activation of NH₃, CO₂, and H₂ by **11** is indicative of the highly



Scheme 8. The activation of CO₂ by **11** to yield oxadisilacyclobutanone **14**.

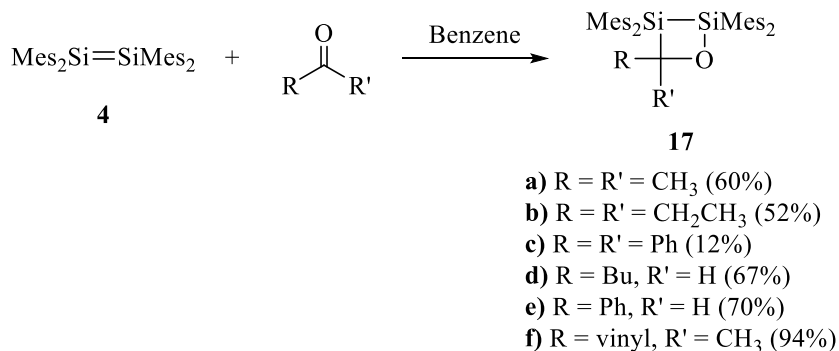
reactive Si=Si bond, which may be attributed to the strongly donating N-heterocyclic imine (Nt'Bu) substituents which lead to increased *trans*-bending and twisting at the Si centres. Future investigations by Inoue and co-workers will focus on transferring the CO₂ moiety of **14** to other substrates. Scheschkewitz *et al.* reported the partial reduction of CO using cyclotrisilene **15**.²¹ Exposure of cyclotrisilene to CO at room temperature resulted in the incorporation of one equivalent of CO per molecule of **15**, yielding the tricyclic compound, bis(silene) **16** (Scheme 9). The facile activation of CO by **15** can be explained, in part, by the release of ring strain in the three-membered ring featuring the Si=Si bond.



Tip = 2,4,6-triisopropylphenyl

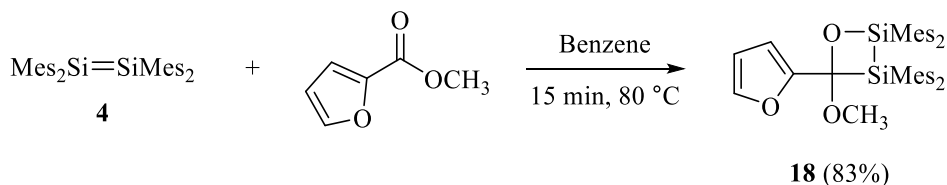
Scheme 9. Partial reduction of CO by cyclotrisilene **15**.

Ditetrelenes are also known to react with other carbonyl containing compounds. The reaction of ketones and aldehydes with tetramesityldisilene **4**, reported by West, undergoes cycloaddition to form 2,3-disilaoxetanes **17a-f** (Scheme 10).²² The reactions with the aldehydes and ketones listed in Scheme 10 went to completion within minutes at room temperature, with the exception of the reaction of benzophenone with **4** which was heated to 50 °C for 1 hour to form **17c** in 12% yield.



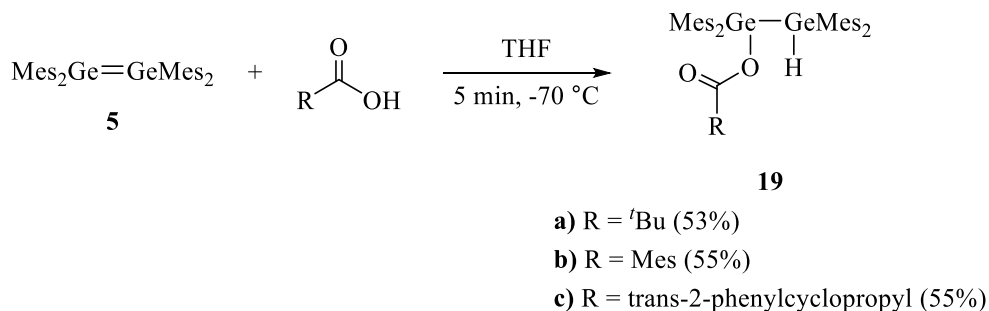
Scheme 10. The addition of aldehydes and ketones to tetramesityldisilene **4**.

Interestingly, disilene **4** was unreactive towards esters including ethyl acetate, methyl benzoate and ethyl *p*-(dimethylamino)benzoate, even at elevated temperatures over 3 days.²² Reactivity was observed only with the activated carbonyl in methyl furoate to give the cycloadduct **18**, analogous in structure to adducts **17a-f** (Scheme 11). The lack of reactivity of esters towards **4** can be accounted for by the less polar C=O bond in esters. Evidently, a moderately strongly polarized π -bond is required for the reaction to proceed.



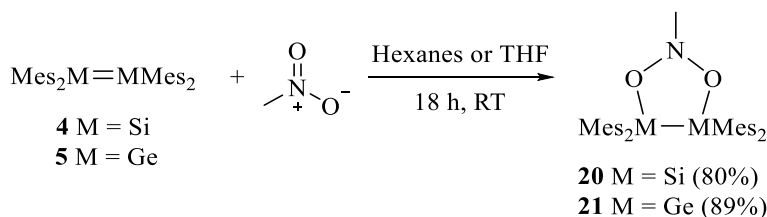
Scheme 11. The addition of methyl furoate to **4**.

In contrast to the cycloaddition observed in the reaction of disilene **4** with aldehydes and ketones, the addition of carboxylic acids to digermene **5** resulted in a 1,2-addition that yielded digermyl esters **19a-c** (Scheme 12).¹³ Carboxylic acids also react rapidly with **5** at room temperature, similar to the conditions for the reactions of aldehydes and ketones with disilene **4**.



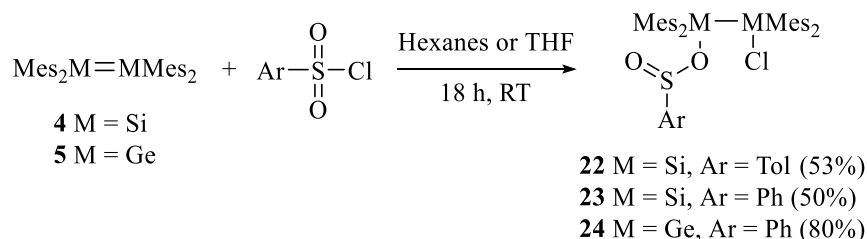
Scheme 12. The 1,2-addition of carboxylic acids to digermene **5**.

The reaction of ditetrelenes and compounds featuring double bonds between oxygen and main group elements other than carbon have also been investigated. Baines *et al.* reported the addition of nitromethane to tetramesityldisilene **4** and -digermene **5** at room temperature, resulting in the formation of 1,3,2-dioxazolidines, **20** and **21**, respectively (Scheme 13).²³ The cycloaddition results in a selective two-electron reduction of the nitrogen in nitromethane. The synthesis of **20** and **21** is facile in comparison to the analogous reactions in alkene chemistry. The generation of a 1,3,2-dioxazolidine ring system by cycloaddition of a nitro group to an alkene only occurs under



Scheme 13. The addition of nitromethane to ditetrelenes **4** and **5**.

special circumstances; either photochemically²⁴ or thermally, using highly strained alkenes and aromatic nitro compounds.²⁵ Since the reduction of nitromethane by ditetrelenes **4** and **5** was a novel, selective two electron reduction and resulted in the formation of new heterocyclic ring systems, Baines and co-workers were interested in exploring the reaction of other organic main group oxides with ditetrelenes. The reactivity of disilene **4** and digermene **5** towards arylsulfonyl chlorides was also explored.²⁶ Similar to the reaction with nitromethane, a two electron reduction occurs at the sulfur centre of the sulfonyl chlorides to give arylsulfinates **22**, **23** and **24** (Scheme 14). Unlike the reaction with nitromethane, the reduction of the arylsulfonyl chlorides occurs through a 1,3-addition. For both nitroalkanes and the arylsulfonyl chlorides, the reductions are performed under mild conditions, without the use of a catalyst or heat, unlike the analogous reactions with alkenes.²⁷

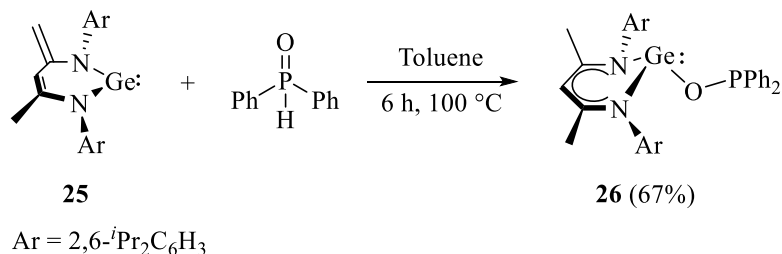


Scheme 14. The reduction of arylsulfonyl chlorides by ditetrelenes **4** and **5**.

1.5 Reactions with Organophosphorus Oxides

The reaction of ditetrelenes with organophosphorus oxides has not been reported in the literature. The only example of the addition of phosphine oxides to a low-valent Group 14 compound was reported by Zhao *et al.*²⁸ Diphenylphosphine oxide and other organic phosphorus compounds such as diphenylphosphine, (2-thienyl)₂PCl, diphenylphosphinic acid and diphenylthiophosphinic acid, were allowed to react with the N-heterocyclic germylene **25**, the germanium analogue of a carbene. In the reaction of **25** with diphenylphosphine oxide at elevated

temperatures, the phosphorus centre is reduced from P(V) to P(III) to give **26** (Scheme 15). This one-step process was envisioned as an alternative to the salt metathesis reactions for the formation of oxyphosphorus-substituted germanium (II) complexes.



Scheme 15. The reactivity of diphenylphosphine oxide with germylene **25**.

In this thesis, the reactivity of tetramesityldisilene **4** and -digermene **5**, prototypical examples of a disilene and a digermene, with organophosphorus oxides, namely, phosphine oxides and phosphites (Figure 6) will be examined. The nature of the phosphorus-oxygen bond has been investigated by Natural Bond Order (NBO)/ Natural Resonance Theory (NRT) calculations. The results of these calculations indicate that the phosphinyl moiety in the phosphine oxides and phosphites is a charge-localized dipole with the best Lewis representation of the bonding being P⁺-O⁻.²⁹ However, throughout the thesis, the phosphorus-oxygen bond of the organophosphorus oxides will be represented as a π bond.

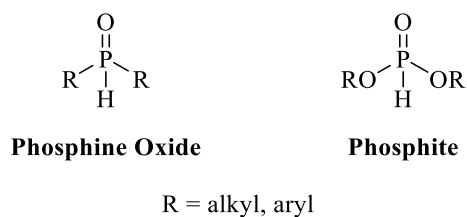
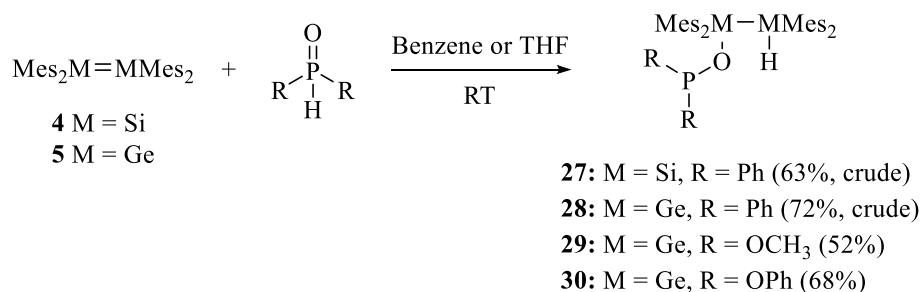


Figure 6. Structure of organophosphorus oxides.

The reactions of **4** and **5** with diphenylphosphine oxide, diphenyl phosphite and dimethyl phosphite have previously been explored in the group.^{30,31} In all reactions, the formation of a 1,3-adduct was observed, resulting in the reduction of the P(V) centre in the phosphine oxide or phosphite reagent to P(III) in compounds **27**, **28**, **29** and **30** (Scheme 16). Since compounds **27** and **28** were not sufficiently pure for publication, these reactions will be repeated and the spectroscopic assignments will be reassessed.

In addition to the re-examination of the reactions of **4** and **5** with diphenylphosphine oxide, the scope of the reaction of phosphorus(V) compounds with ditetrelenes **4** and **5**, will be expanded upon in this thesis. Specifically, the reaction of **4** and **5** with dipentylphosphine oxide, an alkylphosphine oxide, and the reaction of **4** with diphenyl phosphite and dimethyl phosphite will be explored.



Scheme 16. The addition of phosphine oxides and phosphites to **4** and **5**.

1.6 References

1. For reactivity of disilenes: a) Rammo, A.; Scheschkewitz, D. *Chem. Eur. J.* **2018**, *24*, 6866; b) Milnes, K. K.; Pavelka, L. C.; Baines, K. M. *Chem. Soc. Rev.* **2016**, *45*, 1019; c) Iwamoto, T.; Ishida, S. Multiple Bonds with Silicon: Recent Advances in Synthesis, Structure, and Functions of Stable Disilenes. In *Functional Molecular Silicon Compounds II Low Oxidation States*; Scheschkewitz, D., Ed.; Springer International Publishing: Switzerland, 2013; p 125; d) Mitsuo, K.; Iwamoto, T. *Adv. Organomet. Chem.* **2006**, *54*, 73; For reactivity of digermenes: e) Barrau, J.; Escudié, J.; Satgé, J. *Chem. Rev.* **1990**, *90*, 283; f) Tokitoh, N.; Okazaki, R. Multiply bonded germanium, tin and lead compounds. In *The Chemistry of Organic Germanium, Tin and Lead Compounds*; Rappoport, Z., Ed.; John Wiley & Sons Ltd: New York, 2002; p 844.
2. Majumdar, M.; Bejan, I.; Huch, V.; White, A. J. P.; Whittell, G. R.; Schäfer, A.; Manners, I.; Scheschkewitz, D. *Chem Eur. J.* **2014**, *20*, 9225.
3. Duke, C.B. *Chem. Rev.* **1996**, *96*, 1237.
4. Hardwick, J. A.; Baines, K. M. *Angew. Chem. Int. Ed.* **2015**, *54*, 6600.
5. Filler, M. A.; Mui, C.; Musgrave, C. B.; Bent, S. F. *J. Am. Chem. Soc.* **2003**, *125*, 4928.
6. Mui, M.; Filler, M. A.; Bent, S. F.; Musgrave, C. B. *J. Phys. Chem. B.* **2003**, *107*, 12256.
7. a) Grev, R. S., Schaefer, H.F.; Baines, K. M. *J. Am. Chem. Soc.* **1990**, *112*, 9458; b) Schmidt, M. W.; Truong, P. N.; Gordon, M. S. *J. Am. Chem. Soc.* **1987**, *109*, 5217.
8. Kovács, A.; Esterhuysen, C.; Frenking, G. *Chem. Eur. J.* **2005**, *11*, 1813.
9. Kira, M. *Proc. Jpn. Acad., Ser B, Phys. Biol. Sci.* **2017**, *88*, 167.
10. Lee, V. Y.; Sekiguchi, A. *Organometallic Compounds of Low-Coordinate Si, Ge, Sn and Pb: From Phantom Species to Stable Compounds*; John Wiley & Sons Ltd: Chichester, 2010.
11. Shepherd, B. D.; Campana, C. F.; West, R. *Heteroat. Chem.* **1990**, *1*, 1.
12. Izod, K.; Evans, P.; Waddell, P. G. *Angew. Chem. Int. Ed.* **2017**, *56*, 5593.

13. Hurni, K. L.; Rupar, P. A.; Payne, N. C.; Baines, K. M. *Organometallics* **2007**, *26*, 5569.
14. Kira, M.; Iwamoto, I.; Maruyama, T.; Kabuto, C.; Sakurai, H. *Organometallics* **1996**, *15*, 3767.
15. Hardwick, J. A.; Baines, K. M. *Chem. Eur. J.* **2015**, *21*, 2480.
16. Apeloig, Y.; Bravo-Zhivotovskii, D.; Zharov, I.; Panov, V.; Leigh, W. J.; Sluggett, G. W. *J. Am. Chem. Soc.* **1998**, *120*, 1398.
17. Boudjouk, P.; Han, B. H.; Anderson, K. R. *J. Am. Chem. Soc.* **1982**, *104*, 4992.
18. Weetman, C.; Inoue, S. *ChemCatChem*. **2018**, *10*, 4213.
19. Wendel, D.; Szilvási, T.; Jandl, C.; Inoue, S.; Rieger, B. *J. Am. Chem. Soc.* **2017**, *139*, 9156.
20. Wendel, D.; Szilvási, T.; Henschel, D.; Altmann, P. J.; Jandl, C.; Inoue, S.; Rieger, B. *Angew. Chem. Int. Ed.* **2018**, *57*, 14575.
21. Cowley, M. J.; Ohmori, Y.; Huch, V.; Ichinohe, M.; Sekiguchi, A.; Scheschkewitz, D. *Angew. Chem. Int. Ed.* **2013**, *52*, 13247.
22. Fanta, A. D.; DeYoung, D. J.; Belzner, J.; West, R. *Organometallics* **1991**, *10*, 3466.
23. Tashkandi, N. Y.; Parsons, F.; Guo, J.; Baines, K. M. *Angew. Chem. Int. Ed.* **2015**, *54*, 1612.
24. a) Okada, K.; Saito, Y.; Oda, M. *J. Chem. Soc. Chem. Commun.* **1992**, 1731; b) Charlton, J. L.; Liao, C. C.; de Mayo, P. *J. Am. Chem. Soc.* **1971**, *93*, 2463; c) Charlton, J. L.; de Mayo, P. *Can. J. Chem.* **1968**, *46*, 1041; d) Buchi, G.; Ayer, D. E. *J. Am. Chem. Soc.* **1956**, *78*, 689.
25. Leitich, J. *Angew. Chem. Int. Ed.* **1976**, *15*, 372.
26. Tashkandi, N. Y.; Bourque, J. L.; Baines, K. M. *Dalton Trans.* **2017**, *46*, 15451.
27. For the cycloaddition reaction of alkenes with compounds containing nitro groups: a) Leitich, J. *Angew. Chem. Int. Ed.* **1976**, *15*, 372; For the reaction of alkenes with sulfonyl chlorides: b) Kamigata, N.; Shimizu, T. *Rev. Heteroat. Chem.* **1997**, *17*, 1.

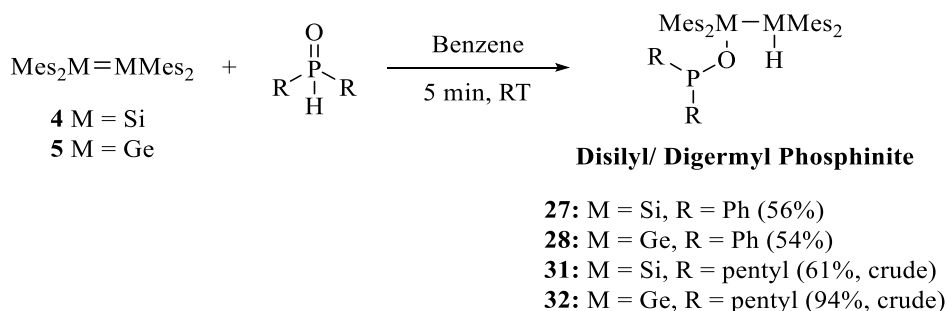
28. Wu, Y.; Liu, L.; Su, J.; Yan, K.; Wang, T.; Zhu, J.; Gao, X.; Gao, Y.; Zhao, Y. *Inorg. Chem.* **2015**, *54*, 4423.
29. Denehy, E.; White, J. M.; Williams, S. J. *Inorg. Chem.* **2007**, *46*, 8871.
30. Tashkandi, N. Y. Cycloaddition Reactions of (Di)tetrelenes. Ph. D. Dissertation, The University of Western Ontario, London, ON, **2016**.
31. Farhadpour, B. Doubly Bonded Derivatives of Si and Ge: Cycloaddition Reactions and Polymer Chemistry. Ph. D. Dissertation, The University of Western Ontario, London, ON **2017**.

Chapter 2

2 Synthesis and Characterization of Disilyl and Digermyl Phosphinites and Phosphites

2.1 The Addition of Organophosphorus Oxides to Ditetrelenes

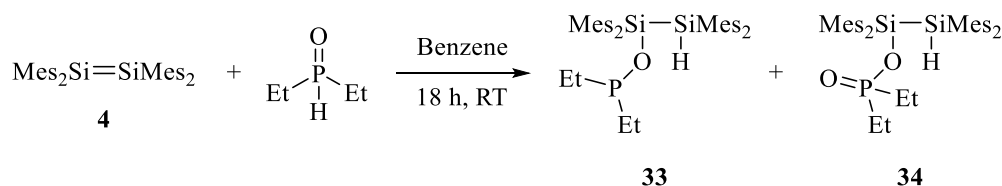
The reactivity of dialkyl and diarylphosphine oxides and phosphites towards ditetrelenes **4** and **5** is reported. The addition of phosphine oxides to a yellow solution of **4** or **5** at room temperature in benzene resulted in the formation of disilyl and digermyl phosphinites **27**, **28**, **31** or **32** (Scheme 17). The reactions occurred rapidly under mild conditions as evidenced by the rapid fading (5 min) of the yellow colour of the solutions to light yellow. The isolation of **27** and **28** was achieved by recrystallization of the crude oil from hexanes to yield white solids in 56% and 54% yield, respectively. By repeating the synthesis of **27** and recollecting the spectroscopic data, the assignment of the chemical shifts for the mesityl moieties could be corrected. For **28**, the ^{13}C chemical shifts for the mesityl *i*- and *p*-carbons were reassigned, and a spectrum with better resolution was obtained which enabled the correct assignment of the broad peaks originally reported in the $^{13}\text{C}\{^1\text{H}\}$ NMR spectrum of **28**. Since, the purification of **31** and **32** was difficult due to the sensitivity of the compounds to air and moisture, characterization of the products was performed on the crude reaction mixtures.



Scheme 17. The addition of diphenyl- and dipentylphosphine oxide to **4** and **5**.

The reaction of diethylphosphine oxide with **4** was also examined. The addition of diethylphosphine oxide (95%, Alfa Aesar) to a solution of **4** resulted in a colour change of the solution from bright yellow to pale yellow after 10 minutes. The solvent was evaporated, resulting in a pale yellow oil which was recrystallized from hexanes to yield an off-white solid which

contained two products, **33** and **34** in a ratio of 1:10, respectively (Scheme 18). The electrospray ionization (ESI) mass spectrum of the recrystallized solid contains a base peak at m/z 677.3 which



Scheme 18. The addition of 95% diethylphosphine oxide to **4**.

is consistent with $\text{C}_{40}\text{H}_{55}\text{O}_2\text{PSi}_2\text{Na}$ (**34** plus Na^+), corresponding to a 1:1 adduct between diethylphosphine oxide and disilene **4** plus an oxygen. A less intense signal was also observed at m/z 639.4 which is consistent with the molecular formula $\text{C}_{40}\text{H}_{56}\text{OPSi}_2$ (**33** plus H^+). The $^{31}\text{P}\{^1\text{H}\}$ NMR spectrum of the solid revealed a signal at 135.4 ppm which is characteristic of a P(III) centre, and therefore, was assigned to **33**. However, it is in minor amounts compared to the signal at 47.5 ppm, which is indicative of a P(V) centre and was assigned to **34**. An attempt was made to separate compounds **33** and **34** by preparative TLC; however, only **34** was isolated as a clear, colourless oil. The oil was recrystallized from benzene to give **34** as clear, colourless crystals. The structure of **34** was determined using X-ray crystallography (Figure 7). All bond lengths and angles in the structure of **34** are within expected ranges.¹

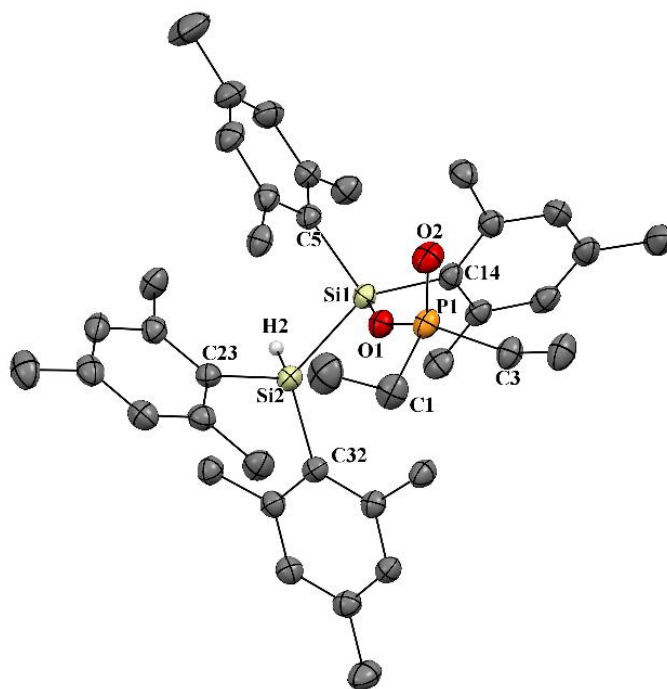


Figure 7. Displacement ellipsoid plot of **34**. Ellipsoids are at the 50% probability level and hydrogen atoms are omitted for clarity except the hydrogen on Si2. Selected bond lengths (Å) and angles (deg): Si1-O1 = 1.6830(17), Si1-Si2 = 2.3742(10), P1-O1 = 1.5802(17), P1-O2 = 1.4711(18), O1-Si1-Si2 = 105.63(7), Si1-Si2-H2 = 100.6(10), P1-O1-Si1 = 150.79(12).

The formation of **34** was surprising given that the reaction was performed under inert conditions. The progress of the reaction was monitored by $^{31}\text{P}\{^1\text{H}\}$ NMR spectroscopy which revealed that **34** is formed during the early stages of the reaction (Figure 8). Analysis of the reagent by $^{31}\text{P}\{^1\text{H}\}$ NMR spectroscopy² revealed that the reagent was primarily diethylphosphinic acid ($\text{Et}_2\text{P}(\text{O})\text{OH}$) with only minor amounts of diethylphosphine oxide present (95: 5 ratio). Evidently, compound **34** is formed by reaction of disilene **4** with diethylphosphinic acid and **33** is formed by reaction of **4** with diethylphosphine oxide. Compound **33** is susceptible to oxidation, as the intensity of the signal at 135.4 ppm decreases over time, while the intensity of the signal at 47.5 ppm increases.

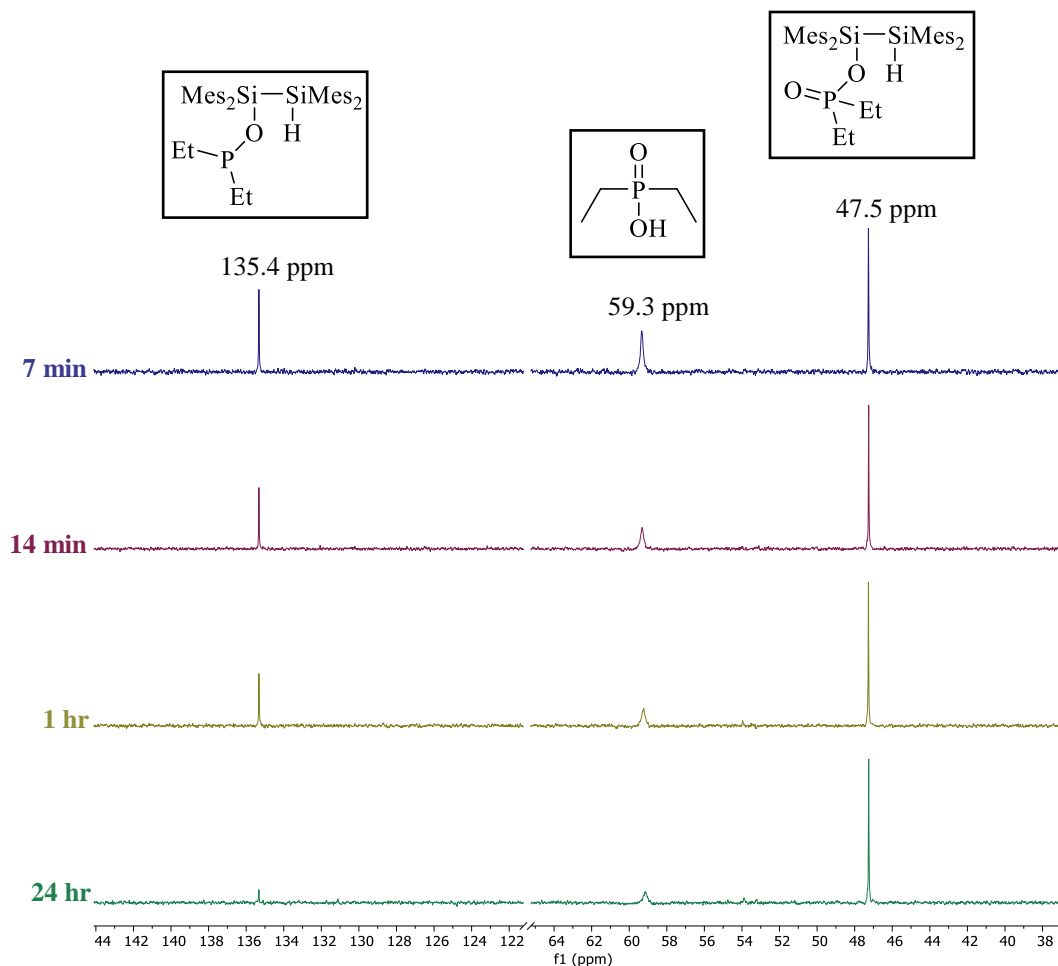
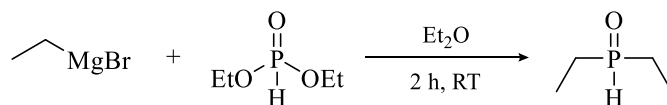


Figure 8. The reaction of **4** with diethylphosphinic acid monitored by $^{31}\text{P}\{^1\text{H}\}$ NMR spectroscopy (C_6D_6 , 162 MHz).

Diethylphosphine oxide was synthesized by the reaction of diethyl phosphite with excess ethylmagnesium bromide in diethyl ether at room temperature (Scheme 19).³ The phosphine oxide was isolated as a white solid after recrystallization of the crude oil from hexanes. Multiple attempts were made to react **4** with diethylphosphine oxide, however, the phosphine oxide was only soluble

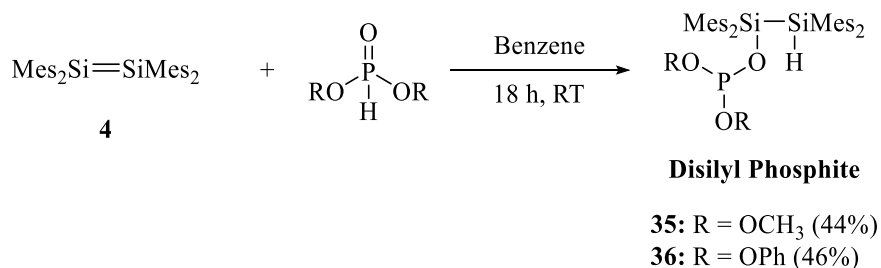


Scheme 19. The synthesis of diethylphosphine oxide.

in water and slightly soluble in chloroform. These solvents could not be used for the reaction of diethylphosphine oxide with **4** since both water and chloroform readily react with **4**.⁴ Since the

reaction of diethylphosphine oxide with **4** proved to be problematic, the study of the reaction of diethylphosphine oxide with **4** was discontinued.

Similar to the addition of diphenyl- and dipentylphosphine oxide to ditetrelenes **4** and **5**, one equivalent of dimethyl or diphenyl phosphite was added to a yellow solution of disilene **4** dissolved in benzene to yield disilyl phosphites **35** and **36**, respectively (Scheme 20). Unlike the phosphine oxides which reacted within 5 minutes, the reaction of the ditetrelenes with the phosphites took 18 hours to go to completion. The purification of **35** involved recrystallization of the crude oil from hexanes to yield clear, colourless crystals. In the reaction of diphenyl phosphite with **4**, excess phosphite was separated by preparative thin layer chromatography (TLC) and **36** was isolated as a white solid by recrystallization from hexanes in 46% yield.



Scheme 20. The addition of dimethyl and diphenyl phosphite to **4**.

2.2 Characterization of Disilyl and Digermyl Phosphinites and Phosphites

The compounds synthesized from the reaction of diorganophosphine oxides and phosphites with ditetrelenes **4** and **5** were characterized by NMR spectroscopy, high resolution mass spectrometry, infrared (IR) spectroscopy, and when appropriate, X-ray crystallography. The exact mass for each compound, as determined by ESI-MS in positive ion mode, was consistent with the formation of a 1: 1 adduct between the diorganophosphine oxide or phosphite and disilene **4** or digermene **5**, plus Na^+ or H^+ .

NMR spectroscopy was extremely useful in the characterization of the disilyl and digermyl phosphinites and phosphites as the compounds contained multiple NMR active nuclei including ^1H , ^{13}C , ^{31}P , and ^{29}Si (for the derivatives formed from the reactions with tetramesityldisilene **4**). The most diagnostic nucleus for assessing the outcome of the reactions was ^{31}P .

Diorganophosphites with a P(III) centre, resonate downfield in comparison to compounds with P(V) centres as exemplified by the ^{31}P chemical shifts of trimethyl phosphite ($\text{P}(\text{OCH}_3)_3$) and trimethyl phosphate ($\text{O}=\text{P}(\text{OCH}_3)_3$) which resonate at 142.0 ppm and 3.7 ppm, respectively.⁵ The same trend is seen in the reaction of phosphine oxides and phosphites with ditetrelenes **4** or **5**. The phosphine oxides and phosphite reagents containing a P(V) centre resonate below 40 ppm, whereas the disilyl and digermyl phosphinite and phosphite derivatives formed, containing a P(III) centre, resonate at chemical shifts significantly shifted downfield (above 100 ppm) compared to the starting phosphorus reagent (Table 2).

Table 2. ^{31}P chemical shifts of P(V) reagents, disilyl/ digermyl phosphinites and phosphites.

$\begin{array}{c} \text{O} \\ \\ \text{R}-\text{P}-\text{R} \\ \\ \text{H} \end{array}$	^{31}P Chemical Shift (ppm) ^a	$\begin{array}{c} \text{Mes}_2\text{M}-\text{MMes}_2 \\ \text{R}-\text{P}-\text{O}-\text{H} \\ \\ \text{R} \end{array}$	^{31}P Chemical Shift (ppm) ^a
R = Ph	16.9	M = Si, R = Ph (27)	107.2
		M = Ge, R = Ph (28)	104.5
R = pentyl	29.7	M = Si, R = pentyl (31)	130.6 ^b
		M = Ge, R = pentyl (32)	129.0
R = OCH ₃	9.8	M = Si, R = OCH ₃ (35)	132.8
R = OPh	-0.4	M = Si, R = OPh (36)	133.3

^a Measured in C₆D₆.

^b Tentatively assigned.

For the reactions with tetramesityldisilene **4**, ^1H - ^{29}Si gHMBC (gradient heteronuclear multiple bond correlation) spectroscopy also provided valuable structural information. In HMBC spectroscopy, correlations are seen between heteronuclei and hydrogens which are 1 to 3 bonds away, which gives insight into the connectivity of the molecule. Two signals were consistently observed in the disilyl phosphinite and phosphite derivatives synthesized with ^{29}Si chemical shifts of approximately -55 and -5 ppm and coupling constants of ~ 180 Hz and 15 Hz, respectively (Table 3). For example, the ^1H NMR spectrum of **35** revealed a signal at 5.67 ppm, which integrated to 1H and was assigned to the Si-H moiety. In the ^1H - ^{29}Si gHMBC spectrum of disilyl phosphite **35**, each signal in the ^{29}Si dimension correlates to the signal at 5.67 ppm in

Table 3. The ^{29}Si chemical shifts and coupling constants of disilyl phosphinites and phosphites.

$\begin{array}{c} \text{Mes}_2\text{Si}_A-\text{Si}_B\text{Mes}_2 \\ \\ \text{R}-\text{P}-\text{O}-\text{H} \\ \\ \text{R} \end{array}$	^{29}Si chemical shifts of Si_A (ppm)	$^2J_{\text{Si-H}}$ coupling constant (Hz)	^{29}Si chemical shifts of Si_B (ppm)	$^1J_{\text{Si-H}}$ coupling constant (Hz)
R = Ph (27)	-1.8	15	-56.4	175
R = pentyl (31)	-5.6	13	-54.8	177
R = OCH ₃ (35)	-7.3	13	-55.3	180
R = OPh (36)	-5.9	15	-55.7	179

the ^1H dimension. The signal at -55.3 ppm correlates through a J coupling of 180 Hz and this, was assigned to an Si-H moiety on the basis of the magnitude of the J and the chemical shift. The signal at -7.3 ppm correlates through a J coupling of 13 Hz and thus, was assigned to Si_A (Figure 9).

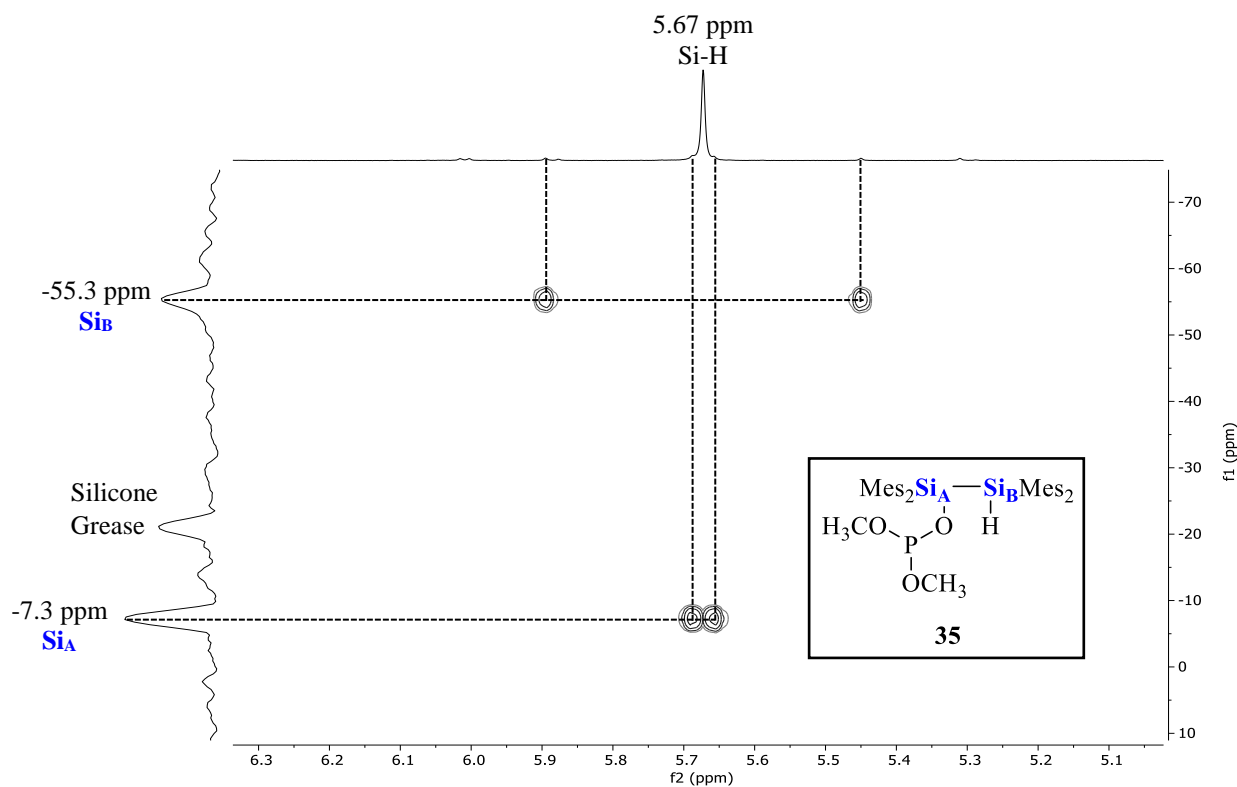


Figure 9. The ^1H - ^{29}Si gHMBC spectrum of **35** showing the correlations to the signal at 5.67 ppm in the ^1H dimension.

The structures of **27**⁶ and **35** (Figure 10) were identified unambiguously through single crystal X-ray diffraction. The phosphorus centre of **35** exhibits trigonal pyramidal geometry; the displacement of the phosphorus atom from the plane of the attached atoms is 0.764 Å. The geometry at the phosphorus centre is indicative of the P(III) oxidation state. All bond lengths and angles in **35** are within expected ranges. For example, the Si2-H2 (1.39 Å), Si1-O1 (1.67 Å), Si1-Si2 (2.38 Å) and P1-O1 (1.60 Å) bond lengths in **35** are within the ranges of 1.39-1.45, 1.64-1.71, 2.35-2.40 and 1.59-1.66 Å, respectively, for related compounds.⁷ In some crystal samples of disilyl phosphite **35**, a disorder was observed in the molecular structure where a hydroxyl group was bound to Si2, 5% of the time, instead of a hydrogen, as a result of oxidation of the Si-H centre.

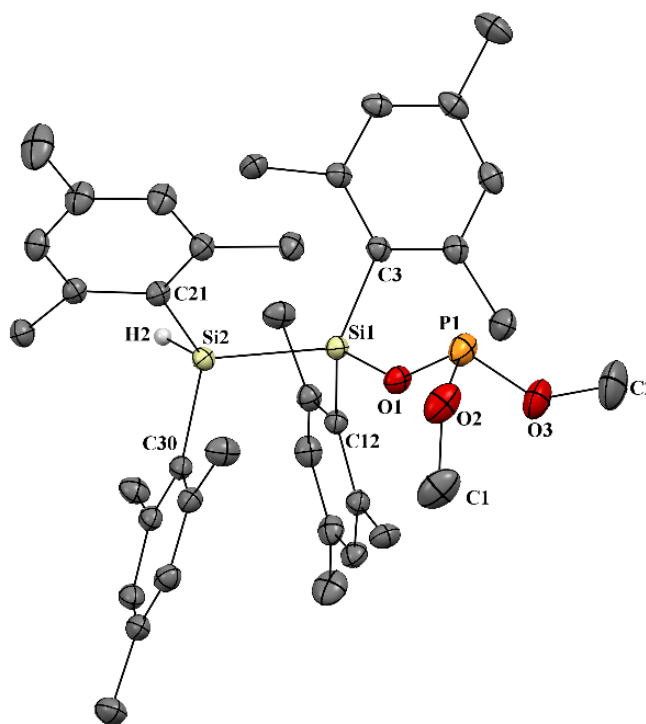


Figure 10. Displacement ellipsoid plot of **35**. Ellipsoids are at the 50% probability level and hydrogen atoms are omitted for clarity except the hydrogen on Si2. Selected bond lengths (Å) and angles (deg): Si1-O1 = 1.6685(11), Si1-Si2 = 2.3806(7), P1-O1 = 1.6043(11), O1-Si1-Si2 = 108.52(4), Si1-Si2-H2 = 100.0(7), P1-O1-Si1 = 141.92(7).

Infrared spectroscopy is also useful in this chemistry. The appearance of the characteristic signals for Si-H (or Ge-H) groups and the disappearance of the signals characteristic of the P=O moiety of the phosphine oxides and phosphites are particularly diagnostic. For example, the IR spectrum of **36** (Figure 11) shows a medium intensity signal at 2129 cm⁻¹, which is characteristic of an Si-H stretching vibration (typically 2250 – 2100 cm⁻¹). Additionally, the absence of strong

signals in the regions $2425 - 2325\text{ cm}^{-1}$ and $1350 - 1300\text{ cm}^{-1}$, corresponding to phosphorus ester P-H stretching and aromatic P=O stretching, respectively, indicates the lack of a $\text{O}=\text{P}(\text{V})\text{-H}$ moiety in the compound. Instead, a strong signal at 851 cm^{-1} is observed and can be assigned to the P(III)-O stretching of the P(III)-(OPh)₂ functional group, which are typically found in the range of $875 - 830\text{ cm}^{-1}$.⁸

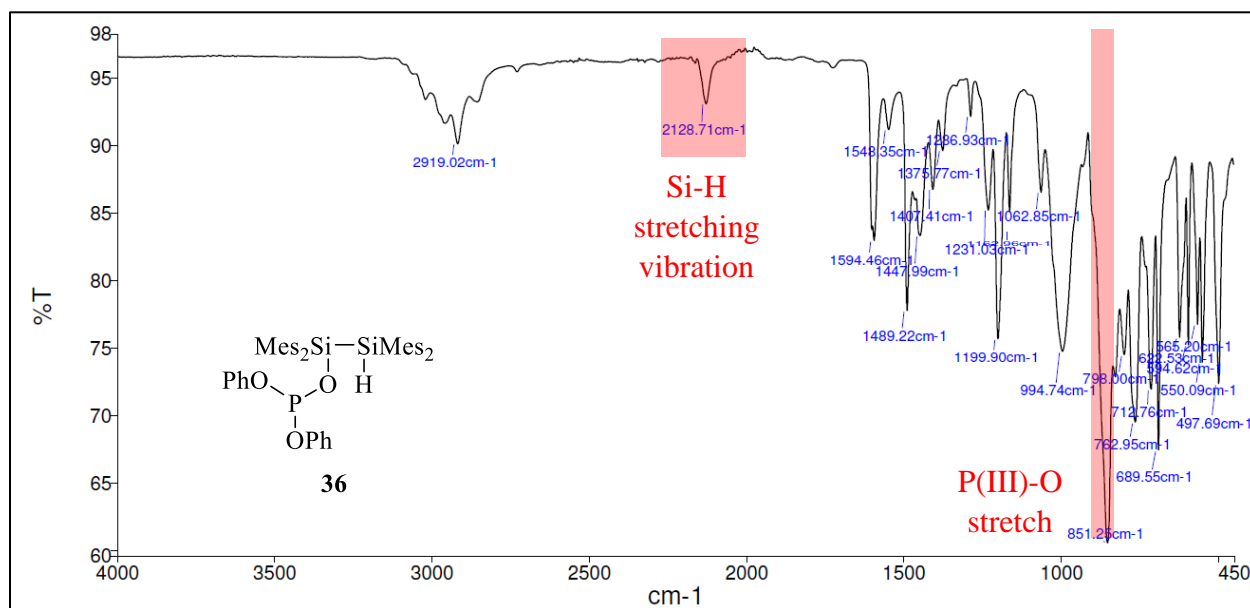
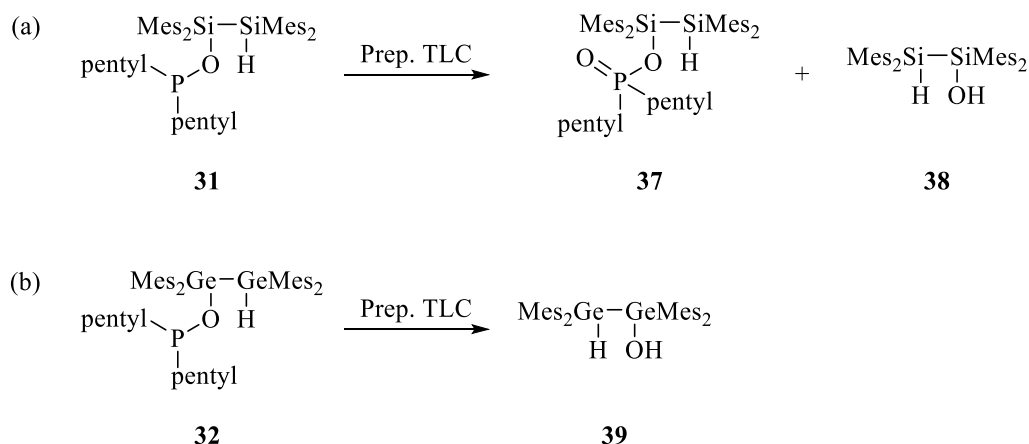


Figure 11. IR spectrum of compound **36**.

2.3 Reactivity of Disilyl and Digermyl Phosphinites and Phosphites

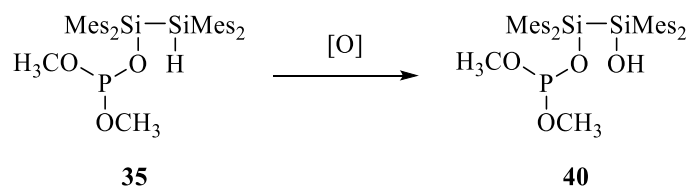
The disilyl and digermyl adducts **31**, **32**, **35**, and **36** were prone to oxidation of the M-H bond, hydrolysis at the P-OR bond or oxidation of the P(III) centre. The reactions were typically accelerated by chromatography, except for the oxidation of the Si-H bond of disilyl phosphite **35**. The dialkyldisilyl and digermyl phosphinites were particularly prone to oxidation of the P(III) centre and hydrolysis of the P-O moiety bound to the M centre.

Attempted purification of **31** by preparative TLC resulted in the isolation of two compounds, **37** and **38**. Compound **37** is a result of the oxidation of the P(III) centre in **31** and compound **38** is proposed to form through hydrolysis of the P-O moiety bound to the Si centre. (Scheme 21a). Compound **39** was the only compound isolated from the attempted purification of **32** by preparative TLC and is proposed to form by hydrolysis of the P-O moiety bound to the Ge centre, similar to the formation **38** (Scheme 21b).



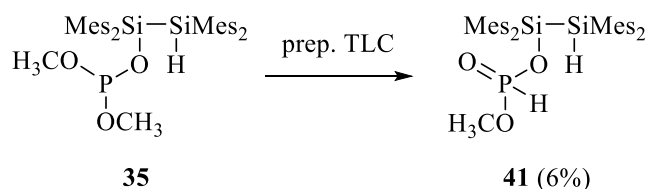
Scheme 21. The secondary reactivity observed for (a) disilyl phosphinite **31** and (b) digermyl phosphinite **32**.

Dimethyldisilyl phosphite **35** was also susceptible to oxidation of the Si-H bond to form compound **40** (Scheme 22). The presence of **40** was observed in the molecular structure obtained from single-crystal X-ray diffraction, and in the ESI mass spectrum at m/z 681.3 of samples of **35**.



Scheme 22. The oxidation of the Si-H moiety of **35**.

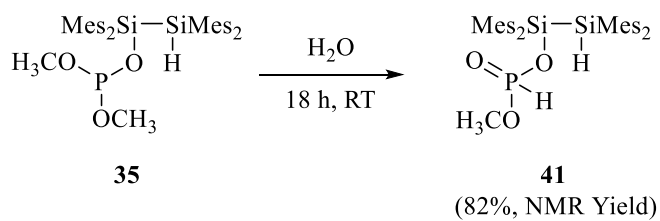
Attempts to separate **35** and **40** by preparative TLC resulted in the isolation of compound **41** in 6% isolated yield (Scheme 23). The ESI mass spectrum of **41**, revealed a base peak at m/z 651.3 corresponding to the molecular formula $\text{C}_{37}\text{H}_{49}\text{O}_3\text{PSi}_2$ plus Na^+ , which is consistent with a 1:1 adduct between **35** and water, and the loss of methanol. Consistent with the loss of CH_3O , in the ^1H NMR spectrum of **41**, the doublet assigned to the methoxy group at 3.24 ppm integrates to



Scheme 23. The formation of **41** following preparative TLC.

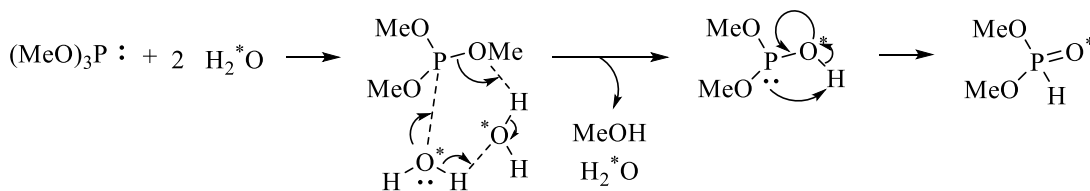
3H relative to the signal at 5.66 ppm which was assigned to the Si-H moiety. An additional doublet appears at 6.80 ppm. The coupling constant of the doublet is 690 Hz, which is typical of a one-bond hydrogen-phosphorus(V) coupling, and therefore, is assigned to the hydrogen directly bonded to the P(V) centre.⁹ In the $^{31}\text{P}\{^1\text{H}\}$ NMR spectrum of **41**, a signal is observed at -5.2 ppm which is shifted upfield compared to the chemical shift of the signal for disilyl phosphite **35** at 132.8 ppm, consistent with a P(V) centre. These data are consistent with the structure proposed for **41**.

The formation of compound **41** was proposed to occur through the hydrolysis of the P-OCH₃ bond in **35**, followed by tautomerization. Indeed, **41** could be formed independently by hydrolysis to give a white solid consisting of **41** in an 82% yield as determined by ^{31}P NMR spectroscopy (Scheme 24).



Scheme 24. The direct hydrolysis of dimethyldisilyl phosphite **35**.

Preparative TLC of a sample of **35** also resulted in the formation of **41**, indicating the hydrolysis was accelerated by chromatography. The hydrolysis of trialkyl phosphites to give dialkyl phosphites is well known; the mechanism for the hydrolysis of P(OMe)₃ has been studied by Alam *et al.* and the results are consistent with the observations reported herein (Scheme 25).¹⁰



Scheme 25. The hydrolysis of trimethyl phosphite with ^{17}O -labelled water.¹⁰

Diphenyldisilyl phosphite **36** is not as susceptible to hydrolysis or oxidation in comparison to the dialkyldisilyl phosphite since **36** was successfully isolated from the TLC plate as a white solid, although minor contaminants were observed. On the basis of ESI mass spectrometry and ^{31}P NMR

spectroscopy the contaminants were identified as triphenyl phosphite ($\text{P}(\text{OPh})_3$) and compounds **42**, **43**, and **44**; the ratio of **36** relative to the contaminants was 100: 12: 1: 1: 1, respectively (Figure 12). Compound **42** is proposed to form through the hydrolysis of the P-OPh bond in **36**, followed by tautomerization, similar to the formation of **41**. The formation of **43** can be explained by the oxidation of the P(III) centre, and **44** is a result of the oxidation of both the P(III) centre and the Si-H moiety.

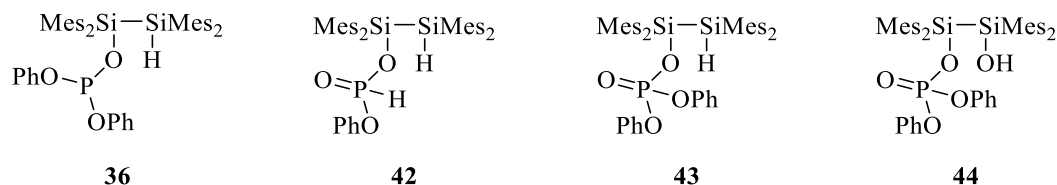
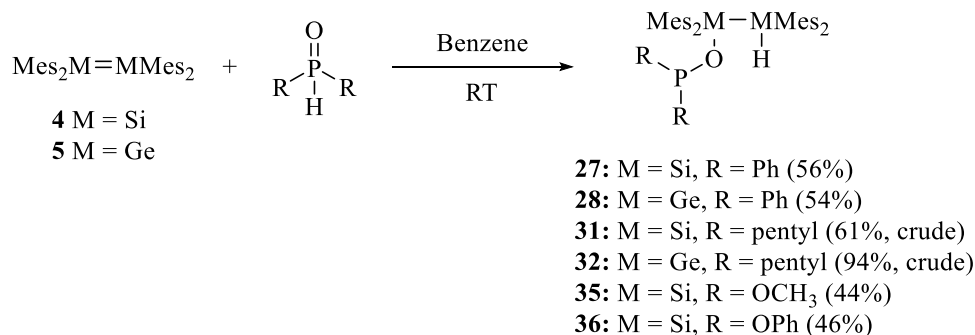


Figure 12. Compounds isolated from the preparative TLC plate.

The diaryldisilyl and digermyl phosphinites **27** and **28** showed no signs of further chemistry. Upon exposure to air, **27** and **28** were stable, and no oxidation or hydrolysis was observed by NMR spectroscopy. The diaryl phosphinites and phosphites were more stable in comparison to the dialkyl derivatives. This observation is in line with the computational studies performed on the stability of dialkyl and diarylphosphines by Higham *et al.*¹¹ In order for a phosphine to be oxidized, it must go through a cationic radical intermediate $[\text{R}_2\text{HP}]^{+\bullet}$. The authors report that $[\text{Ph}_2\text{HP}]^{+\bullet}$ is more stable due to the steric bulk and conjugation provided by the aryl groups in comparison to the dialkyl derivative $[\text{Et}_2\text{HP}]^{+\bullet}$. As a result, the P(III) centre of diethylphosphine is more susceptible to oxidation compared to diphenylphosphine.

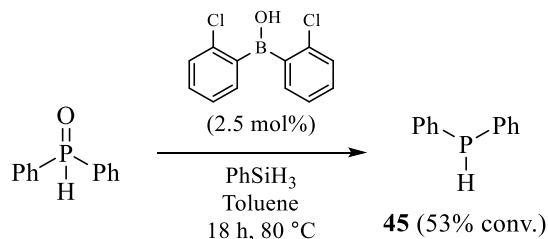
2.4 Discussion

The reactivity of ditetrelenes **4** and **5** towards compounds containing P=O bonds, resulted in the formation of 1,3-adducts **27**, **28**, **31**, **32**, **35** and **36** under mild conditions (Scheme 26). In each case, the reaction resulted in the formation of an M-O and M-H bond, and the breaking of a P-H bond to reduce the P(V) centre in the phosphine oxides and phosphites to P(III) in the adducts.



Scheme 26. The addition of organophosphorus oxides to **4** and **5**.

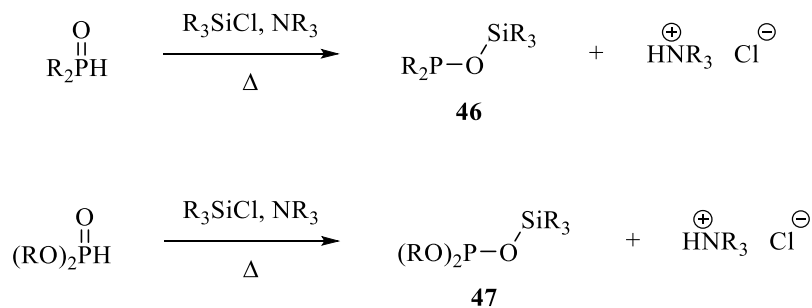
Reductions of phosphine oxides to form phosphines are often achieved using aluminohydride or chlorosilane reagents such as LiAlH_4 or HSiCl_3 at elevated temperatures.¹² The use of hydrosilanes as alternatives to aluminohydrides and chlorosilane reagents has also been explored in the reduction of phosphine oxides, although this method requires a catalyst to activate the Si-H bond.¹³ While these methods have been extensively investigated with tertiary phosphine oxides ($\text{O}=\text{PR}_3$), the reduction of secondary phosphine oxides ($\text{O}=\text{PHR}_2$) has been explored to a lesser extent. Blanchet *et al.* recently reported the reduction of tertiary and secondary phosphine oxides using bis(2-chlorophenyl)borinic acid as a precatalyst and phenylsilane as the hydride source.¹⁴ The reduction of diphenylphosphine oxide by the borinic acid precatalyst to form diphenylphosphine **45** was conducted at 80 °C (Scheme 27). In contrast, the reduction of diphenyl- and dipentylphosphine oxide by disilene **4** and digermene **5** yields phosphinite ($\text{R}_2\text{P}(\text{OR}')$) derivatives **27**, **28**, **31** and **32**, and not dialkyl- or diarylphosphines. While the formal oxidation number for P is (III) in both types of products, the chemical state of P in the phosphinite derivatives is intermediate between that of phosphine oxides and phosphines.



Scheme 27. Reduction of diphenylphosphine oxide by a borinic acid precatalyst.

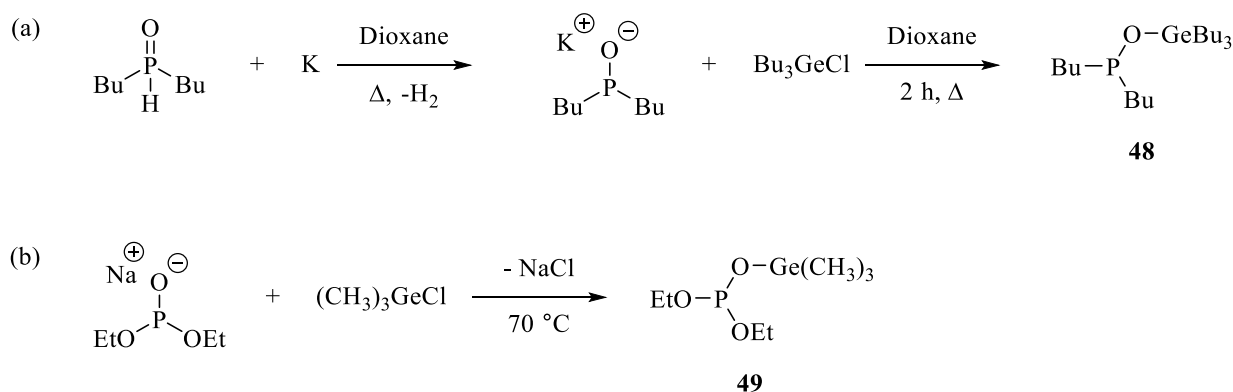
The reduction of diorganophosphine oxides and phosphites by disilene **4** is reminiscent of the reaction of diorganophosphine oxides and phosphites with chlorosilanes at elevated temperatures

in the presence of an amine which also gives silyl phosphinite and phosphite derivatives **46** and **47**, respectively (Scheme 28).¹⁵ However, in the reactivity with disilene **4**, the Lewis acid and Lewis base are contained within the same molecule, and the reaction can be performed under neutral conditions and at room temperature.



Scheme 28. Reaction of diorganophosphine oxides and phosphites with chlorosilanes in the presence of amines.

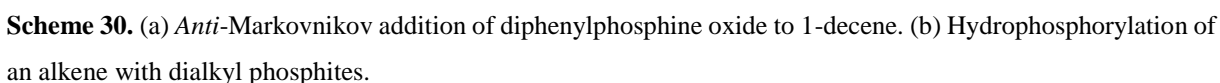
The synthesis of germyl phosphinite **48** has previously been reported to occur through the reduction of dibutylphosphine oxide by potassium to form the salt derivative (R₂POK). A salt metathesis reaction occurs when the salt is added to Bu₃GeCl to yield germyl phosphinite **48** (Scheme 29a).¹⁶ Similarly, diethylgermyl phosphite **49** is synthesized from the reaction of a phosphite salt with a chlorogermane at 70 °C (Scheme 29b).¹⁷



Scheme 29. The synthesis of (a) germyl phosphinite **48** and (b) germyl phosphite **49** through a salt metathesis reaction.

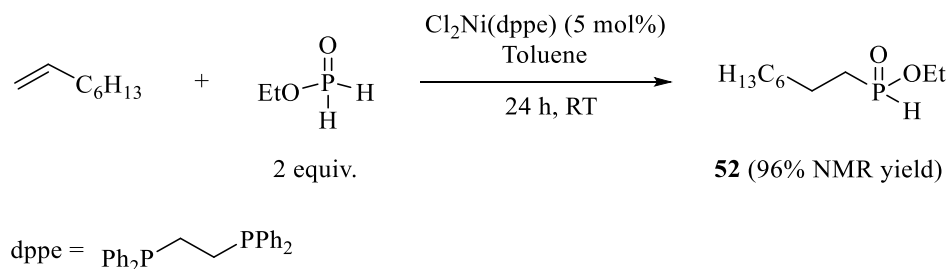
In the salt metathesis method, the P(V) centre of dibutylphosphine oxide and diethyl phosphite is already reduced to a P(III) centre in the salt derivative. In this case, the germane is only involved in a substitution reaction. In contrast, the formation of the digermyl phosphinites and phosphites

The reaction of diorganophosphine oxides and phosphites with ditetrelenes is in stark contrast to that with alkenes. The reaction of diorganophosphine oxides and phosphites with alkenes leads to cleavage of the P-H bond and the formation of a C-P bond and requires the use of heat with or without a transition metal catalyst. For example, the addition of diphenylphosphine oxide to 1-decene yields the *anti*-Markovnikov adduct **50** at 80 °C (Scheme 30a).¹⁸ In another example, the hydrophosphorylation of alkenes with dialkyl phosphites is catalyzed by Mn(OAc)₂ at high temperatures (ranging from 90 to 110 °C) to yield dialkyl phosphonates **51** (Scheme 30b)¹⁹. In both examples, the reaction of the organophosphorus oxide with the alkene involves addition of the P-H across the C=C bond.



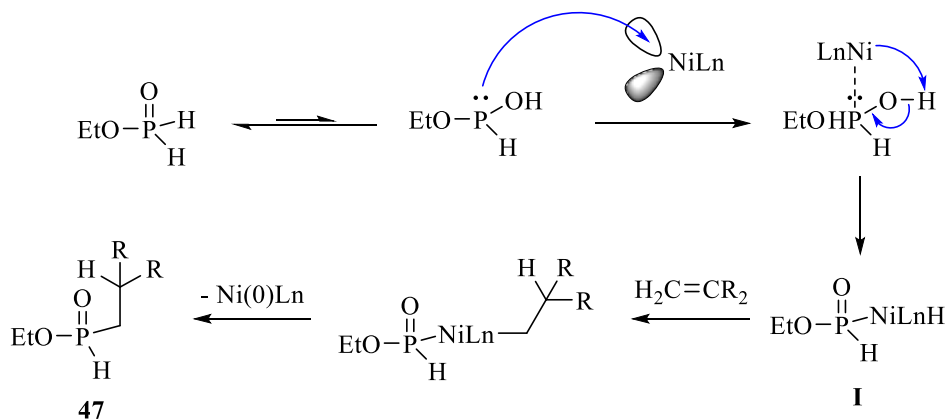
Since ditetrelenes **4** and **5** successfully activated organophosphorus oxides, it is also interesting to compare the reactivity of phosphine oxides and phosphites with transition metals, particularly those used to facilitate the addition to alkenes. In the Ni-catalyzed hydrophosphinylation of 1-octene with a primary phosphite, ethyl phosphinate (EtOP(O)H₂), the

anti-Markovnikov adduct **52** was formed in 96% yield as determined by ^{31}P NMR spectroscopy (Scheme 31).²⁰



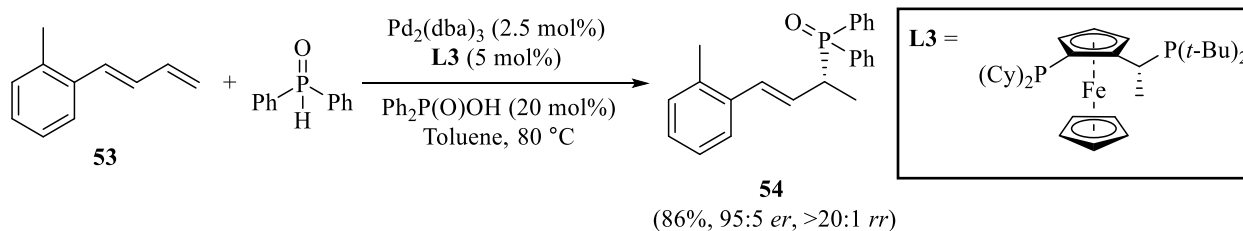
Scheme 31. The Ni-catalyzed hydrophosphinylation of 1-octene.

The mechanism proposed by the authors (Scheme 32) involves the coordination of the ethyl phosphinate tautomer to the Ni(0) centre, to generate intermediate species **I**. Following the complexation of Ni(0) to the phosphinate tautomer, intermediate **I** can add to the alkene. Subsequent reductive elimination would regenerate the Ni catalyst and yield the functionalized product **52**.



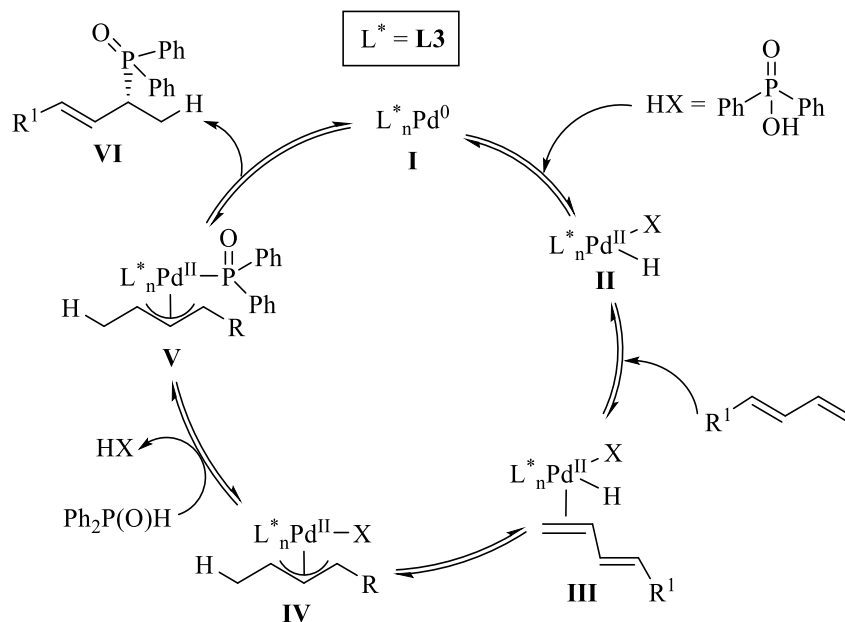
Scheme 32. Proposed mechanism for the hydrophosphinylation of 1-octene.²⁰

The enantioselective hydrophosphinylation of diene **53** with diphenylphosphine oxide is facilitated by a Pd-based catalyst and diphenylphosphinic acid as a co-catalyst to yield the Markovnikov adduct **54** in 86% yield (Scheme 33).²¹ The authors proposed the mechanism depicted in Scheme 34 based on literature precedence and experimental observations. The Pd(0)



Scheme 33. The Pd-catalyzed hydrophosphinylation of **54**.

precatalyst undergoes ligand substitution with the Josiphos ligand (**L3**) to form chiral species **I**. Subsequent oxidative addition of co-catalyst (diphenylphosphinic acid), yields the Pd-H species **II**. Addition of the 1,3-diene results in coordination of the Pd to the less hindered alkene to form species **III**. Species **III** undergoes hydopalladation to generate the Pd- π -allyl intermediate **IV**, which is subjected to ligand exchange upon addition of diphenylphosphine oxide. As a result of the substitution of diphenylphosphinic acid with $\text{Ph}_2\text{P}(\text{O})\text{H}$, a Pd-P(V) intermediate **V** is formed and the co-catalyst is regenerated. Reductive elimination results in the formation of the functionalized product **VI** and regeneration of chiral species **I**.



Scheme 34. Proposed mechanism for the Pd-catalyzed hydrophosphinylation of 1,3-dienes.

In the Pd-catalyzed hydrophosphinylation of 1,3-dienes, the alkene is activated before addition of the phosphine oxide; whereas, in the Ni-catalyzed hydrophosphinylation of terminal alkenes with primary phosphites, the phosphite is activated first, then addition to the alkene occurs.

While the mechanism for the transition metal catalyzed hydrophosphinylation of alkenes differs between reactions with phosphine oxides and phosphites, a similarity is seen where the phosphorus reagent binds to the transition metal through the P atom. In contrast, for the reactions of phosphine oxides and phosphites with ditetrelenes, the phosphine oxide or phosphite is attached to the metal centre through the oxygen. The reactivity observed between phosphine oxides and phosphites with **4** and **5** is evidently governed by the strong M-O bond that is formed from addition of the P⁺-O⁻ bond of the organophosphorus oxide to the M=M bond. This imparts unique reactivity to the reactions of ditetrelenes with phosphine oxides and phosphites which can be utilized in further chemistry.

2.5 Summary

The reaction of phosphine oxides and phosphites with disilene **4** and digermene **5** resulted in a mild two electron reduction of the P centre, to yield diorganodisilyl and digermyl phosphinites and phosphites (Figure 13). The formation of diorganodisilyl phosphinites and phosphites by **4** provides an alternative synthetic route to the traditional reduction of phosphine oxides and

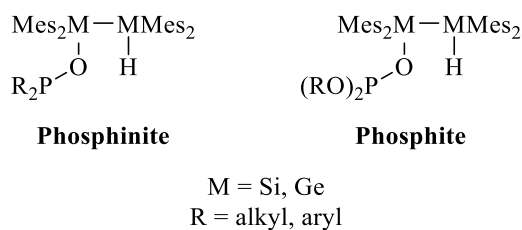


Figure 13. General structures of disilyl and digermyl phosphinites and phosphites.

phosphites by chlorosilanes in the presence of amines at elevated temperatures, under neutral conditions at room temperature. For the previous synthesis of a diorganogermyl phosphinite, the phosphine oxide was reduced by potassium to form a salt of the phosphine oxide, followed by a salt metathesis reaction with a chlorogermene. The new synthesis of diorganodigermyl phosphinites with **5** shows the reduction of the P(V) centre of the phosphine oxide directly by the Ge centre.

The formation of an M-O bond in the disilyl and digermyl phosphinites and phosphites is in contrast to alkene chemistry, which adds the P-H moiety of the phosphine oxide or phosphite across the C=C bond to form a C-P bond. Furthermore, alkenes require heat and/or a catalyst to

facilitate the addition of phosphine oxides and phosphites. The reactions of organophosphorus oxides with ditetrelenes **4** and **5** are performed under mild conditions, without the use of a catalyst. Therefore, ditetrelenes **4** and **5** are capable of activating organophosphorus oxides. However, the reactivity of phosphine oxides and phosphites with ditetrelenes differs from the reactivity with transition metals. Transition metals react directly with the P centre, often through a P-OH containing species, whereas ditetrelenes react with the oxygen of the P⁺-O⁻ moiety. The reaction of organophosphorus oxides with **4** and **5** provides another example of the activation of organic main group oxides by ditetrelenes, in addition to the activation of nitromethane,²² arylsulfonyl chlorides,²³ CO²⁴ and CO₂.²⁵

While all reactions lead to the formation of a 1,3-adduct containing a P(III) centre, secondary reactions of certain adducts were observed. Upon exposure to air and moisture, three classes of secondary reactions were observed: i) hydrolysis of the P-OR bond, ii) oxidation of the M-H bond and iii) oxidation of the P(III) centre. The dipentylidisilyl and digermyl phosphinites were the most susceptible to secondary reactions, while the diphenyldisilyl and digermyl phosphinites were the most stable. This trend can be rationalized by the steric bulk of the aryl derivatives providing increased stability of the P(III) center.¹¹

The importance of the purity of commercially available reagents is exemplified in the attempted addition of diethylphosphine oxide to **4**. The 95% reagent that was purchased was made up of diethylphosphinic acid, and only about 5% diethylphosphine oxide. The addition of diethylphosphinic acid to **4** resulted in the formation of **34**, containing a P(V) centre.

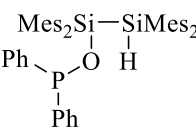
2.6 Experimental

2.6.1 General Experimental Details

All reactions were carried out using flame dried apparatus under an inert atmosphere of argon using general Schlenk techniques or in an MBraun glovebox under an atmosphere of nitrogen, unless otherwise stated. All anhydrous solvents were collected from an Innovative Technology solvent purification system and dried over 4 Å molecular sieves. All reagents were purchased from Millipore Sigma or Alfa Aesar. Disilene **4** was prepared by photolysis of Mes₂Si(Si(CH₃)₃)₂ in hexanes in a quartz tube with Ushio G8T5 Mercury UV-C lamps (254 nm)

and cooled to -45 °C using a Thermo Scientific Neslab ULT 80 bath circulator. Digermene **5** was prepared through a similar procedure as **4**, by the photolysis of (Mes₂Ge)₃ in THF at 350 nm. NMR spectra were acquired using a Varian INOVA I600 FT-NMR spectrometer or a Bruker AvIII HD 400 spectrometer. The ¹H and ¹³C chemical shifts (δ) are listed in ppm against residual C₆D₅H (7.15 ppm) and C₆D₆ (128 ppm) relative to tetramethylsilane, respectively. The chemical shifts for the ³¹P{¹H} NMR spectrum were referenced externally to 85% H₃PO₄. The ²⁹Si chemical shifts were obtained from the ²⁹Si dimension of the ¹H-²⁹Si gHMBC spectrum relative to tetramethylsilane. Electrospray ionization time of flight mass spectrometry was performed using the Bruker microOTOF 11 instrument in positive ion mode. Infrared spectra were collected through Attenuated Total Reflectance (ATR)-IR spectroscopy on a solid sample using the Perkin Elmer Spectrum Two IR Spectrometer. Reaction mixtures were purified outside of the glovebox using preparative thin-layer chromatography on 20 x 20 cm plastic TLC plates consisting of silica gel coated with a fluorescent indicator and purchased from Millipore Sigma.

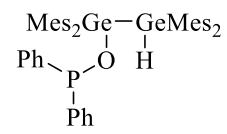
2.6.2 Addition of Diphenylphosphine Oxide to Tetramesityldisilene **4**


 Diphenylphosphine oxide (19 mg, 0.10 mmol) was added to a yellow solution, consisting of tetramesityldisilene **4** (52 mg, 0.10 mmol) dissolved in benzene (4 mL), at room temperature; the colour of the solution immediately changed to pale yellow. The benzene was evaporated giving a colourless oil which was redissolved in a minimal amount of hexanes. The flask was placed in the freezer (-20 °C) for 24 hours. A white precipitate formed and the solid was isolated by decantation (37 mg, 56 %). mp: 186 – 190 °C; ATR-FTIR (solid, cm⁻¹) 2919 (m), 2132 (m, Si-H), 1602 (m), 1435 (m), 940 (s), 842 (m), 795 (m), 696 (s); ¹H NMR (C₆D₆, 600 MHz) δ 7.57 – 7.52 (m, 4H, Ph *m*-H), 7.06 – 6.98 (m, 6H, Ph *o*- and *p*-H), 6.67 (s, 4H, Mes *m*-H), 6.63 (s, 4H, Mes *m*-H), 5.66 (s, 1H, Si-H), [2.32 (s, Mes *o*-CH₃), 2.31 (s, Mes *o*-CH₃) all together 24H], 2.07 (br s, 12H, Mes *p*-CH₃); ¹³C{¹H} NMR (C₆D₆, 151 MHz) δ 145.41 (Mes *o*-C), 144.19 (Mes *o*-C), 143.94 (d, *J* = 24 Hz, Ph *i*-C), 139.19 (Mes *p*-C), 138.56 (Mes *p*-C), 135.06 (Mes *i*-C), 131.73 (d, *J* = 25 Hz, Ph *o*-CH), 131.49 (Mes *i*-C), 129.71 (Mes *m*-CH), 129.22 (Ph *p*-CH), 128.86 (Mes *m*-CH), 128.1 (Ph *m*-CH)^a, 25.14 (Mes *o*-CH₃), 25.12 (Mes *o*-CH₃), 25.06 (br s, Mes *o*-CH₃), 21.05 (Mes *p*-CH₃), 20.99 (Mes *p*-CH₃); ²⁹Si (C₆D₆)

^a Chemical shift extracted from ¹³C-¹H gHMBC spectrum.

δ -1.8 (Si-O), -56.4 (Si-H); $^{31}\text{P}\{^1\text{H}\}$ (C_6D_6 , 243 MHz) δ 107.2; ESI-MS for $[\text{C}_{48}\text{H}_{55}\text{Si}_2\text{OP} + \text{H}^+]$ calcd: 735.3607, found: 735.3604.

2.6.3 Addition of Diphenylphosphine Oxide to Tetramesityldigermene **5**


 Diphenylphosphine oxide (28 g, 0.14 mmol) was added to a yellow solution of tetramesityldigermene **5** (85 mg, 0.14 mmol) dissolved in benzene (5 mL), at room temperature. The colour of the solution changed to light yellow after 5 minutes. The benzene was evaporated to give a light yellow oil. The oil was dissolved in a minimal amount of hexanes and stored in the freezer (-20 °C) for 24 hours. A white precipitate formed and the solid was isolated by decantation (72 mg, 54 % contaminated with 9% $\text{Ph}_2\text{P}(\text{O})\text{H}$). mp: 196 – 200 °C; FTIR (thin film, cm^{-1}) 2918 (m), 2024 (m, Ge-H), 1601 (m), 1556 (m), 1436 (s), 1290 (w), 1186 (s), 1122 (m), 1026 (m), 953 (m), 846 (s), 737 (s), 693 (s); ^1H NMR (C_6D_6 , 600 MHz) δ 7.65 – 7.63 (m, 4H, Ph *o*-H), 7.09 – 7.06 (m, 4H, Ph *m*-H), 7.01 – 6.99 (m, 2H, Ph *p*-H), 6.68 (s, 4H, Mes *m*-H), 6.63 (s, 4H, Mes *m*-H), 5.98 (s, 1H, Ge-H), [2.332 (s, Mes *o*-CH₃), 2.327 (s, Mes *o*-CH₃) all together 24H], [2.07 (s, Mes *p*-CH₃), 2.06 (s, Mes *p*-CH₃) all together 12H]; $^{13}\text{C}\{^1\text{H}\}$ NMR (C_6D_6 , 151 MHz) δ 147.06 (d, $J = 25$ Hz, Ph *i*-C)^b, 144.02 (Mes *o*-C), 143.18 (Mes *o*-C), 139.07 (Mes *p*-C), 138.43 (d, $J = 2.2$ Hz, Mes *i*-C), 138.31 (Mes *p*-C), 135.01 (Mes *i*-C), 130.90 (d, $J = 24$ Hz, Ph *o*-CH)^a, 129.67 (Mes *m*-CH), 128.96 (Mes, *m*-CH), 128.63 (Ph *p*-CH), 128.29 (Ph *m*-CH), 25.22 (d, $J = 2.6$ Hz, Mes *o*-CH₃), 24.59 (d, $J = 1.8$ Hz, Mes *o*-CH₃), 20.97 (Mes *p*-CH₃), 20.95 (Mes *p*-CH₃); $^{31}\text{P}\{^1\text{H}\}$ NMR (C_6D_6 , 243 MHz) δ 104.8; ESI-MS for $[\text{C}_{48}\text{H}_{55}\text{OP}^{70}\text{Ge}_2 + \text{Na}^+]$ calcd: 841.2373, found: 841.2398.

2.6.4 Addition of Dipentylphosphine Oxide to Tetramesityldisilene **4**

Dipentylphosphine oxide (15 mg, 0.079 mmol) was added to a yellow solution of tetramesityldisilene (42 mg, 0.079 mmol) dissolved in C_6D_6 (4 mL). The colour of the solution faded to light yellow after 1 minute of stirring at room temperature. The C_6D_6 was removed under vacuum, yielding **31** as a light yellow oil (35 mg, 61%), which was contaminated with compound **40**, formed from the oxidation of the Si-H bond (16%)^c and dipentylphosphine (20%)^d. Attempts

^b Similar magnitude for J found in $\text{PhCH}_2\text{P}(\text{Ph})_2$.²⁶

^c Tentatively assigned by ^{31}P chemical shift.

^d Assigned on the basis of ^{31}P chemical shift reported in the literature.²⁷

at purification by preparative TLC (silica gel; 30: 70 DCM to hexanes) resulted in the isolation of **37** and Mes₂HSiSiOHMes₂.⁴ Since purification of **31** was difficult, the characterization of the compound was performed on the crude reaction mixture.

$$\begin{array}{c} \text{Mes}_2\text{Si}-\text{SiMes}_2 \\ | \quad | \\ \text{pentyl}-\text{P}-\text{O}-\text{H} \\ | \\ \text{pentyl} \end{array}$$
31: ¹H NMR (C₆D₆, 600 MHz) δ 6.75 (s, 4H, Mes *m*-H), 6.66 (s, 4H, Mes *m*-H), 5.64 (s, 1H, Si-H), 2.46 (br s, Mes *o*-CH₃), 2.38 (s, 12H, Mes *o*-CH₃), 2.11 (s, 6H, Mes *p*-CH₃), 2.09 (br s, Mes *p*-CH₃), 1.73 – 1.56 (m, P-CH₂), 1.44 – 1.31 (m, P-CH₂CH₂), 1.30 – 1.20 (m, CH₂CH₂CH₃), 0.88 (t, *J* = 7.0 Hz, 6H, CH₃); ¹³C{¹H} NMR (C₆D₆, 151 MHz) δ 145.47 (Mes *o*-C), 144.09 (Mes *o*-C), 139.10 (Mes *p*-C), 138.64 (Mes *p*-C), 135.58 (Mes *i*-C), 131.71 (Mes *i*-C), 129.73 (Mes *m*-CH), 128.98 (Mes *m*-CH), 35.58 (d, *J* = 25 Hz, P-CH₂), 34.06 (d, *J* = 12 Hz, CH₂CH₂CH₃), 25.22 (br, Mes *o*-CH₃), 25.01 (Mes *o*-CH₃), 24.29 (d, *J* = 15 Hz, P-CH₂CH₂), 22.84 (CH₂CH₃), 21.14 (Mes *p*-CH₃), 21.04 (Mes *p*-CH₃), 14.27 (CH₃); ²⁹Si (C₆D₆) δ -5.6 (Si-O), -54.8 (Si-H); ³¹P{¹H} (C₆D₆, 162 MHz) δ 130.6. Satisfactory ESI-MS high resolution data could not be obtained likely due to a contaminant with the same *m/z* as **31**.

$$\begin{array}{c} \text{Mes}_2\text{Si}-\text{SiMes}_2 \\ | \quad | \\ \text{O}=\text{P}-\text{O}-\text{H} \\ | \quad | \\ \text{pentyl} \quad \text{pentyl} \end{array}$$
37: ¹H NMR (C₆D₆, 400 MHz) δ 6.73 (s, 4H, Mes *m*-H), 6.66 (s, 4H, Mes *m*-H), 5.66 (d, *J* = 1.8 Hz) 1H, Si-H), 2.42, 2.41 [(br s and s, 24 H all together, Mes *o*-CH₃)], 2.10 (s, 6H, Mes *p*-CH₃), 2.06 (s, 6H, Mes *p*-CH₃), 1.61 – 1.49 (m, P-CH₂CH₂)^e, 1.42 – 1.26 (m, P-CH₂CH₂)^e, 1.22 – 1.07 (m, CH₂CH₂CH₃)^e, 0.84 (t, *J* = 6.9 Hz, 6H, CH₃); ²⁹Si (C₆D₆) δ -5.2 (Si-O), -55.6 (Si-H); ³¹P{¹H} (C₆D₆, 162 MHz) δ 44.7; ESI-MS for [C₄₆H₆₇Si₂O₂P + Na⁺] calcd: 761.4315, found: 761.4326.

2.6.5 Addition of Dipentylphosphine Oxide to Tetramesityldigermene **5**

$$\begin{array}{c} \text{Mes}_2\text{Ge}-\text{GeMes}_2 \\ | \quad | \\ \text{pentyl}-\text{P}-\text{O}-\text{H} \\ | \\ \text{pentyl} \end{array}$$
 Dipentylphosphine oxide (31 mg, 0.16 mmol) was added to a yellow solution of tetramesityldigermene (0.10 g, 0.16 mmol) dissolved in benzene (3 mL), and the reaction was allowed to stir at room temperature. The colour of the solution changed to light yellow after 5 min. The benzene was evaporated under vacuum, yielding **32** as a light yellow oil (0.12 g, 94%), likely contaminated by the compound formed upon oxidation of the P(III) centre (5%). Attempts to purify **32** by preparative TLC or micropipette

^e Tentatively assigned on the basis of chemical shifts.

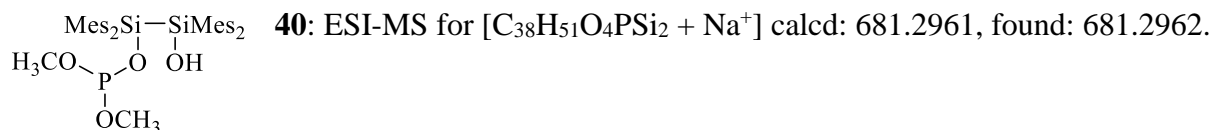
columns under inert conditions resulted in hydrolysis of the Ge centre with the P(III) moiety to give Mes₂HGeGeOHMes₂.²⁸ Since purification was difficult, **32** was characterized from the crude reaction mixture. ¹H NMR (C₆D₆, 600 MHz) δ 6.75 (s, 4H, Mes *m*-H), 6.67 (s, 4H, Mes *m*-H), 5.93 (s, 1H, Ge-H), 2.47 (s, 12H, Mes *o*-CH₃), 2.41 (s, 12H, Mes *o*-CH₃), 2.10 (s, 6H, Mes *p*-CH₃), 2.07 (s, 6H, Mes *p*-CH₃), 1.63 (t, *J* = 7.9 Hz, 4H, P-CH₂), 1.47 – 1.37 (m, P-CH₂CH₂)^f, 1.34 – 1.23 (m, CH₂CH₂CH₃)^a, 0.88 (t, *J* = 7.1 Hz, 6H, CH₃); ¹³C{¹H} NMR (C₆D₆, 151 MHz) δ 144.17 (Mes *o*-C), 143.11 (Mes *o*-C), 138.99 (Mes *p*-C), 138.81 (Mes *i*-C), 138.32 (Mes *p*-C), 135.19 (Mes *i*-C), 129.67 (Mes *m*-CH), 129.04 (Mes *m*-CH), 36.31 (d, *J* = 25 Hz, P-CH₂), 34.29 (d, *J* = 10 Hz, CH₂CH₂CH₃), 25.30 (Mes *o*-CH₃), 24.62 (d, *J* = 5.6 Hz, Mes *o*-CH₃), 24.22 (d, *J* = 16 Hz, P-CH₂CH₂), 22.94 (CH₂CH₃), 21.05 (Mes *p*-CH₃), 21.00 (Mes *p*-CH₃), 14.33 (CH₃); ³¹P{¹H} NMR (C₆D₆, 162 MHz) δ 129.0; ESI-MS for [C₄₆H₆₇OP⁷⁰Ge₂ + Na⁺] calcd: 829.3312, found: 829.3306.

2.6.6 Addition of Dimethyl Phosphite to Tetramesityldisilene **4**

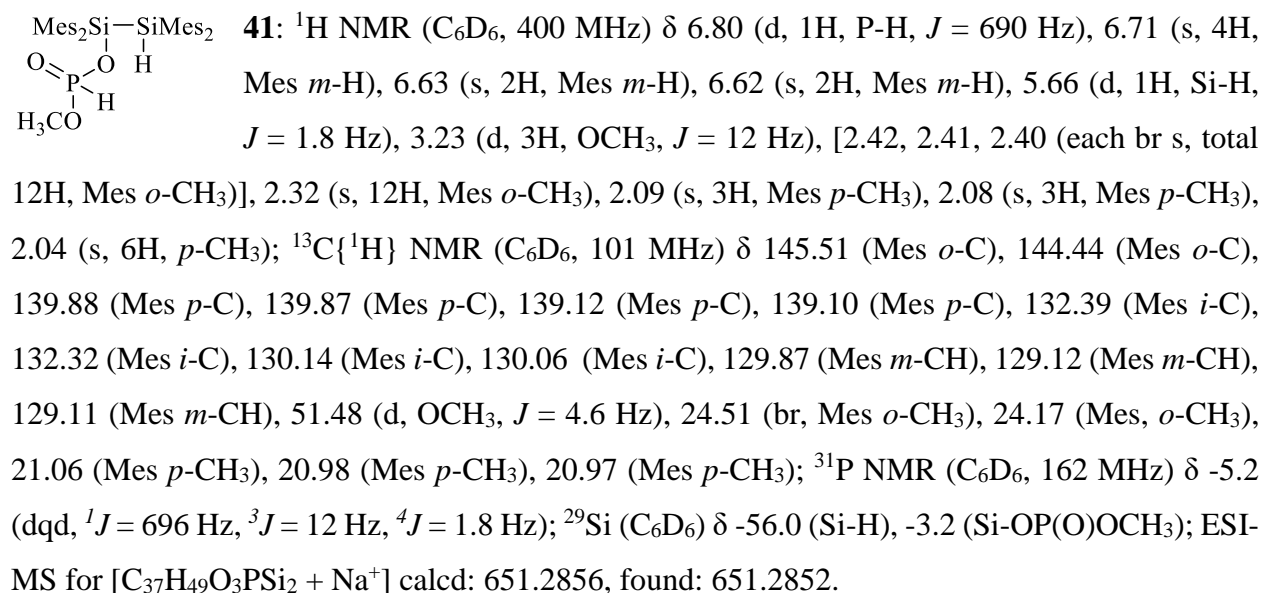
Dimethyl phosphite (0.011 mL, 0.12 mmol) was added to a yellow solution of tetramesityldisilene **4** (66 mg, 0.12 mmol) dissolved in benzene (5 mL) and the solution was allowed to stir at room temperature. After 18 hours, the colour of the solution changed from yellow to pale yellow. The benzene was evaporated under vacuum to give a pale yellow oil which was re-dissolved in a minimal amount of hexanes. The vial was stored in the freezer (-20 °C) for 7 days. Clear, colourless crystals of **35** and **40** (36 mg, 19:1) were isolated.

$$\begin{array}{c}
 \text{Mes}_2\text{Si} - \text{SiMes}_2 \\
 | \quad | \\
 \text{H}_3\text{CO} - \text{P} - \text{O} - \text{H} \\
 | \\
 \text{OCH}_3
 \end{array}$$
35: mp: 168 – 172 °C; ATR-FTIR (solid, cm⁻¹) 2916 (m), 2147 (m, Si-H), 1603 (m), 1445 (m), 1011 (s), 940 (m), 847 (s), 733 (s); ¹H NMR (C₆D₆, 400 MHz) δ 6.73 (s, 4H, Mes *m*-H), 6.67 (s, 4H, Mes *m*-H), 5.67 (s, 1H, Si-H), 3.20 (d, 6H, OCH₃, *J* = 11 Hz), 2.46 (br s, 12H, Mes *o*-CH₃), 2.37 (s, 12H, Mes *o*-CH₃), 2.10 (s, 6H, Mes *p*-CH₃), 2.06 (s, 6H, Mes *p*-CH₃); ¹³C{¹H} NMR (C₆D₆, 101 MHz) δ 145.56 (Mes *o*-C), 144.31 (Mes *o*-C), 139.26 (Mes *p*-C), 138.74 (Mes *p*-C), 134.32 (Mes *i*-C), 131.20 (Mes *i*-C), 129.73 (Mes *m*-CH), 128.97 (Mes *m*-CH), 48.34 (d, OCH₃, *J* = 4.9 Hz), 24.80 (br, Mes *o*-CH₃), 24.53 (d, Mes, *o*-CH₃, *J* = 3.3 Hz), 21.08 (Mes *p*-CH₃), 21.00 (Mes, *p*-CH₃); ³¹P{¹H} NMR (C₆D₆, 162 MHz) δ 132.8; ²⁹Si (C₆D₆) δ -55.3 (Si-H), -7.3 (Si-OP(OCH₃)₂); ESI-MS for [C₃₈H₅₁O₃PSi₂ + Na⁺] calcd: 665.3012, found: 665.3006.

^f Chemical shifts extracted from ¹³C-¹H gHSQC spectrum.



The reaction was repeated and the crude yellow oil was dissolved in a minimal amount of dichloromethane (DCM) and purified by preparative TLC. The mixture was separated into two bands using an 80: 20 DCM to hexanes solvent ratio. Compound **41** (4.5 mg, 6%) was isolated as a pale yellow oil from the band closest to the baseline and is contaminated with a compound tentatively identified as $(\text{Mes}_2\text{SiH})_2\text{O}$ (10%).

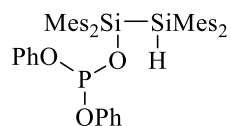


$(\text{Mes}_2\text{SiH})_2\text{O}$ was isolated cleanly from the second band in the TLC plate, directly above **41**, and was tentatively assigned by ^1H NMR spectroscopy and mass spectrometry. ^1H NMR (C_6D_6 , 400 MHz) δ 6.70 (s, 8H, Mes *m*-H), 6.11 (s, 2H, Si-H), 2.41 (s, 24H, Mes *o*-CH₃), 2.09 (s, 12H, Mes *p*-CH₃); ESI-MS m/z 550.3.

2.6.7 Direct Hydrolysis of **35**

Degassed water (4 mL, 0.17 mmol) was added to the yellow solid **35** (58 mg, 0.090 mmol), and the reaction stirred at room temperature. The colour of the solid changed from yellow to white after 18 hours. The water was removed under vacuum to yield a white solid consisting of a mixture of **35** and **41** (57 mg, 1:5).

2.6.8 Addition of Diphenyl Phosphite to Tetramesityldisilene **4**



Diphenyl phosphite (0.023 mL, 0.12 mmol) was added to a yellow solution of tetramesityldisilene **4** (66 mg, 0.12 mmol) dissolved in benzene (5 mL), and the reaction was allowed to stir at room temperature. The colour of the solution changed to light yellow after 18 hours. The benzene was removed under vacuum, yielding a light yellow oil. The oil was redissolved in a minimal amount of DCM and purified by preparative TLC (silica gel; 20:80 DCM to hexanes) Compound **36** was extracted as a colourless oil from the band of silica closest to the baseline. The oil was redissolved in a minimal amount of hexanes and stored in the freezer for 7 days (-8 °C). A white solid consisting of **36** (42 mg, 46%) with contaminants including P(OPh)₃^g, **42**, **43** and **44**^h present in a 100: 12: 1: 1: 1 ratio relative to **36**, was isolated. mp: decomposes at 60 °C; ATR-FTIR (solid, cm⁻¹) 2919 (m), 2129 (m, Si-H), 1594 (m), 1489 (m), 1200 (m), 995 (m), 851 (s), 763 (m), 690 (m); ¹H NMR (C₆D₆, 600 MHz) δ 6.94 – 6.98 (m, 4H, Ph *m*-CH), 6.88 – 6.91 (m, 4H, Ph *o*-CH), 6.78 – 6.82 (m, 2H, Ph *p*-CH), 6.70 (s, 4H, Mes *m*-CH), 6.64 (s, 4H, Mes *m*-CH), 5.72 (s, 1H, Si-H), 2.50 (br s, 12H, Mes *o*-CH₃), 2.40 (s, 12H, Mes *o*-CH₃), 2.08 (s, 6H, Mes *p*-CH₃), 2.06 (s, 6H, Mes *p*-CH₃); ¹³C{¹H} NMR (C₆D₆, 151 MHz) δ 152.85 (d, Ph *i*-C, *J* = 8.1 Hz), 145.64 (Mes *o*-C), 144.33 (Mes *o*-C), 139.47 (Mes *p*-C), 138.86 (Mes *p*-C), 133.90 (Mes *i*-C), 130.74 (Mes *i*-C), 129.86 (Mes *m*-CH), 129.72 (Ph *m*-CH), 129.03 (Mes *m*-CH), 123.61 (Ph *p*-CH), 120.85 (d, Ph *o*-CH, *J* = 9.0 Hz), 24.83 (br, Mes *o*-CH₃), 24.63 (d, Mes *o*-CH₃, *J* = 3.6 Hz), 21.08 (Mes *p*-CH₃), 20.99 (Mes *p*-CH₃); ²⁹Si (C₆D₆) δ -55.7 (Si-H), -5.9 (Si-OP(OPh)₂); ³¹P{¹H} NMR (C₆D₆, 243 Hz) δ 133.3; ESI-MS for [C₄₈H₅₅O₃PSi₂ + Na⁺] calcd: 789.3325, found: 789.3328.

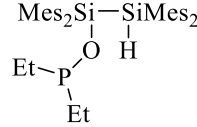
2.6.9 Addition of Diethylphosphinic Acid to Tetramesityldisilene **4**

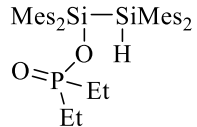
Diethylphosphinic acid (15 mg, 0.12 mmol) was added to a yellow solution of **4** (66 mg, 0.12 mmol) dissolved in benzene (5 mL) and the solution was allowed to stir at room temperature. After 10 minutes, the colour of the solution changed to pale yellow. The benzene was evaporated under vacuum, yielding a light yellow oil which was redissolved in a minimal amount of hexanes. The vial was stored in the freezer (-20 °C) for 24 hours, yielding a mixture of **33** and **34** as an off-

^g P(OPh)₃ is a contaminant in diphenyl phosphite and was characterized by ¹H, ³¹P{¹H}, ¹³C{¹H} NMR spectroscopy.²⁹

^h Compounds **42**, **43**, and **44** are tentatively assigned by ³¹P{¹H} and ³¹P NMR spectroscopy and ESI-MS.

white solid. The solid was dissolved in a minimal amount of DCM and the compounds were separated by preparative TLC (silica gel; 50:50 DCM to hexanes). Compound **34** (3.8 mg, 39%) was isolated as a clear, colourless oil from the silica and recrystallized in a minimal amount of benzene to yield clear, colourless crystals. In a separate band, Mes₂HSiSi(OH)Mes₂ (4.2 mg, 43%) was isolated.⁴


33: ¹H and ²⁹Si chemical shifts are not listed because the signals for the product overlapped with those assigned to **34** in the NMR spectra of the mixture, and thus, were not easily distinguished. ³¹P{¹H} NMR (C₆D₆, 162 MHz) δ 135.4; ESI-MS for [C₄₀H₅₅OPSi₂ + H⁺] calcd: 639.3607, found: 639.3612.


34: ¹H NMR (C₆D₆, 400 MHz) δ 6.71 (s, 4H, Mes *m*-CH), 6.63 (s, 4H, Mes *m*-CH), 5.64 (d, 1H, Si-H, *J* = 1.9 Hz), 2.38, (s, 12H, Mes *o*-CH₃), 2.37 (br s, 12H, Mes *o*-CH₃), 2.10 (s, 6H, Mes *p*-CH₃), 2.04 (s, 6H, Mes *p*-CH₃), 1.39 – 1.54 (m, 4H, CH₂CH₃), 0.96 (dt, 6H, CH₂CH₃, *J* = 7.6 Hz, 18 Hz); ¹³C{¹H} NMR (C₆D₆, 101 MHz) δ 145.21 (Mes *o*-C), 144.49 (Mes *o*-C), 139.71 (Mes *p*-C), 138.92 (Mes *p*-C), 133.59 (Mes *i*-C), 130.99 (Mes *i*-C), 129.84 (Mes *m*-CH), 128.97 (Mes *m*-CH), 24.80 (Mes *o*-CH₃), 23.36 (d, CH₂CH₃, *J* = 94 Hz), 21.07 (Mes *p*-CH₃), 20.97 (Mes *p*-CH₃), 7.04 (d, CH₂CH₃, *J* = 5.0 Hz); ³¹P{¹H} NMR (C₆D₆, 162 MHz) δ 47.6; ²⁹Si (C₆D₆) δ -55 (Si-H), -5 (Si-OP(CH₂CH₃)₂); ESI-MS for [C₄₀H₅₅O₂PSi₂ + Na⁺] calcd: 677.3376, found: 677.3402.

2.7 References

1. Cottrell, T. *The Strengths of Chemical Bonds*, 2nd ed.; Butterworths Sci. Pubs.: London, 1958.
2. For the chemical shifts of diethylphosphinic acid: a) Aksnes, G.; Majewski, P. *Phosphorus and Sulfur* **1968**, 26, 261.; For the chemical shifts of diethylphosphine oxide: b) Zhang, W.; Ye, G.; Chen, J. *J. Mater. Chem. A* **2013**, 1, 12706.
3. Hays, H. R. *J. Org. Chem.* **1968**, 33, 3690.
4. Fink, M. J.; DeYoung, D. J.; West, R. *J. Am. Chem. Soc.* **1983**, 105, 1070.
5. Maryasin, B.; Zipse, H. *Phys. Chem. Chem. Phys.* **2011**, 13, 5150.
6. Tashkandi, N. Y. Cycloaddition Reactions of (Di)tetrelenes. Ph. D. Dissertation, The University of Western Ontario, London, ON, **2016**.
7. a) Hussein, S.; Priester, D.; Beet, P.; Cottom, J.; Hart, S. J.; James, T.; Thatcher R.; Whitwood, A. C.; Slattery, J. M. *Chem. Eur. J.* **2019**, 25, 2262; b) Tashkandi, N.; Bourque, J. L.; Baines, K. M. *Dalton Trans.* **2017**, 46, 15451; c) van der Vlugt, J. I.; Akerstaff, J.; Dijkstra, T. W.; Mills, A. M.; Kooijman, H.; Spek, A. L.; Meetsma, A.; Abbenhuis, H. C. L.; Vogt, D. *Adv. Synth. Catal.* **2014**, 346, 399; d) Meltzer, A.; Majumdar, M.; White, A. J. P.; Huch, V.; Scheschkewitz, D. *Organometallics* **2013**, 32, 6844; e) Rupert, B. L.; Tiedemann, B. E. F.; Vespremi, S. M. *Acta. Crystallogr., Sect. E.* **2003**, 59, o934; f) Dehnert, U.; Schär, D.; Rhode, B.; Müller, P.; Usón, I. *J. Organomet. Chem.* **2002**, 649, 25.; g) Greene, N.; Taylor, H.; Kee, T. P.; Thornton-Pett, M. *J. Chem. Soc., Dalton Trans.* **1993**, 821.
8. Stuart, B. Infrared Spectroscopy: Fundamentals and Applications. In *Analytical Techniques in the Sciences*; Ando, D. J., Ed.; Wiley: New York, 2004; p 85.
9. Pavia, D. L.; Lampman, G. M.; Kriz, G. S.; Vyvyan, J. R. Introduction to Spectroscopy, 5th ed.; Cengage Learning: Connecticut, 2015; p 349.
10. McIntyre, S. K.; Alam, T. M. *Magn. Reson. Chem.* **2007**, 45, 1022.
11. Stewart, B.; Harriman, A.; Higham, L. J. *Organometallics* **2011**, 30, 5338.

12. Kovacs, T.; Keglevich, G. *Curr. Org. Chem.* **2017**, *21*, 569.
13. Coumbe, T.; Lawrence, N. J.; Muhammad, F. *Tetrahedron Lett.* **1994**, *35*, 625.
14. Chardon, A.; Maubert, O.; Rouden, J.; Blanchet, J. *ChemCatChem* **2017**, *9*, 4460.
15. Evans, D. A.; Hurst, K. M. Takacs, M. *J. Am. Chem. Soc.* **1978**, *100*, 3467.
16. Issleib, K.; Walther, B. *Angew. Chem. Int. Ed.* **1967**, *6*, 88.
17. Novikova, Z. S.; Mashoshina, S. N.; Lutsenko, I. F. *Russ. J. Gen. Chem.* **1975**, *45*, 1486.
18. Hirai, T.; Han, L. *Org. Lett.* **2007**, *9*, 54.
19. Tayama, O.; Nakano, A.; Iwahama, T.; Sakaguchi, S.; Ishii, Y. *J. Org. Chem.* **2004**, *69*, 5494.
20. Ortial, S.; Fisher, H. C.; Montchamp, J. L. *J. Org. Chem.* **2013**, *78*, 6599.
21. Nie, S. Z.; Davison, R. T.; Dong, V. M. *J. Am. Chem. Soc.* **2018**, *140*, 16450.
22. Tashkandi, N. Y.; Parsons, F.; Guo, J.; Baines, K. M. *Angew. Chem. Int. Ed.* **2015**, *54*, 1612.
23. Tashkandi, N. Y.; Bourque, J. L.; Baines, K. M. *Dalton Trans.* **2017**, *46*, 15451.
24. Cowley, M. J.; Ohmori, Y.; Huch, V.; Ichinohe, M.; Sekiguchi, A.; Scheschkewitz, D. *Angew. Chem. Int. Ed.* **2013**, *52*, 13247.
25. Wendel, D.; Szilvási, T.; Henschel, D.; Altmann, P. J.; Jandl, C.; Inoue S.; Rieger. B. *Angew. Chem. Int. Ed.* **2018**, *57*, 14575.
26. Kühl, O. *Phosphorus-31 NMR Spectroscopy: A Concise Introduction for the Synthetic and Organometallic Chemist*; Springer: Berlin, 2008; p 19.
27. Baccolini, G.; Boga, C.; Mazzacurati, M.; Sangirardi, F. *Org. Lett.* **2006**, *8*, 1677.
28. Baines, K. M.; Cooke, J. A.; Dixon, C. E.; Lui, H. W.; Netherton, M. R. *Organometallics* **1994**, *13*, 631.
29. Bodner, G. M.; Gaul, M. *J Organomet. Chem.* **1975**, *101*, 63.

Chapter 3

3 Mechanistic Studies and Competition Experiments

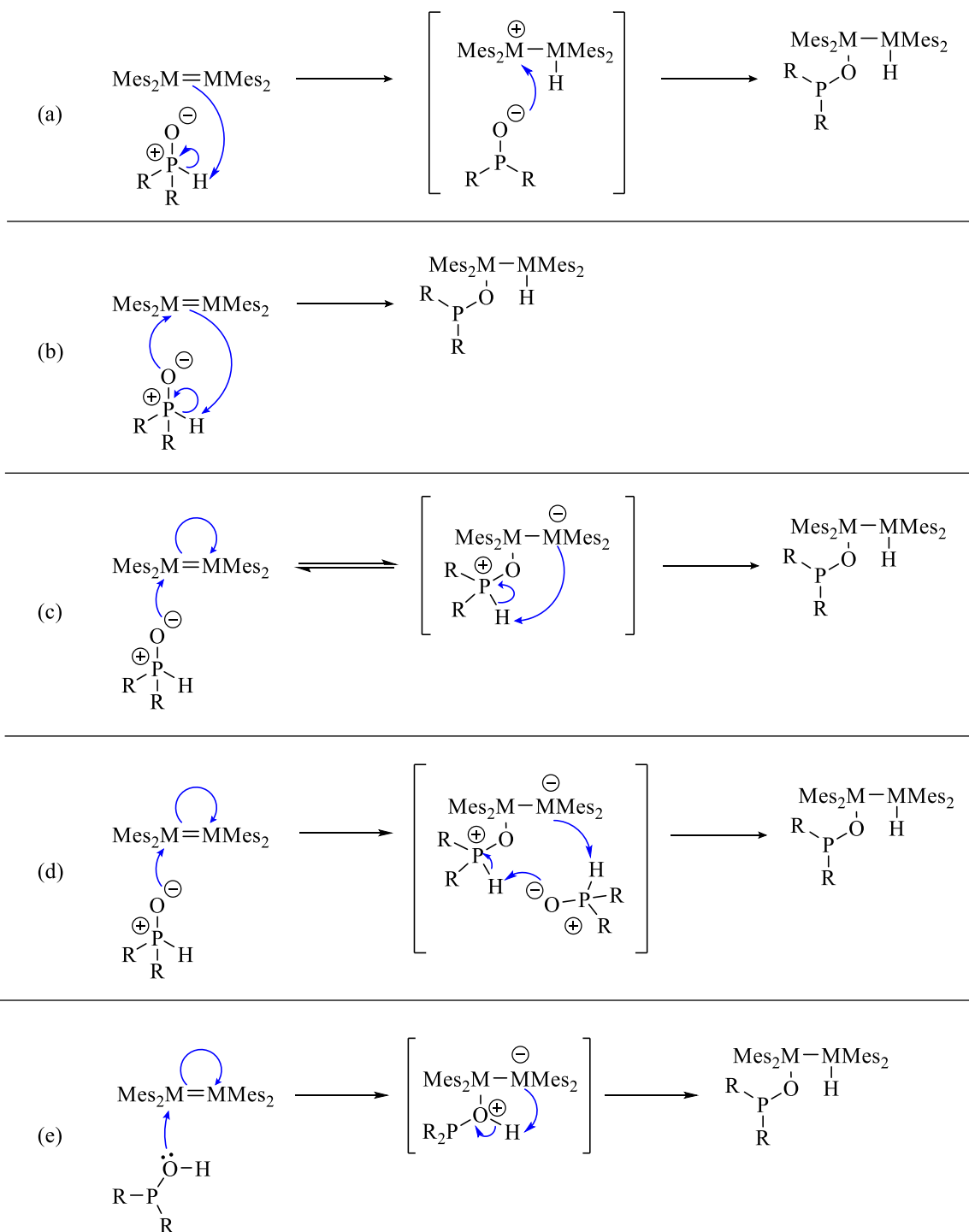
3.1 Introduction

In this chapter, the mechanism for the addition of organophosphorus oxides to ditetrelenes **4** and **5** will be discussed. Five plausible mechanisms can be envisioned for the reaction (Scheme 35). Stepwise electrophilic addition, which is common in alkene chemistry, would involve abstraction of a proton from the secondary phosphine oxide or phosphite, followed by addition of the conjugate base to the disilyl or digermyl cation to give disilyl and digermyl phosphinites or phosphites (Scheme 35a). Another option is a concerted addition where the abstraction of the proton from the organophosphorus oxide and nucleophilic addition of the oxygen in the phosphine oxide or phosphite towards the M centre occurs in one step (Scheme 35b). A stepwise nucleophilic addition mechanism should also be considered. In this pathway, the nucleophilic addition of the oxygen in the phosphine oxide or phosphite towards the M centre generates a disilyl or digermyl anion which undergoes intramolecular proton abstraction to form the disilyl or digermyl phosphinites and phosphites (Scheme 35c). An intermolecular proton abstraction between the disilyl or digermyl anion and another molecule of phosphine oxide or phosphite is also plausible following nucleophilic addition of the oxygen from the organophosphorus oxide (Scheme 35d). The last mechanism involves the addition of the phosphine oxide or phosphite tautomer (R_2P-OH) to **4** and **5** (Scheme 35e). The alcoholic oxygen attacks the M centre to generate the disilyl or digermyl anion intermediate, which undergoes intramolecular or intermolecular proton abstraction to form the product.

On the basis of previous mechanistic studies on the addition of water, alcohols and HCl to disilenes,^{1,2} the electrophilic addition mechanism was eliminated since phosphine oxides and phosphites are weak acids and ditetrelenes **4** and **5** are weak bases. The mechanism which involves addition through the organophosphorus oxide tautomer (R_2P-OH) was also eliminated since the oxygen of the P^+-O^- bond in the organophosphorus oxide is expected to be more nucleophilic than the hydroxyl oxygen of the tautomer and higher in concentration compared to the tautomer.

To distinguish between the concerted or stepwise nucleophilic addition mechanisms, deuterium labelling and kinetic isotope effect experiments were performed. In addition,

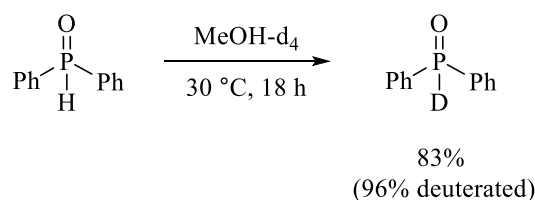
competition experiments between dialkyl and diarylphosphine oxides were investigated to determine which derivative reacts more readily with digermene **5**.



Scheme 35. Plausible reaction mechanisms for the addition of organophosphorus oxides to **4** and **5**.

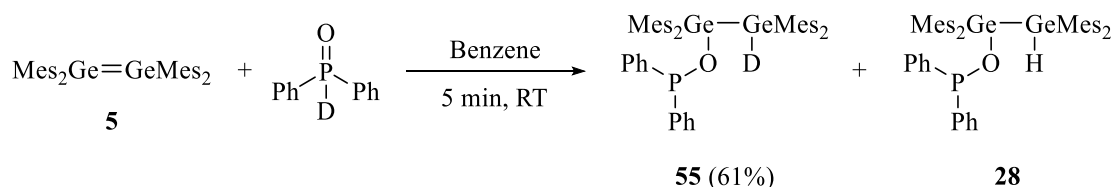
3.2 Deuterium Labelling Experiment

The addition of organophosphorus oxides to **4** or **5** is proposed to proceed through either a concerted or a stepwise nucleophilic addition mechanism. In both, the P-H bond is broken and a M-H bond is formed. To determine if the hydrogen of the phosphine oxide or phosphite is transferred to the ditetrelene, deuterated diphenylphosphine oxide was added to digermene **5**. Diphenylphosphine oxide-*d*₁ was synthesized by stirring diphenylphosphine oxide in excess MeOH-*d*₄ at 30 °C for 18 hours (Scheme 36).³



Scheme 36. The synthesis of diphenylphosphine oxide-*d*₁.

One equivalent of diphenylphosphine oxide-*d*₁ was added to a yellow solution of **5** dissolved in benzene and the reaction was allowed to stir at room temperature (Scheme 37). After 5 minutes, the colour of the solution faded from yellow to light yellow. Evaporation of benzene



Scheme 37. The addition of diphenylphosphine oxide-*d*₁ to **5**.

yielded a light yellow oil which was recrystallized from hexanes to give **55** as a white solid in 61% yield. The ¹H chemical shifts of **55** matched the chemical shifts observed in the ¹H NMR spectrum of the protonated analogue **28** within experimental error (± 0.01 ppm). A signal at 5.98 ppm in the ¹H NMR spectrum of **55** was observed and was assigned as the Ge-H from residual amounts of **28**. Since the signal at 5.98 ppm integrated to 0.08 relative to the signals assigned to the mesityl protons of **55**, 92% of **55** was deuterated in both the crude and recrystallized product. The level of deuterium incorporation in the phosphine oxide reagent and **55** are within experimental error. In the ²H NMR spectrum of **55**, only one signal appeared at 5.99 ppm, which was assigned to the

Ge-D moiety. The isolation of **55** confirms that the hydrogen attached to the P of the phosphine oxide is transferred exclusively to a Ge of the former digermene **5**, during the reaction.

3.3 Kinetic Isotope Effect

Kinetic isotope effect (KIE) experiments are a useful experimental technique to gain an understanding of which bonds are broken, formed or rehybridized in the rate determining step (rds) of a reaction. The KIE is a measurement of the change in the rate of the reaction when an atom is replaced with its isotope, the most common exchange being H/D. KIEs are expressed as a ratio of the rate constants of the reaction for the protonated and the deuterated analogues ($KIE = k_H/k_D$). If the value for $k_H/k_D \gg 1$, then a primary isotope effect is observed meaning the labelled atom is transferred in the rate determining step of the reaction. The maximum k_H/k_D value for a primary isotope effect is 6.5 – 7 at 298 K.⁴ In contrast, if the labelled atom is not transferred in the rds, a secondary isotope effect where $k_H/k_D \approx 1$ (normally 1.1–1.2, estimated theoretical maximum is 1.4) is observed.⁵

Diphenylphosphine oxide, and its deuterated analog were combined in a 1:1 ratio (0.05 M stock solution in C₆D₆ for each reagent). The phosphine oxide mixture was added to a 0.06 M solution of **5** dissolved in C₆D₆. The reaction was monitored by following the disappearance of the ³¹P chemical shifts for the deuterated and protonated phosphine oxide over time, since **28** and **55** have indistinguishable ³¹P chemical shifts.

Figure 14 shows the graph of the absolute integrals of the deuterated and non-deuterated phosphine oxides versus time. Even though the protonated phosphine oxide was present in a slightly higher concentration, both reagents are consumed at similar rates. After 20 minutes, the plot for both reagents plateaus, indicating the reaction has gone to completion. The KIE for the reaction was calculated according to Equation (1) which expresses the KIE ratio as the change in concentration over time of the protonated species over the deuterated species. To account for the higher concentration of the protonated phosphine oxide, the integrals at each time point for the protonated and deuterated species were subtracted from the integrals at t_0 .

$$KIE = \frac{k_H}{k_D} = \frac{\Delta[H]}{\Delta[D]} \approx \frac{Int_{H(t_0)} - Int_{H(t)}}{Int_{D(t_0)} - Int_{D(t)}} \quad (1)$$

From the integrals, the average k_H/k_D value over all time points was calculated to be 1.3, which is indicative of a secondary isotope effect. This result provides evidence against a concerted mechanism since the P-H/P-D bond is not broken in the rds. Therefore, the 1,3-addition of diorganophosphine oxides and phosphites to **4** and **5** is proposed to proceed through a stepwise nucleophilic addition mechanism, with the nucleophilic attack of the oxygen atom in the P^+-O^- bond at the M centre as the rds. However, the KIE results cannot distinguish whether the subsequent step involves an intramolecular or intermolecular abstraction of the hydrogen.

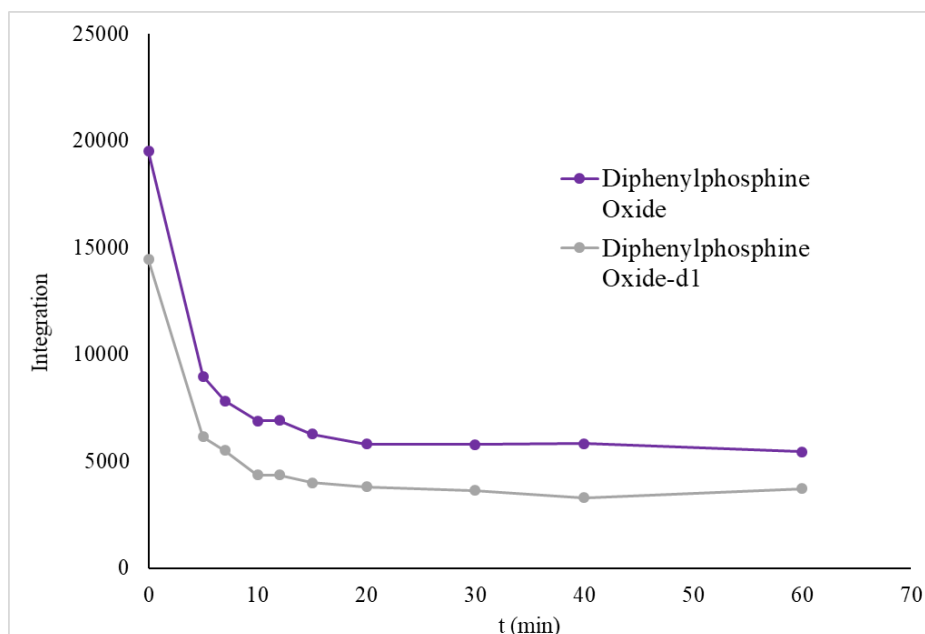
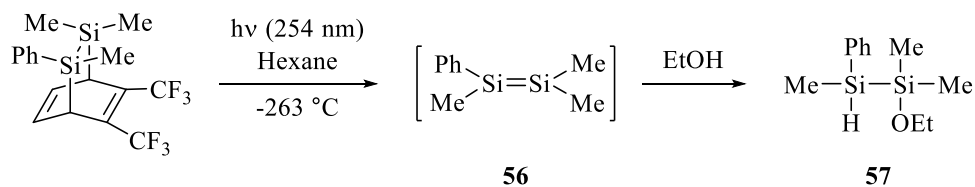


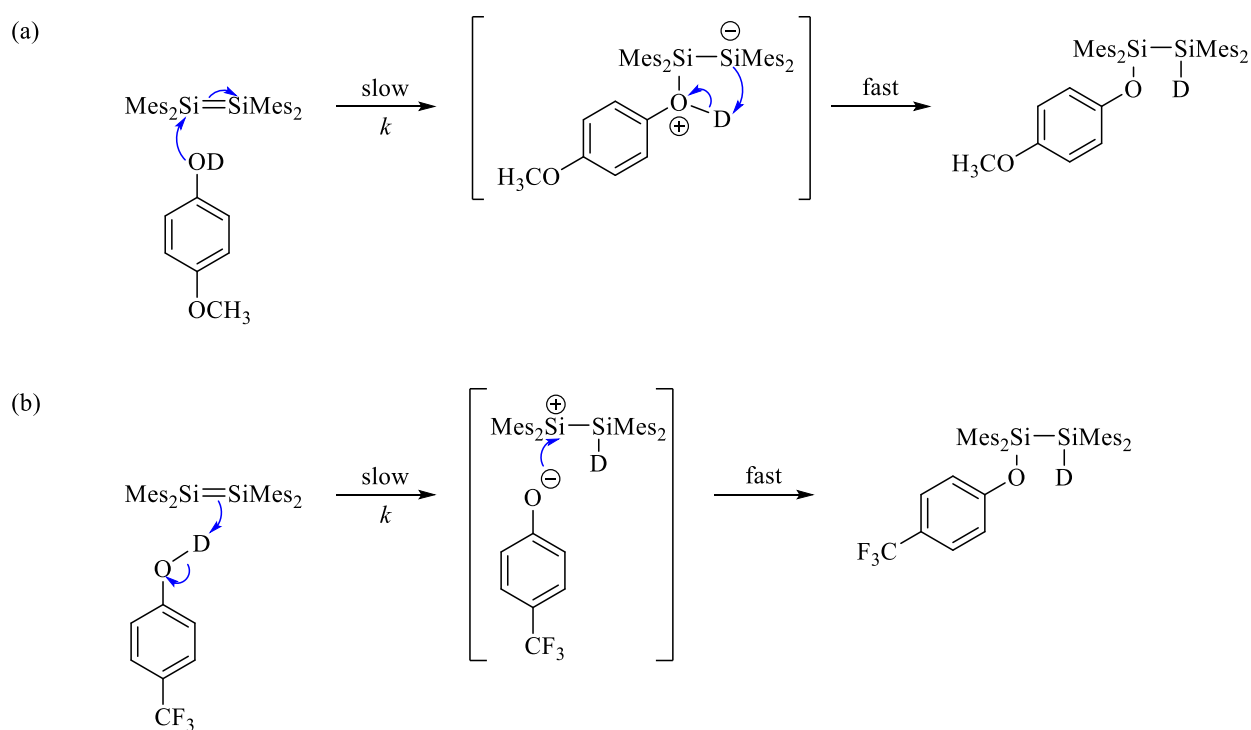
Figure 14. Consumption of protonated and deuterated diphenylphosphine oxide in the reaction with digermene **5**.

The addition of ethanol to disilene **56** to regioselectively form ethoxydisilane **57** was also proposed to take place by nucleophilic addition on the basis of KIE experiments (Scheme 38).⁶ When ethanol- d_1 was allowed to react with **56**, no significant isotope effect was observed, which suggests a concerted addition is not the rds.



Scheme 38. The addition of ethanol to transient disilene **56**.

The mechanism of the addition of phenol derivatives to disilene **4** was investigated by Apeloig *et al.* through KIE experiments.⁷ The authors observed a trend where electron-donating substituents on the phenol, resulted in k_H/k_D values close to 1. For example, the addition of deuterated 4-methoxyphenol to **4** had a k_H/k_D value of 0.71, which is consistent with the rate determining step involving nucleophilic attack of the alcoholic oxygen to the Si centre (Scheme 39a). In contrast, the addition of phenols containing electron-withdrawing substituents resulted in primary KIEs. The addition of deuterated 4-(trifluoromethyl)phenol to **4** resulted in a large KIE value of 5.27, indicating a primary KIE. The primary KIE strongly supports an electrophilic addition where the phenolic H or D is transferred to **4** in the rds which is rationalized by the increased acidity of the phenolic H (Scheme 39b).



Scheme 39. The (a) nucleophilic addition and (b) electrophilic addition of phenols to disilene **4**.

Since diphenylphosphine oxide is a weak acid (pK_a is approximately 25),⁸ an electrophilic addition to digermene **5** is not likely. The KIE results for the addition of diphenylphosphine oxide to **5** are consistent with the results from the addition of electron-donating substituted phenols to disilene **4**, which takes place through a stepwise nucleophilic addition. In both reactions, the nucleophilic addition by an oxygen atom to the M centre is involved in the rate determining step of the reaction.

3.4 Relative Rate Studies and Exchange Reactivity on the Addition of Phosphine Oxides to Tetramesityldigermene **5**

A competition experiment between dipentyl- and diphenylphosphine oxide was performed to determine the relative rates of reaction between the dialkyl and diarylphosphine oxide with digermene **5**. A 1:1 mixture of dipentylphosphine oxide and diphenylphosphine oxide was added to a yellow solution of **5** dissolved in C₆D₆. The colour of the solution faded to light yellow within 5 minutes after adding the phosphine oxide mixture. The reaction was monitored by ³¹P{¹H} NMR spectroscopy (Figure 15), which revealed the appearance of two new signals within 5 minutes at 104.5 and 129.0 ppm, assigned to **28** and **32**, respectively. At the 5 minute time point, **28** and **32** are present in a 3:1 relative ratio, indicating that diphenylphosphine oxide reacts with **5** more readily compared to dipentylphosphine oxide. The ¹H NMR spectrum of the reaction after 20 minutes confirms the reaction has gone to completion which was indicated by the disappearance of the signals for digermene **5** in the ¹H NMR spectrum of the reaction mixture. Interestingly, the relative ratio of **28** to **32** changes over time, which is noticeable at the 24 hour time point where the relative ratio of products is 7:1. The change in the relative ratio of products is not due to oxidation of **32** since no new signals appeared in the ³¹P{¹H} NMR spectrum. The increase of **28** and decrease of **32** over time suggests that the OP(pentyl)₂ group can be exchanged for a OPPh₂ group.

The faster rate for the addition of diphenylphosphine oxide to digermene **5** compared to the addition of dipentylphosphine oxide suggests the oxygen of the aryl substituted phosphine oxide is more nucleophilic than the alkyl substituted phosphine oxide. These conclusions were made based on the assumption that diphenyldigermyl phosphinite **28** is the kinetic product. However, it is possible that dipentyldigermyl phosphinite **32** could be the kinetic product and the exchange with the OPPh₂ group likely occurs because **28** is the thermodynamic product. The early stages of the reaction should be monitored to determine which phosphinite is the kinetic product.

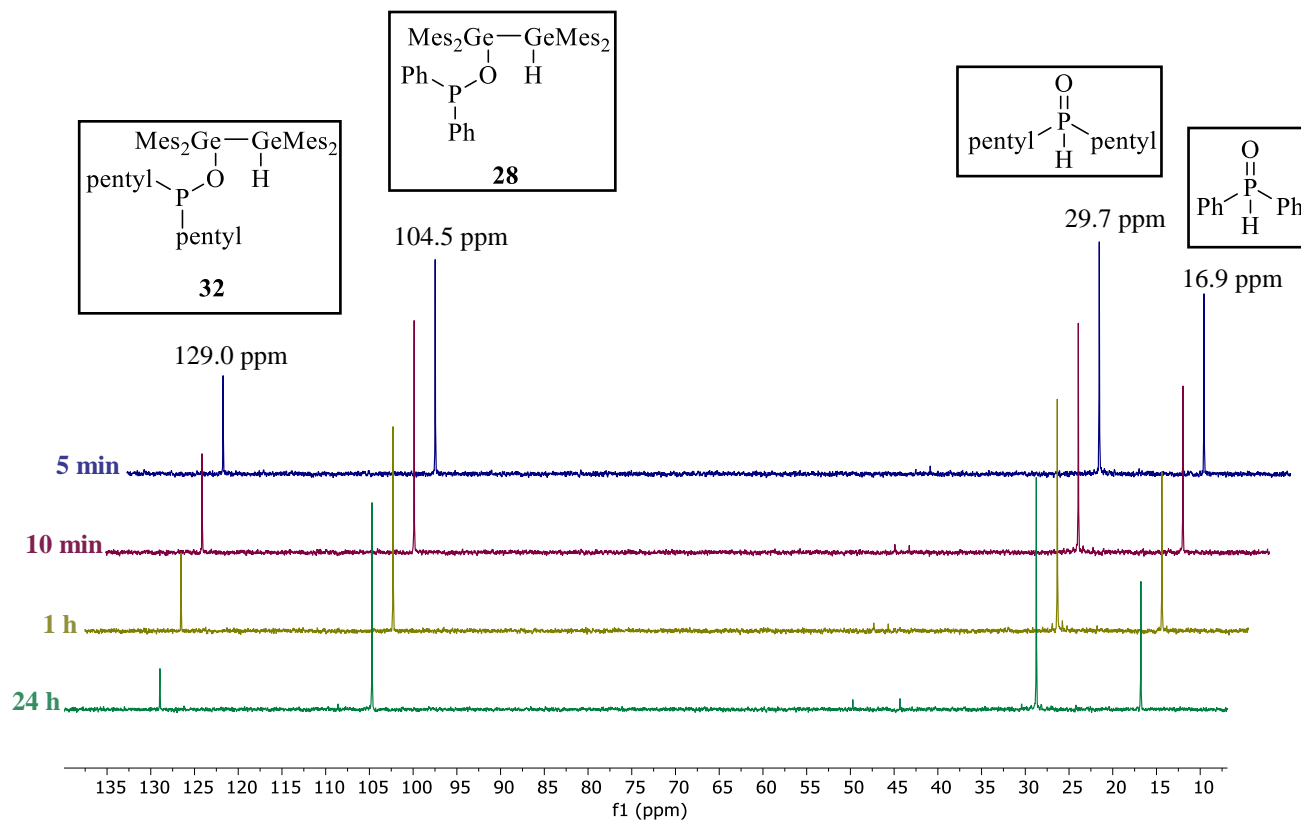


Figure 15. $^{31}\text{P}\{^1\text{H}\}$ NMR (C_6D_6 , 162 MHz) spectra of the competition reaction between dipentyl- and diphenylphosphine oxide with digermene **5**.

To probe the exchange between the $\text{OP}(\text{pentyl})_2$ moiety and the OPPh_2 group, excess diphenylphosphine oxide was added to a crude sample of dipentyldigermyl phosphinite **32**, and the reaction was monitored by $^{31}\text{P}\{^1\text{H}\}$ NMR spectroscopy using OPe_3 (^{31}P chemical shift = 46.1 ppm) as an internal standard inside a sealed capillary tube (Figure 16). Within the first 10 minutes of the reaction, the appearance of a signal at 104.7 ppm was observed and assigned to diphenyldigermyl phosphinite **28**. The appearance of another signal at 29.2 ppm is indicative of the regeneration of dipentylphosphine oxide, which is in line with the disappearance of the signal at 128.9 ppm, assigned to dipentyldigermyl phosphinite **32**. The reaction occurs quite rapidly under mild conditions, as evident at the 1 hour time point, where the signal for **32** has almost disappeared. The reverse reaction, where excess dipentylphosphine oxide was added to diphenyldigermyl phosphinite **28**, was also monitored by $^{31}\text{P}\{^1\text{H}\}$ NMR spectroscopy; however, appearance of a signal at 128.9 ppm was not observed after 24 hours, indicating no reaction occurred.

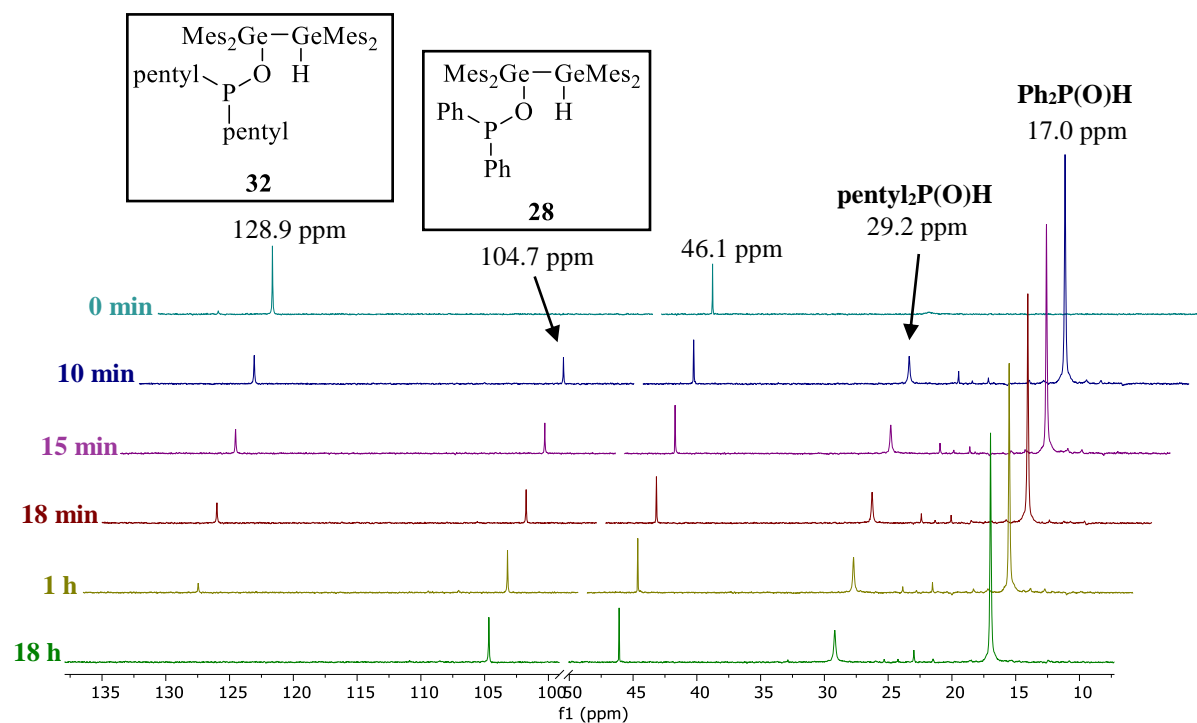
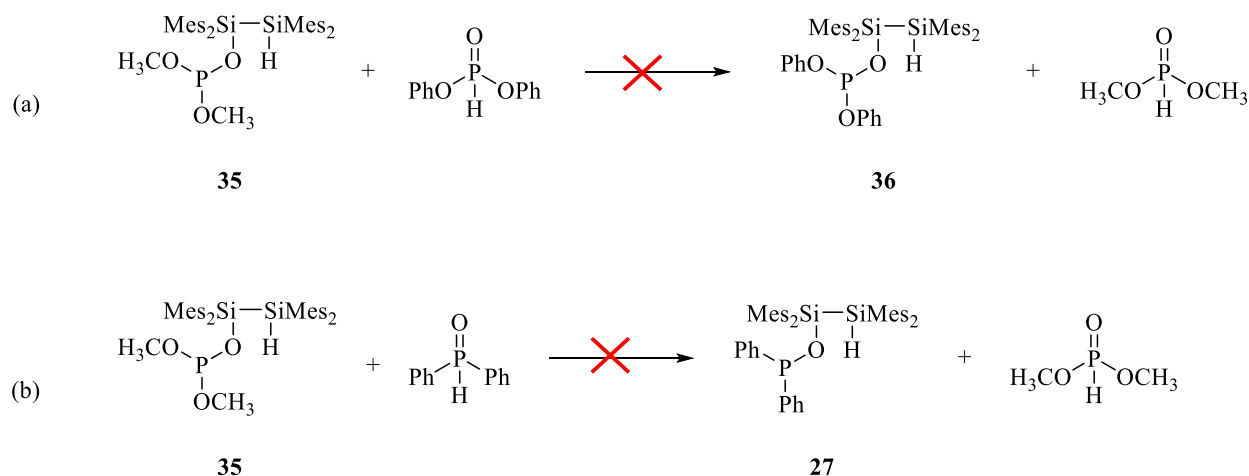


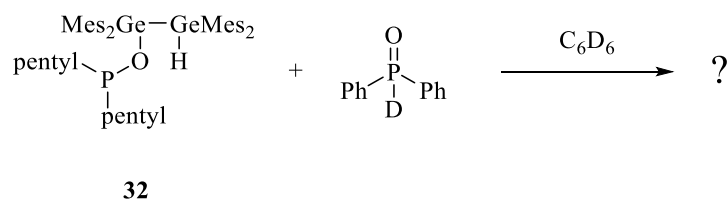
Figure 16. $^{31}\text{P}\{^1\text{H}\}$ NMR (C_6D_6 , 162 MHz) spectra of the addition of diphenyl phosphine oxide to dipentyl digermyl phosphinite **32**.

The exchange phenomenon was also explored with the disilene derivatives. The addition of excess diphenyl phosphite to dimethyldisilyl phosphite **35** (Scheme 40a) was monitored by $^{31}\text{P}\{^1\text{H}\}$ NMR spectroscopy. After 18 hours at room temperature, no change in the $^{31}\text{P}\{^1\text{H}\}$ NMR spectrum was observed. Since no reaction was observed, the mixture was heated at 50 °C for an additional 18 hours, however, no change was observed in the $^{31}\text{P}\{^1\text{H}\}$ NMR spectrum. The reaction of **35** with excess diphenylphosphine oxide (Scheme 40b) was also tested, however after 22 hours, no change was observed in the $^{31}\text{P}\{^1\text{H}\}$ NMR spectrum. On the basis of the results from these two experiments, the exchange of the $\text{OP}(\text{OCH}_3)_2$ group in **35** for another OPR_2 group is not possible under the reaction conditions examined.



Scheme 40. The addition of (a) diphenyl phosphite and (b) diphenylphosphine oxide to **35**.

The mechanism of the reaction of diphenylphosphine oxide with dipentyldigermyl phosphinite **32** was explored by adding excess diphenylphosphine oxide-*d*₁ to a crude sample of **32** (Scheme 41). The reaction was monitored by ³¹P{¹H} NMR spectroscopy (Figure 17a).



Scheme 41. The addition of diphenylphosphine oxide-*d*₁ to **32**.

Within 10 minutes, the appearance of signals at 104.7 and 29.2 ppm are observed, which were assigned to dipentyldigermyl phosphinite **28** and dipentylphosphine oxide, respectively. At the 30 minute time point, it is clear that the deuterium label is incorporated in the dipentylphosphine oxide that is formed based on the appearance of a triplet at 28.4 ppm, which is isotopically shifted from the protonated analog (Figure 17b). The integration of the signal for **28** stopped increasing after 15 hours, indicating dipentyldigermyl phosphinite **28** was no longer being formed. In the ²H{¹H} NMR spectrum, two doublets were observed at 7.80 ppm (*J* = 73 Hz) and 6.60 ppm (*J* = 70 Hz) and are assigned to diphenylphosphine oxide-*d*₁ and dipentylphosphine oxide-*d*₁, respectively. The observed coupling constants are within 3 Hz of the calculated coupling constants for Ph₂P(O)D (72 Hz) and pentyl₂P(O)D (67 Hz). A third doublet at 7.33 ppm (*J* = 22 Hz) was also observed, however the identity of this compound is unknown, although the magnitude of the coupling

constant suggests a 2 to 3 bond D-P coupling. The absence of a signal at 5.98 ppm indicates the deuterium label was not being incorporated into **28**.

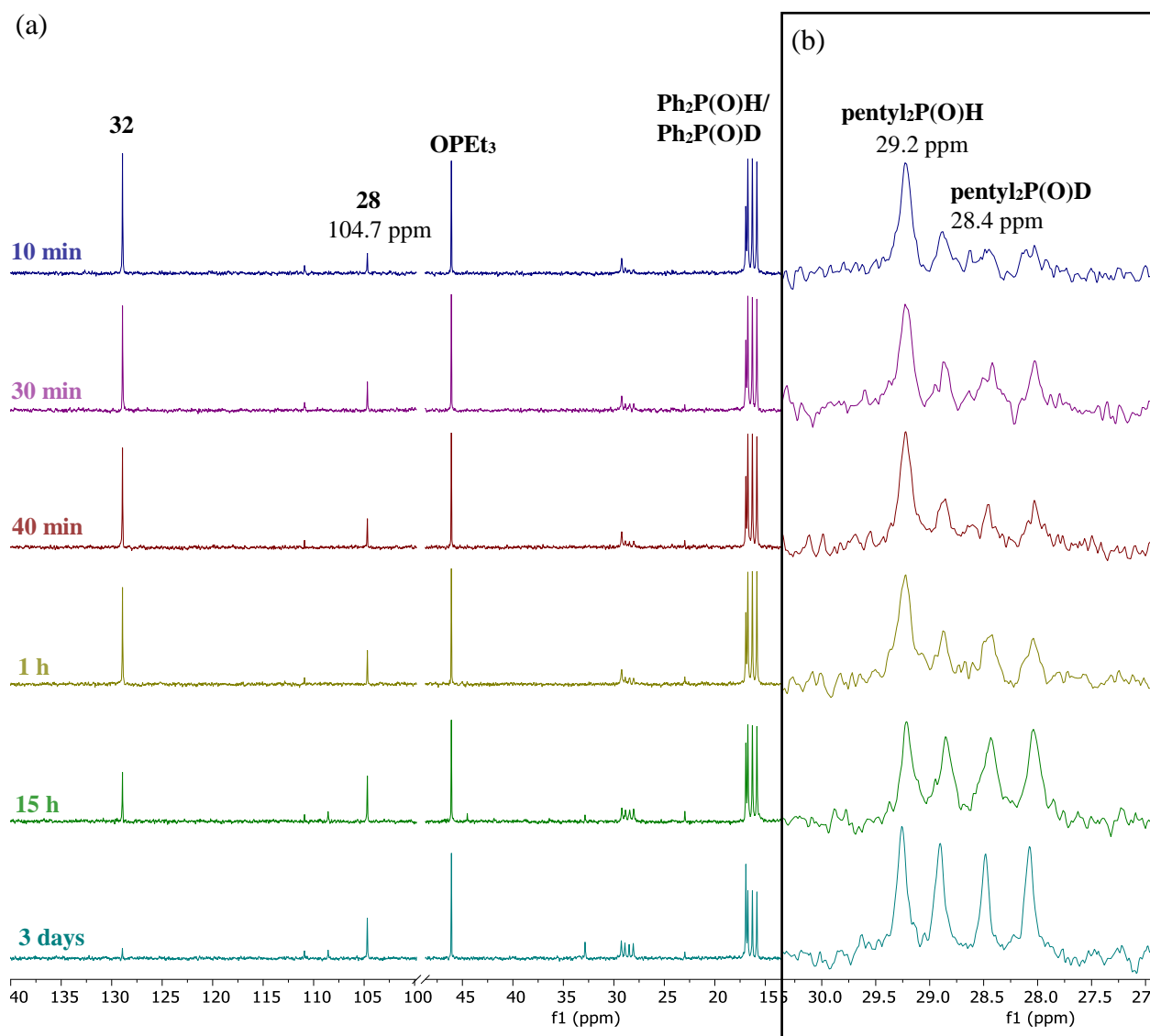
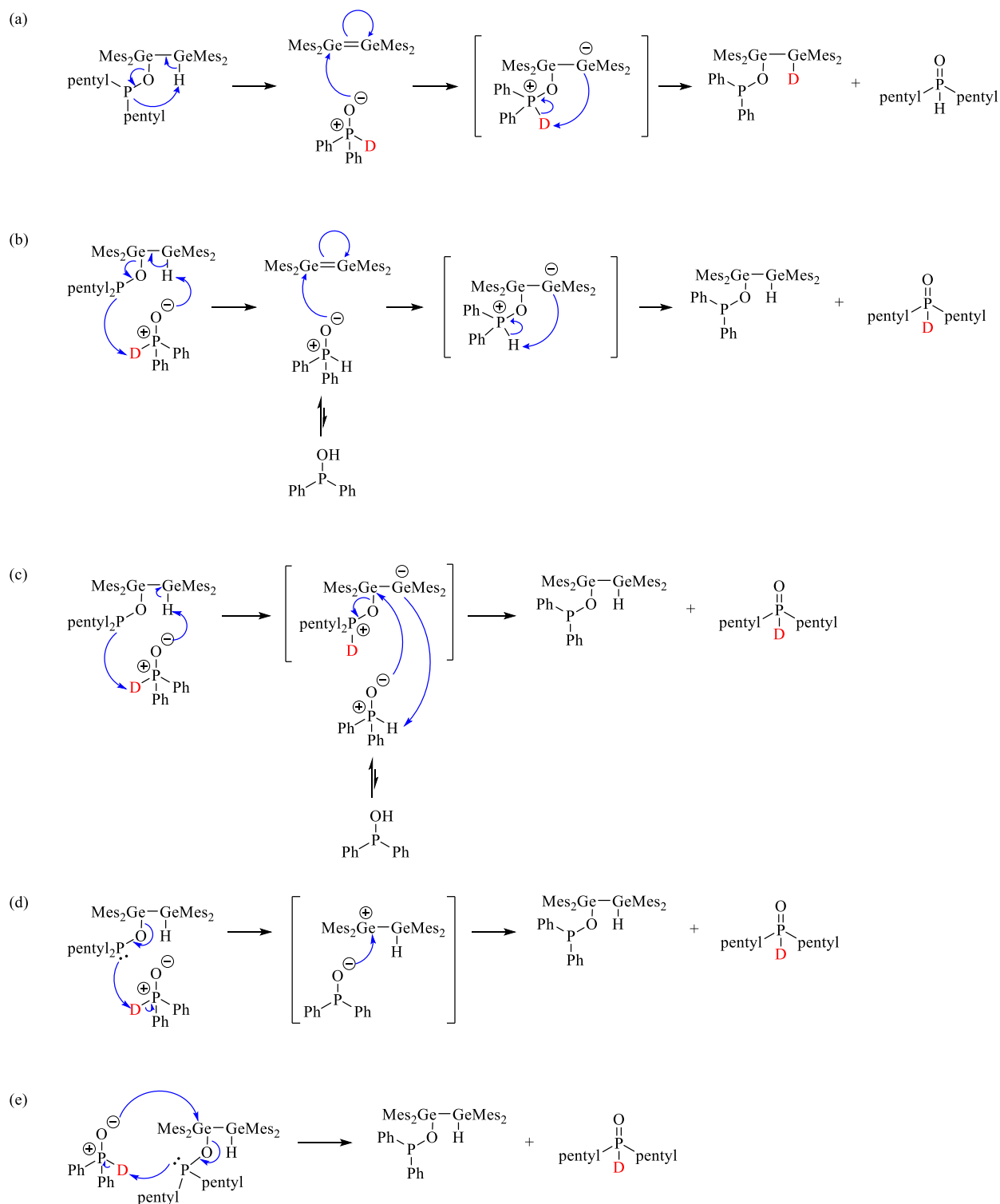


Figure 17. $^{31}\text{P}\{^1\text{H}\}$ NMR (C₆D₆, 162 MHz) spectra of the addition of diphenylphosphine oxide-*d*₁ to **32**. (a) Shows all signals present in the spectra. (b) Expansion shows the zoomed region containing the signals for protonated and deuterated dipentylphosphine oxide.

Five mechanisms can be envisioned for the reaction of diphenylphosphine oxide-*d*₁ with **32** (Scheme 42). In the first mechanism, an intramolecular abstraction of the Ge-H proton results in the regeneration of digermene **5**, followed by the stepwise addition of diphenylphosphine oxide to form deuterated diphenyldigermyl phosphinite **28**. Mechanisms (b) and (c) involve the intermolecular abstraction of the Ge-H proton by diphenylphosphine oxide. In mechanism (b), **5**

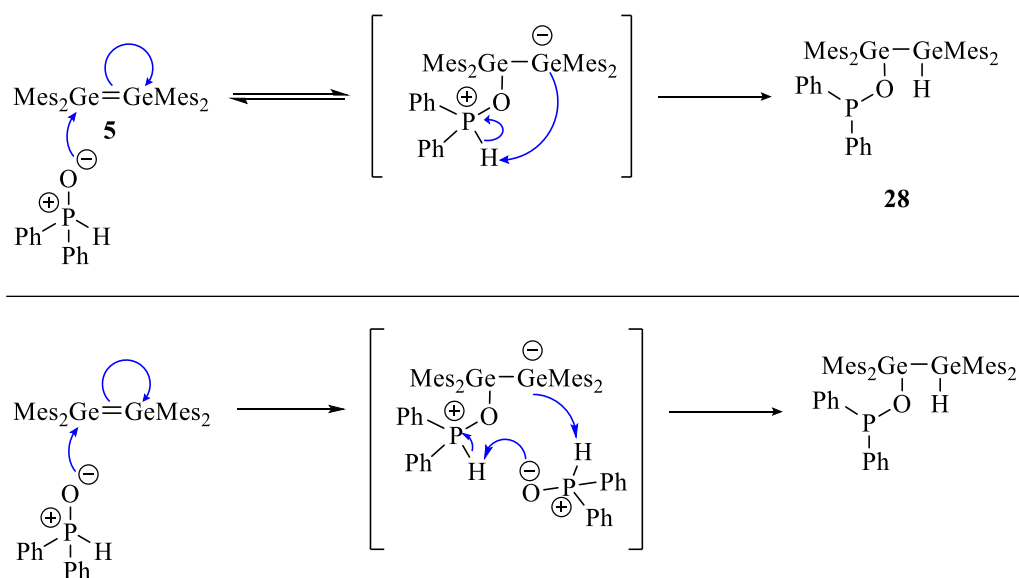
is regenerated and adds to diphenylphosphine oxide by stepwise nucleophilic addition; while in mechanism (c), a digermyl anion adds to diphenylphosphine oxide. The remaining mechanisms, (d) and (e), are substitution pathways. In mechanism (d), an S_N1 type mechanism is shown where dissociation of the $OP(pentyl)_2$ group forms a digermyl cation intermediate, which forms **28** by nucleophilic addition to the Ge cation. A direct substitution mechanism is depicted in mechanism (e) where nucleophilic attack of diphenylphosphine oxide and dissociation of the $OP(pentyl)_2$ moiety occurs in the same step. In mechanisms (b), (c), (d) and (e), the deuterium label is incorporated on the regenerated dipentylphosphine oxide and not dipenyldigermyl phosphinite **28**. On the basis of the results from the deuterium labelling experiment where diphenylphosphine oxide- d_1 was added to **5**, mechanism (a) can be eliminated, since there was no signal for the Ge-D moiety of **28** in the $^2H\{^1H\}$ NMR spectrum. Since deuterium is incorporated in dipentylphosphine oxide instead of **28**, mechanisms (b), (c), (d), and (e) are all plausible, although the mechanism cannot be distinguished with the results obtained. If the Ge-H of **32** is retained, then the reaction likely proceeds through substitution mechanisms (d) or (e). However, if the Ge-H of **32** is broken, then the reaction likely proceeds through either mechanism (b) or (c). Digermyl cations are not readily formed, so the reaction proceeding through mechanism (d) is not likely. Since no deuterium is incorporated into the Ge-H position of **28**, the direct substitution, mechanism (e), is proposed to be the most plausible mechanism since some deuterium incorporation into the Ge-H moiety is expected to occur in mechanisms (b) and (c).



Scheme 42. Proposed reaction mechanisms for the addition of diphenylphosphine oxide- d_1 to **32**.

3.5 Summary

The reaction mechanism for the addition of organophosphorus oxides to ditetrelenes **4** and **5** was investigated. The addition of diphenylphosphine oxide-*d*₁ to **5**, confirmed the breaking of the P-H bond and formation of the Ge-H bond to yield compound **28**. Furthermore, the reaction was confirmed to proceed through a stepwise nucleophilic addition and not a concerted reaction pathway by a KIE experiment. The $k_{\text{H}}/k_{\text{D}}$ value of 1.3 obtained from the KIE experiment indicates a secondary isotope effect, suggesting the breaking of the P-D bond or formation of the Ge-D bond is not involved in the rate determining step, thereby, providing evidence which supports a nucleophilic addition mechanism. However, the KIE experiments could not distinguish between an intramolecular or intermolecular proton abstraction in the second step of the mechanism (Scheme 43).

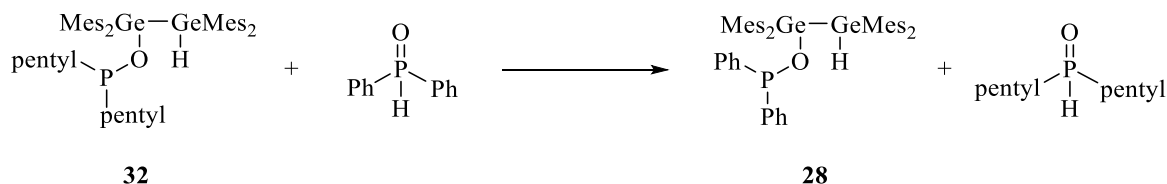


Scheme 43. Plausible mechanisms for the nucleophilic addition of diphenylphosphine oxide to **5**.

A competition experiment between diphenyl- and dipentylphosphine oxide was also explored to determine which reagent reacted with digermene **5** more readily. Since **28** was formed in larger amounts, it can be concluded that diphenylphosphine oxide reacts more rapidly with **5**.

Interestingly, the relative ratio of products changed after 24 hours to favour the formation of **28**, giving evidence that the OP(pentyl)₂ group can be exchanged with a OPPh₂ group. The

exchange phenomenon of the reaction was confirmed by adding excess diphenyl phosphine oxide to dipentyldigermyl phosphinite **32** (Scheme 44).



Scheme 44. The addition of diphenylphosphine oxide to **32** to yield diphenyldigermyl phosphinite **28**.

The exchange phenomenon was not observed in the reverse reaction, the addition of dipentylphosphine oxide to diphenyldigermyl phosphinite **28**. In addition, the $\text{OP}(\text{OCH}_3)_2$ group of dimethyldisilyl phosphite **35** could not be exchanged with either OPPh_2 or $\text{OP}(\text{OPh})_2$ groups.

Lastly, the mechanism for the exchange of the $\text{OP}(\text{pentyl})_2$ group of **32** with a PPh_2 group was explored by adding diphenylphosphine oxide- d_1 to a crude sample of **32**. Since the deuterium label was not incorporated into diphenyldigermyl phosphinite **28**, four plausible mechanisms can still be considered including mechanisms involving intermolecular abstraction of the Ge-H moiety or substitution mechanisms. However, more work is required to determine whether the Ge-H of **32** remains intact to distinguish between the plausible mechanisms remaining.

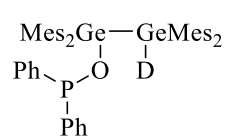
3.6 Experimental

3.6.1 General Experimental Details

All reactions were carried out in an MBraun glovebox under an atmosphere of nitrogen. All anhydrous solvents were collected from an Innovative Technology solvent purification system and dried over 4 Å molecular sieves. All reagents were purchased from Millipore Sigma or Alfa Aesar. Disilene **4** was prepared by photolysis of $\text{Mes}_2\text{Si}(\text{Si}(\text{CH}_3)_3)_2$ in hexanes in a quartz tube with Ushio G8T5 Mercury UV-C lamps (254 nm) and cooled to -45°C using a Thermo Scientific Neslab ULT 80 bath circulator. Digermene **5** was prepared through a similar procedure as **4**, by the photolysis of $(\text{Mes}_2\text{Ge})_3$ in THF at 350 nm. NMR spectra were acquired using a Varian INOVA I600 or I400 FT-NMR spectrometer or a Bruker AvIII HD 400 spectrometer. The ^1H and ^{13}C chemical shifts (δ) are listed in ppm against residual $\text{C}_6\text{D}_5\text{H}$ (7.15 ppm) and C_6D_6 (128 ppm) relative to tetramethylsilane, respectively. The chemical shifts for the $^{31}\text{P}\{^1\text{H}\}$ NMR spectrum

were referenced externally to 85% H₃PO₄. Triethylphosphine oxide was used as an internal standard inside a sealed capillary tube for reactions monitored by ³¹P{¹H} NMR spectroscopy, unless otherwise stated. The ²H chemical shifts are listed in ppm against residual C₆H₅D (7.15 ppm).

3.6.2 Addition of Diphenylphosphine Oxide-*d*₁ to Tetramesityldigermene **5**


 Diphenylphosphine oxide-*d*₁ (6.9 mg, 0.034 mmol) was added to a yellow solution of **5** (17 mg, 0.034 mmol) dissolved in C₆D₆. After 5 minutes of stirring the reaction at room temperature, the colour of the solution changed to light yellow. The C₆D₆ was evaporated under vacuum to yield a light yellow oil, which was redissolved in a minimal amount of hexanes and stored in the freezer (-20 °C) for 18 hours. A tan precipitate formed and **55** was isolated as a solid by decantation (20 mg, 61%). ¹H NMR (C₆D₆, 600 MHz) δ 7.66 – 7.62 (m, 4H, Ph *o*-H), 7.10 – 7.05 (m, 4H, Ph *m*-H), 7.02 – 6.98 (m, 2H, Ph *p*-H), 6.68 (s, 4H, Mes *m*-H), 6.63 (s, 4H, Mes *m*-H), 5.98 (s, 0.2H, residual Ge-H from **28**), [2.331, 2.328 (s, all together 24H, Mes *o*-CH₃)], [2.07, 2.06 (s, all together 12H, Mes *p*-CH₃)]; ³¹P{¹H} NMR (C₆D₆, 243 MHz) δ 104.8; ²H{¹H} NMR (C₆H₆, 92 MHz) 5.99 (Ge-D).

3.6.3 Competition Kinetic Isotope Effect

A stock solution of diphenylphosphine oxide (0.05 M, 0.02 mmol) and 94% diphenylphosphine oxide-*d*₁ (0.05 M, 0.02 mmol) were added to a yellow solution of **5** dissolved in C₆D₆ (0.06M, 0.02 mmol) in an NMR tube. The colour of the solution faded to light yellow in 5 minutes. The reaction was monitored by ³¹P{¹H} NMR spectroscopy over 9 time points (5, 7, 10, 12, 15, 20, 30, 40 and 60 minutes).

3.6.4 Addition of Dipentyl- and Diphenylphosphine Oxide to Tetramesityldigermene **5**

A mixture of diphenylphosphine oxide (33 mg, 0.17 mmol) and dipentylphosphine oxide (31 mg, 0.17 mmol) dissolved in C₆D₆ (2 mL) was added to a yellow solution of **5** (0.1 g, 0.17 mmol) dissolved in C₆D₆ (2 mL). The colour of the solution immediately faded to light yellow. An aliquot

of the solution was taken to monitor the reaction by $^{31}\text{P}\{^1\text{H}\}$ NMR spectroscopy, without an internal standard, over 6 time points (5, 10, and 20 minutes, 1, 2, and 24 hours).

3.6.5 Addition of Diphenylphosphine Oxide to Dipentyldigermyl Phosphinite **32**

A stock solution of diphenylphosphine oxide (0.3 M, 0.2 mmol) was added to **32** (17 mg, 0.021 mmol) in an NMR tube. The reaction was monitored by $^{31}\text{P}\{^1\text{H}\}$ NMR spectroscopy over 7 time points (10, 12, 15, 18, 20 and 60 minutes, and 18 hours).

3.6.6 Addition of Dipentylphosphine Oxide to Diphenyldigermyl Phosphinite **28**

A stock solution of dipentylphosphine oxide (0.2 M, 0.08 mmol) in C_6D_6 was added to **28** (8 mg, 0.01 mmol) in an NMR tube. The reaction was monitored by $^{31}\text{P}\{^1\text{H}\}$ NMR spectroscopy over 7 time points (10, 20, 30, 40, 50 and 60 minutes, and 24 hours), however, no reaction was observed after 24 hours.

3.6.7 Addition of Diphenylphosphine Oxide to Dimethyldisilyl Phosphite **35**

A stock solution of diphenylphosphine oxide (0.2 M, 0.09 mmol) in C_6D_6 was added to **35** (7 mg, 0.02 mmol) in an NMR tube. The reaction was monitored by $^{31}\text{P}\{^1\text{H}\}$ NMR spectroscopy over 5 time points (10, 20, 30, and 60 min, and 22 hours), however, no reaction was observed after 22 hours.

3.6.8 Addition of Diphenyl Phosphite to Dimethyldisilyl Phosphite **35**

A stock solution of diphenyl phosphite (0.3 M, 0.1 mmol) in C_6D_6 , was added to **35** (0.01 g, 0.02 mmol) in an NMR tube. The reaction was monitored by $^{31}\text{P}\{^1\text{H}\}$ NMR spectroscopy over 6 time points (12, 20, 30, 40 and 60 min, and 18 hours). After 18 hours, no reaction occurred at room temperature. The reaction was heated at 50 °C for an additional 18 hours, but no reaction was observed.

3.6.9 The Addition of Diphenylphosphine Oxide- d_1 to Dipentylidigermyl Phosphinite **32**

A stock solution of diphenylphosphine oxide- d_1 (0.2 M, 0.07 mmol) in C_6D_6 was added to **32** (14 mg, 0.017 mmol) in an NMR tube. The reaction was monitored by $^{31}P\{^1H\}$ NMR spectroscopy over 9 time points (7, 10, 20, 30, 40, 50 and 60 minutes, 15 hours, and 3 days). $^2H\{^1H\}$ (C_6H_6 , 92 MHz) δ 7.80 (d, $J = 73$ Hz, $Ph_2P(O)D$), 7.33 (d, $J = 22$ Hz)^a, 6.60 (d, $J = 70$ Hz, $pentyl_2P(O)D$).

^a Identity of compound is unknown.

3.7 References

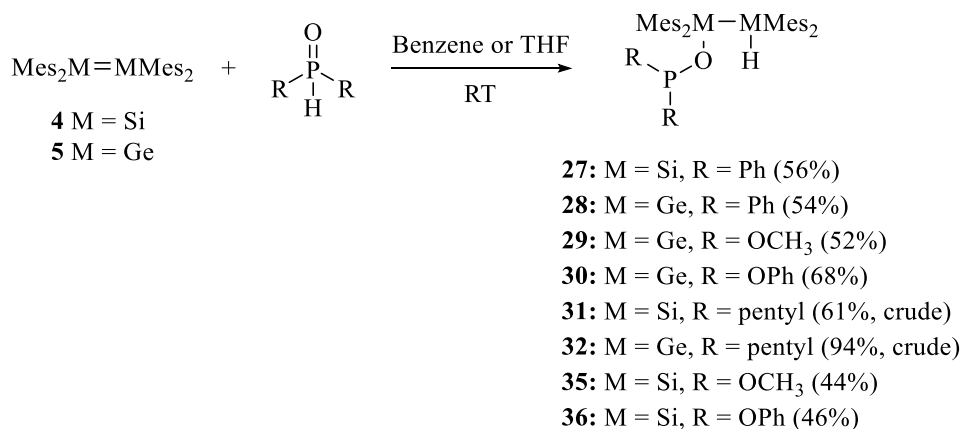
1. Morkin, T. L.; Owens, T. R.; Leigh, W. J. Kinetic studies of the reactions of Si=C and Si=Si bonds. In *The chemistry of organic silicon compounds*; Rappoport, Z.; Apeloig, Y., Ed.; John Wiley & Sons Ltd: New York, 2001; p 949.
2. Hajgató, B.; Takahashi, M.; Mitsuo, K.; Veszprémi, T. *Chem. Eur. J.* 2002, 8, 2126.
3. Nie, S.; Davison, R. T.; Dong, V. M. *J. Am. Chem. Soc.* **2018**, 140, 16450.
4. Melander, L. C. S.; Saunders: W. Reaction Rates of Isotopic Molecules; Krieger: Malabar, FL, 1987.
5. Gómez-Gallego, M.; Sierra, M. A. *Chem. Rev.* **2011**, 111, 4857.
6. Sekiguchi, A.; Maruki, I.; Sakurai, H. *J. Am. Chem. Soc.* **1993**, 115, 11460.
7. Apeloig, Y.; Nakash, M. *J. Am. Chem. Soc.* **1996**, 118, 9787.
8. Grayson, M.; Farley, C. E.; Streuli, C. A. *Tetrahedron* **1967**, 23, 1065.

Chapter 4

4 Conclusions and Future Work

4.1 Summary and Conclusions

This thesis has examined the reactivity of doubly bonded Group 14 species towards organophosphorus oxides. The addition of dialkyl and diaryl phosphine oxides and phosphites with ditetrelenes **4** and **5** was explored (Scheme 45), and in all cases examined, disilyl and digermyl phosphinite and phosphites (**27**, **28**, **29**,¹ **30**,¹ **31**, **32**, **35** and **36**) were isolated. The reaction results in a mild reduction of the P(V) centre of the phosphine oxides and phosphites to give a P centre in the phosphinite and phosphite derivatives that has an intermediate chemical state between $R_3P=O$ and R_3P . The only other method for synthesizing the silyl phosphinite and phosphite derivatives is through the reaction of phosphine oxides or phosphites with chlorosilanes in the presence of amines at elevated temperatures.² In the reactivity with disilene **4**, the Lewis acid and Lewis base are contained within the same molecule and the reaction can be performed under neutral conditions at room temperature. The typical synthesis of germyl phosphinites and phosphites involves the salt metathesis reaction of the phosphine oxide or phosphite salt with chlorogermanes at elevated temperatures.^{3, 4} In the synthesis of digermyl phosphinite and phosphite derivatives using digermene **5**, the Ge centre is directly involved in the partial reduction of the P(V) centre of the phosphine oxide and phosphite.

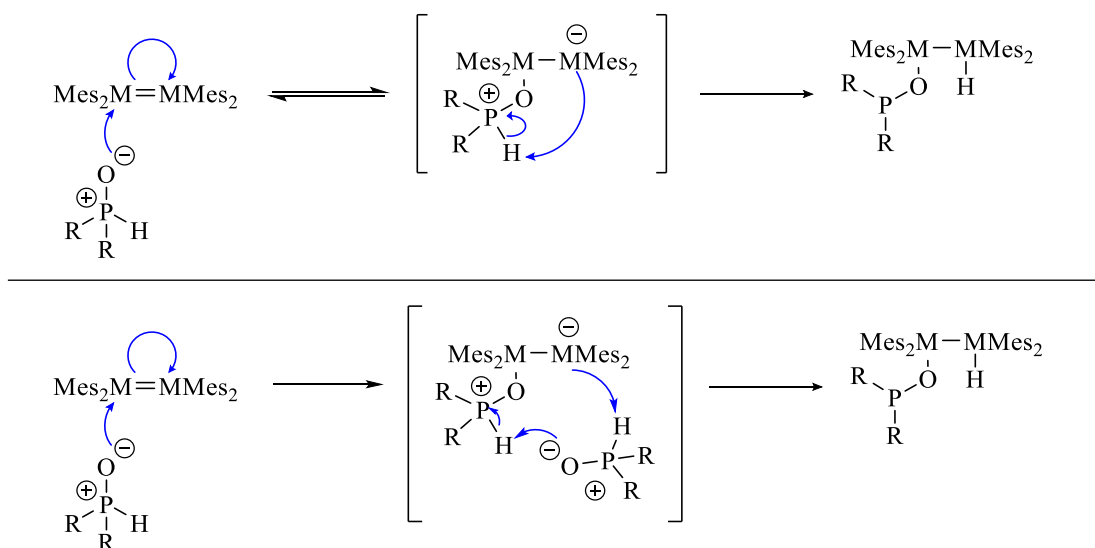


Scheme 45. The addition of organophosphorus oxides to ditetrelenes **4** and **5**.

In the analogous reactivity with alkenes, the P-H bond of the phosphine oxide or phosphite adds across the C=C bond through activation of the P-H bond by a transition metal catalyst to form

a C-P and a C-H bond. In contrast, in the reaction of phosphine oxides and phosphites with ditetrelenes **4** or **5**, an M-O bond is formed, without the use of heat or a catalyst. The reactivity of phosphine oxides and phosphites with ditetrelenes **4** and **5** provides an additional example of the activation of organic main group oxides by doubly bonded Group 14 species, which previously included nitromethane⁵, arylsulfonyl chlorides⁶, carbon monoxide⁷ and carbon dioxide.⁸

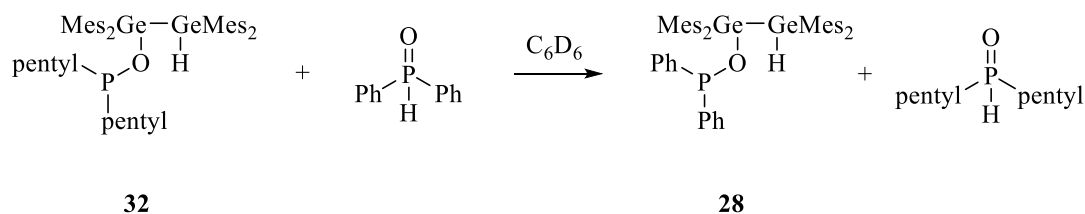
In Chapter 3, the mechanism for the reaction of organophosphorus oxides with ditetrelenes **4** and **5** was explored. On the basis of the results from the KIE experiment, the mechanism was proposed to be a stepwise nucleophilic addition of the organophosphorus oxide across the M=M bond in the ditetrelene (Scheme 46). However, it is not clear whether one or two equivalents of the organophosphorus oxide is involved in the reaction mechanism.



Scheme 46. Plausible mechanisms for the addition of organophosphorus oxides to **4** and **5**.

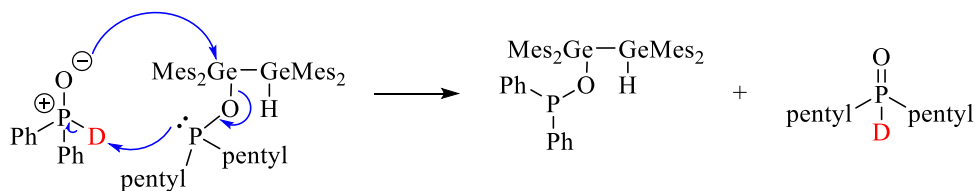
The relative rates of the reactions between dipentyl- or diphenylphosphine oxide with digermene **5** was also investigated by a competition experiment. Since diphenyldigermyl phosphinite **28** was formed in a larger amount, this indicates diphenylphosphine oxide reacts more rapidly with **5**, suggesting higher nucleophilicity of the P⁺-O⁻ moiety in the diaryl-substituted phosphine oxide. Surprisingly, the relative ratio of products changed over time, with the concentration of **28** increasing and the concentration of **32** decreasing, suggesting the OP(pentyl)₂ moiety of **32** can be exchanged for a OPPh₂ group.

The exchange phenomenon was investigated further by adding excess diphenylphosphine oxide to **32** (Scheme 47). This competition experiment confirmed the exchange of the OPR₂ moieties. However, when the reverse reaction was attempted and when disilene derivatives were probed, no exchange occurred. In fact, of all the cases attempted, the only exchange observed was between the OP(pentyl)₂ moiety of **32** and the OPPh₂ group of diphenylphosphine oxide. The exchange seen in the dipentyldigermyl phosphinite derivative **32** may be due to instability of the product which has been proven to readily undergo secondary reactivity such as hydrolysis of the O-P bond on the Ge centre. The exchange with the OPPh₂ group would generate diphenyldigermyl phosphinite **28**, which is a more stable adduct.



Scheme 47. The addition of diphenylphosphine oxide to **32**.

Using a deuterium labelling experiment, the mechanism of the exchange phenomenon was probed by adding diphenylphosphine oxide-*d*₁ to dipentyldigermyl phosphinite **32**. The deuterium label was only incorporated in the dipentylphosphine oxide that was regenerated. On the basis of the results from the deuterium labelling experiment, a direct substitution mechanism is proposed for the exchange of the OP(pentyl)₂ moiety of **32** with a OPPh₂ group (Scheme 48).



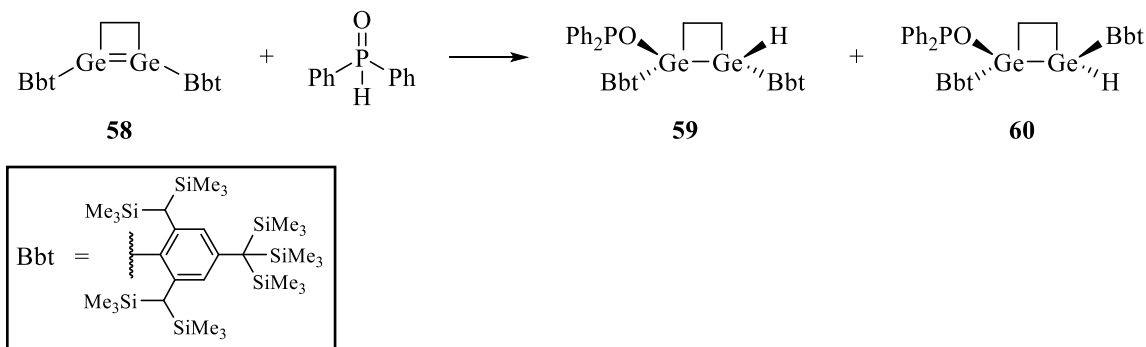
Scheme 48. Plausible mechanism for the exchange phenomenon between **32** and diphenylphosphine oxide.

4.2 Future Work

The scope of this work includes reactions of dialkyl and diarylphosphine oxides and phosphites with ditetrelenes **4** and **5**, however, the reaction scope may be increased by looking at

other compounds containing a P=O group. Potential organophosphorus oxides that could be explored include primary phosphine oxides and phosphites (RP(O)H₂) or diorganophosphinic chlorides (R₂P(O)Cl).

The reaction mechanism for the addition of organophosphorus oxides to **4** and **5** proceeds through a stepwise nucleophilic addition, as confirmed by KIE experiments. However, to determine whether one or two equivalents of diphenylphosphine oxide are required in the reaction mechanism, the order of phosphine oxide in the rate law could be investigated. Diphenylphosphine oxide could also be added to cyclic digermene⁹ **58** (Scheme 49) to gain information on whether one or two equivalents of phosphine oxide are involved in the reaction mechanism. The reaction of **58** with diphenylphosphine oxide could proceed through two pathways, a *syn*-addition to form **59** or *anti*-addition to yield **60**. If **59** is formed as the major product, an intramolecular proton abstraction seems more plausible. However, if a racemic mixture of **59** and **60** is observed, an intermolecular proton abstraction is more likely, since the second equivalent of phosphine oxide could be deprotonated on either face of the Ge=Ge bond.



Scheme 49. The addition of diphenylphosphine oxide to cyclic digermene **58**.

The competition experiment between dipentyl- and diphenylphosphine oxide with digermene **4** should be monitored within the first 5 minutes of the reaction by NMR spectroscopy to determine whether dipentyl digermyl phosphinite **28** or dipentyl digermyl phosphinite **29** is the kinetic product. Since the exchange of the OP(pentyl)₂ moiety of **32** with a OPPh₂ group from diphenylphosphine oxide was successful, expanding on the scope of this reactivity is worthwhile. Diphenyl phosphite or dimethyl phosphite can be added to **32** to determine if an OP(OR)₂ group can also exchange with the OP(pentyl)₂ moiety.

Lastly, the mechanism for the exchange phenomenon can be investigated further by labeling the Ge-H moiety in **32** with deuterium. This labelling experiment would provide information on whether the Ge-H moiety is retained throughout the reaction. If the Ge-H moiety is retained, and the deuterium label is not transferred, this would provide evidence for a substitution mechanism.

4.3 References

- ¹ Farhadpour, B. Doubly Bonded Derivatives of Si and Ge: Cycloaddition Reactions and Polymer Chemistry. Ph. D. Dissertation, The University of Western Ontario, London, ON **2017**.
- ² Evans, D. A.; Hurst, K. M.; Takacs, M. *J. Am. Chem. Soc.* **1978**, *100*, 3467.
- ³ Issleib, K.; Walther, B. *Angew. Chem. Int. Ed.* **1967**, *6*, 88.
- ⁴ Novikova, Z. S.; Mashoshina, S. N.; Lutsenko, I. F. *Russ. J. Gen. Chem.* **1975**, *45*, 1486.
- ⁵ Tashkandi, N. Y.; Parsons, F.; Guo, J.; Baines, K. M. *Angew. Chem. Int. Ed.* **2015**, *54*, 1612.
- ⁶ Tashkandi, N. Y.; Bourque, J. L.; Baines, K. M. *Dalton Trans.* **2017**, *46*, 15451.
- ⁷ Cowley, M. J.; Ohmori, Y.; Huch, V.; Ichinohe, M.; Sekiguchi, A.; Scheschkewitz, D. *Angew. Chem. Int. Ed.* **2013**, *52*, 13247.
- ⁸ Wendel, D.; Szilvási, T.; Henschel, D.; Altmann, P. J.; Jandl, C.; Inoue S.; Rieger. B. *Angew. Chem. Int. Ed.* **2018**, *57*, 14575.
- ⁹ Sasamori, T.; Sugahara, T.; Agou, T.; Sugamata, K.; Guo, J. D.; Nagase, S.; Tokitoh, N. *Chem. Sci.* **2015**, *6*, 5526.

Appendices

Appendix A: NMR Data

Note: ^1H , $^{13}\text{C}\{^1\text{H}\}$ and ^1H - ^{29}Si gHMBC NMR spectra have been expanded to clearly show all signals assigned to the compounds of interest.

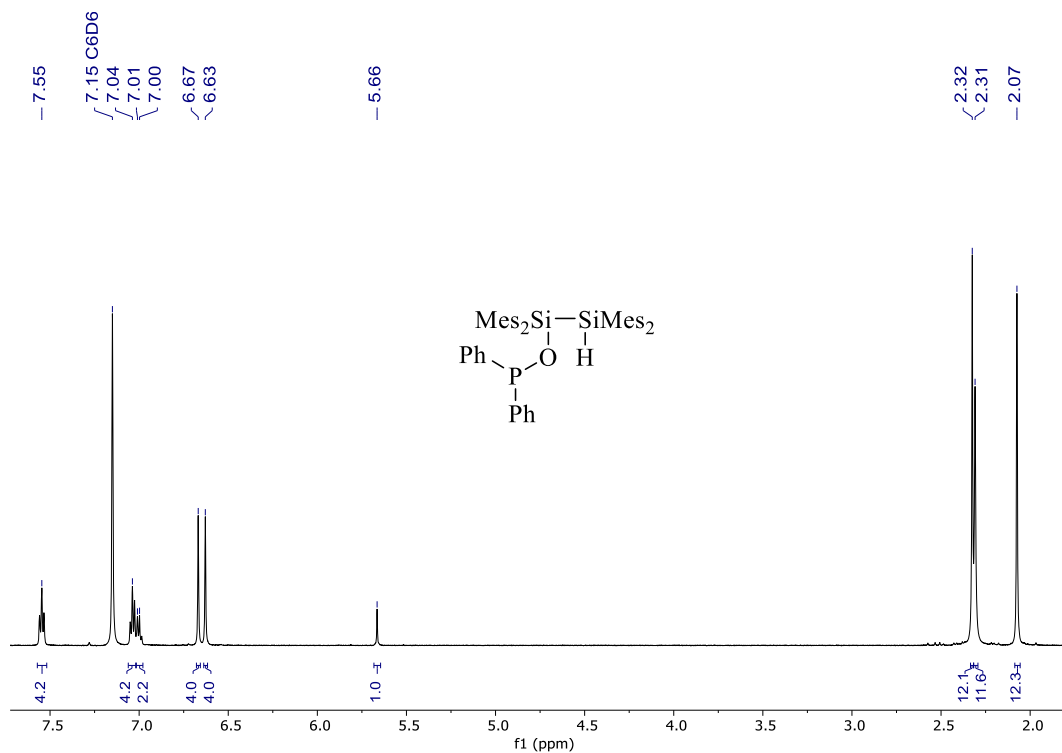


Figure A1: ^1H NMR spectrum (C_6D_6 , 600 MHz) of **27**.

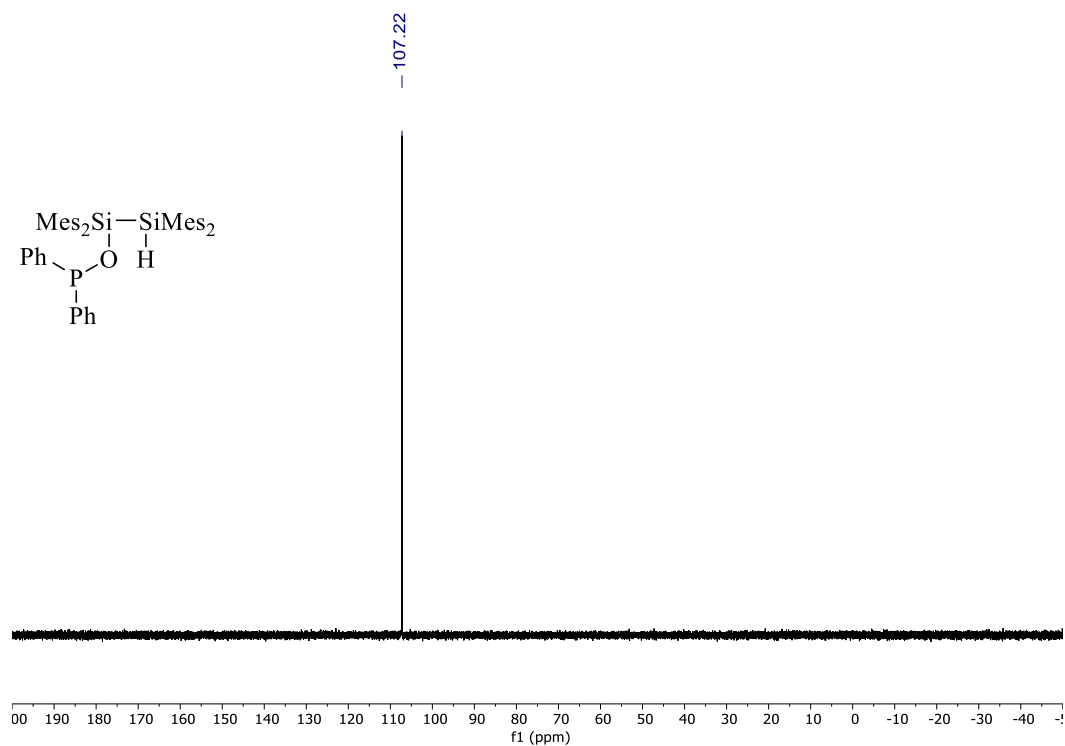


Figure A2: $^{31}\text{P}\{^1\text{H}\}$ NMR spectrum (C_6D_6 , 243 MHz) of **27**.

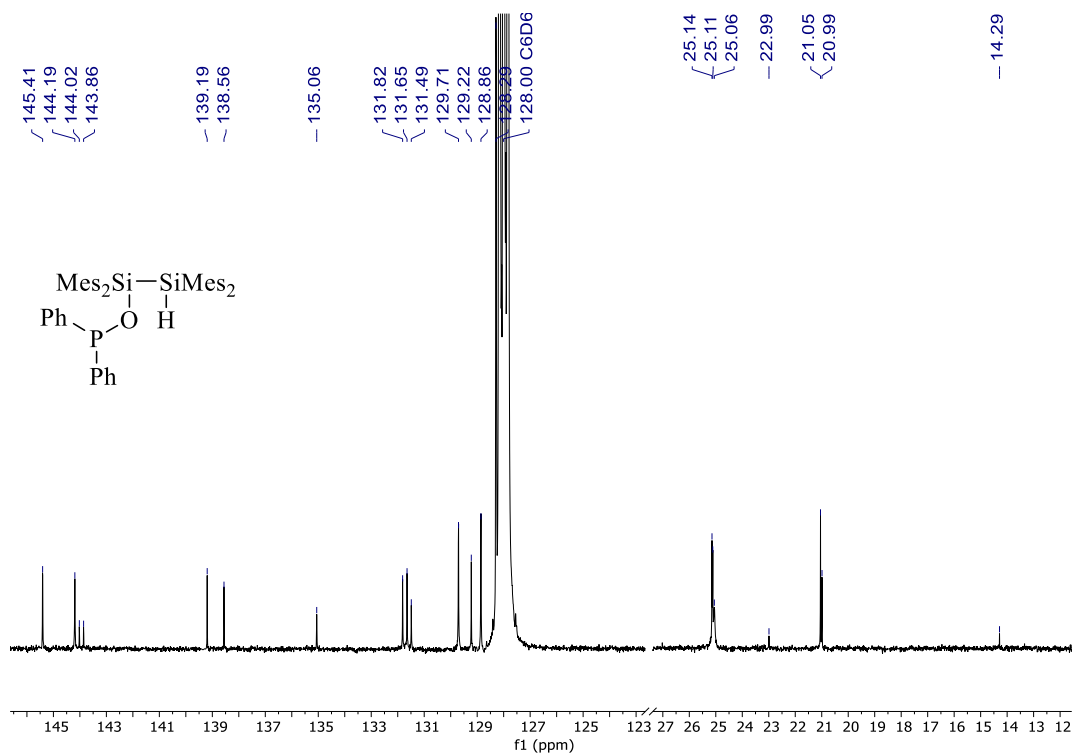


Figure A3: $^{13}\text{C}\{^1\text{H}\}$ NMR spectrum (C_6D_6 , 151 MHz) of **27**. The region of the spectrum from 30 to 120 ppm has been omitted.

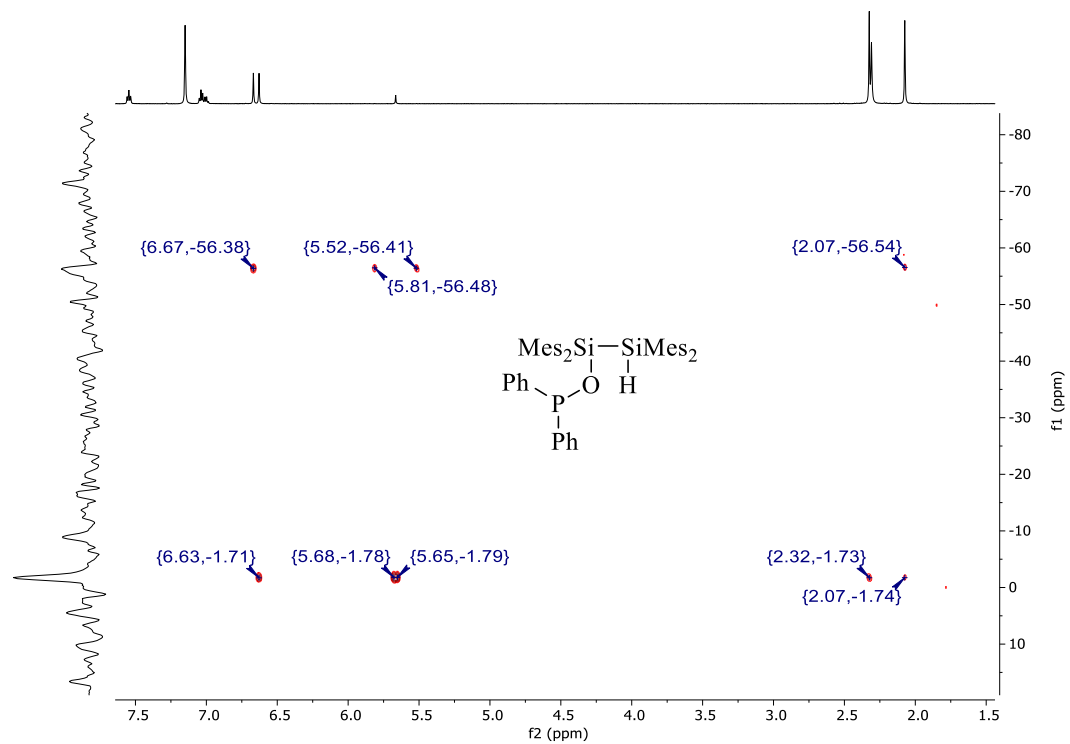


Figure A4: ^1H - ^{29}Si gHMBC NMR spectrum (C_6D_6) of **27**.

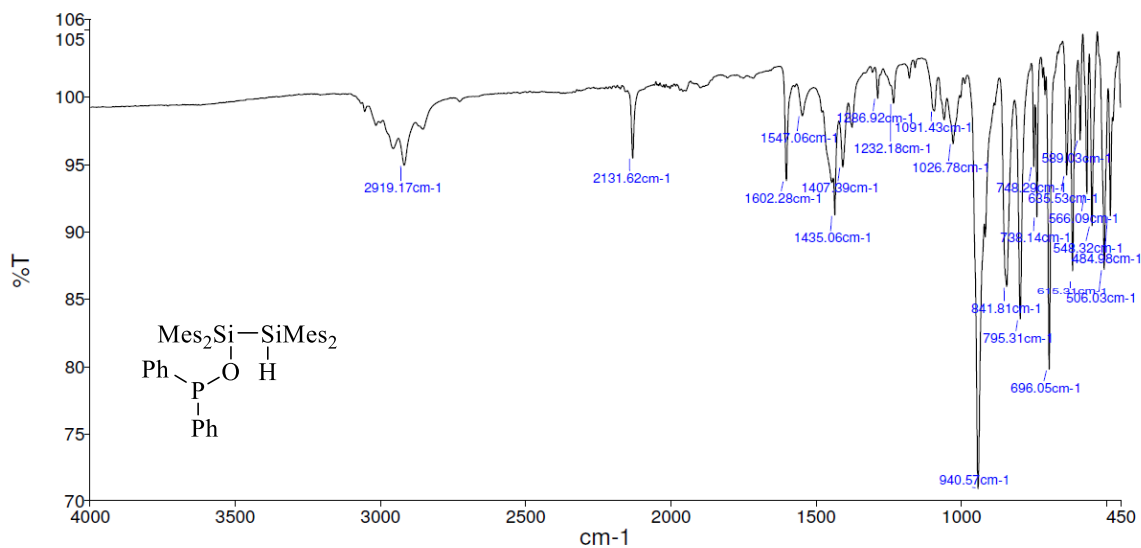


Figure A5: ATR-IR spectrum of **27**.

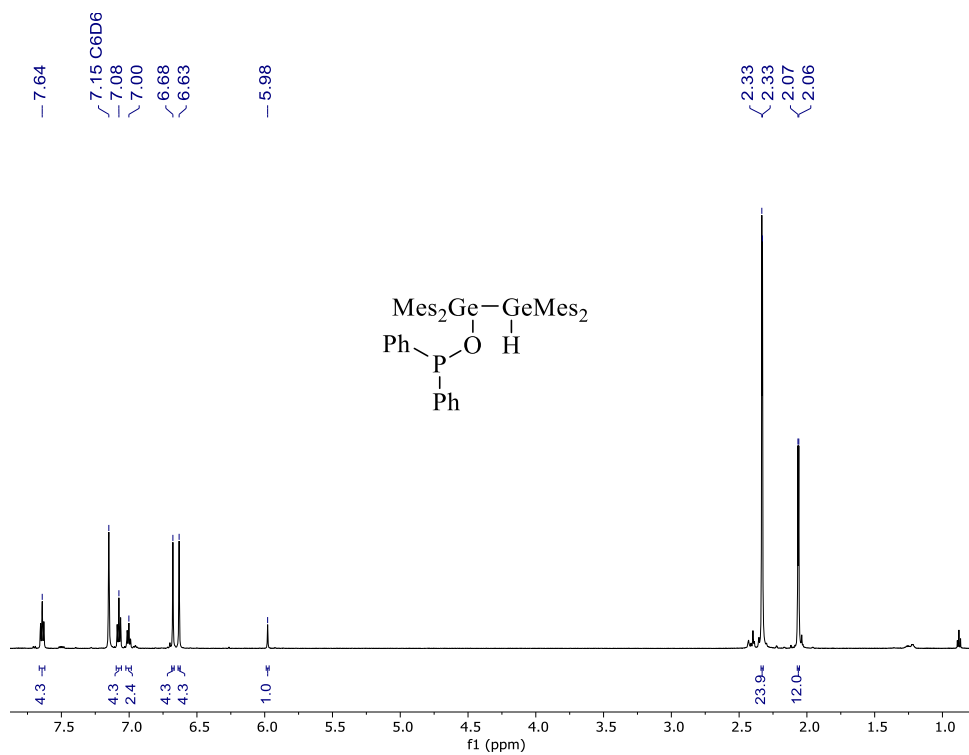


Figure A6: ¹H NMR spectrum (C₆D₆, 600 MHz) of **28**.

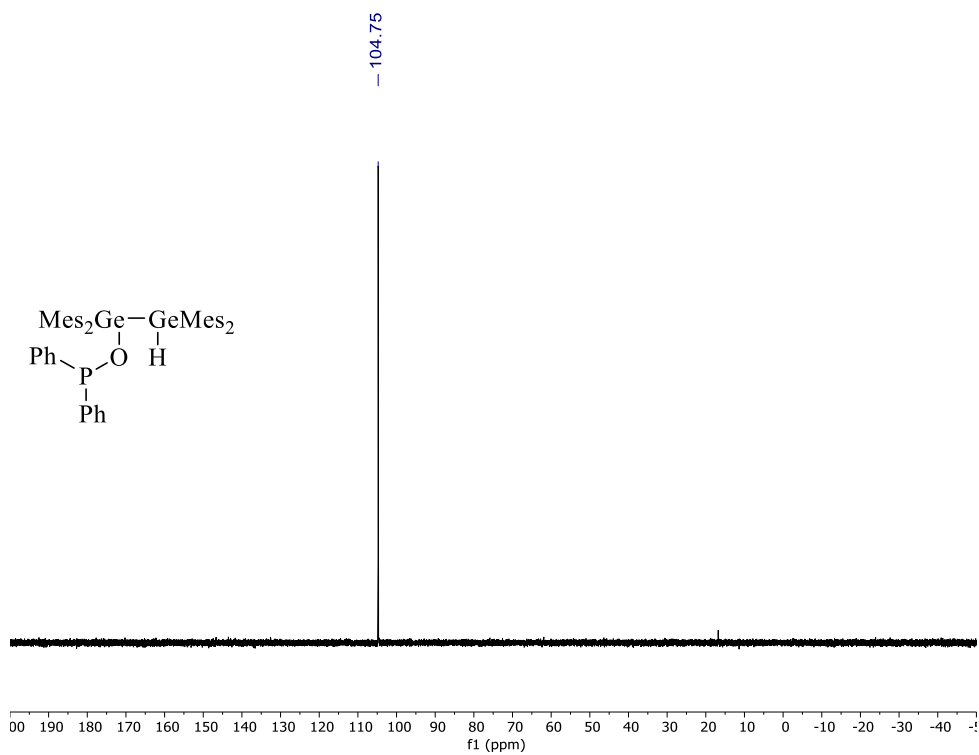


Figure A7: ³¹P{¹H} NMR spectrum (C₆D₆, 243 MHz) of **28**.

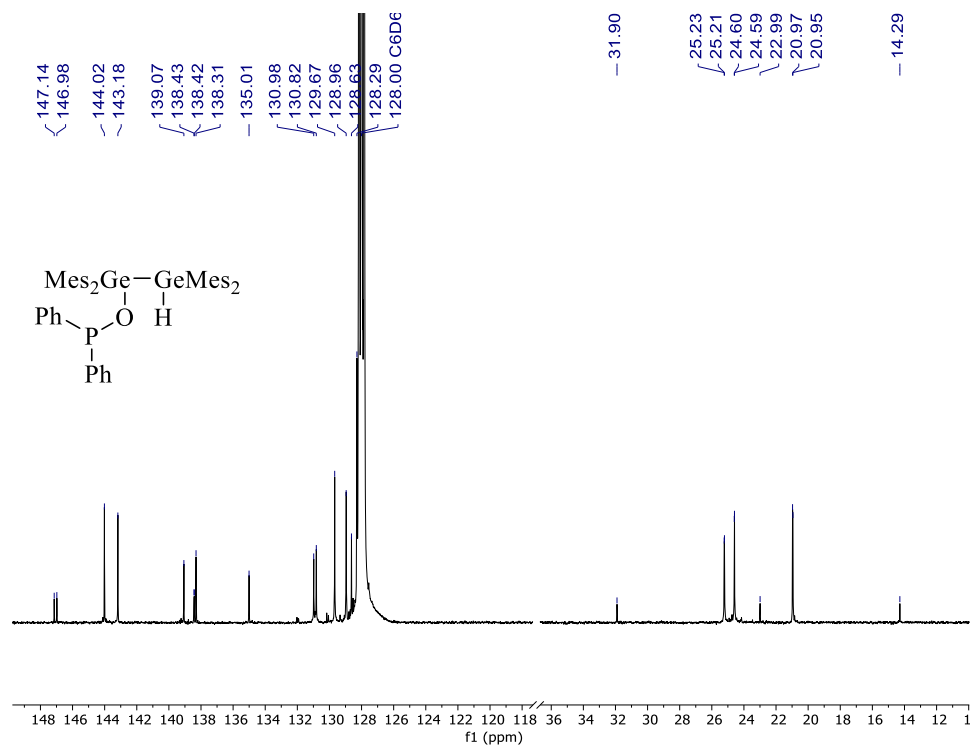


Figure A8: ¹³C{¹H} NMR spectrum (C₆D₆, 151 MHz) of **28**. The region of the spectrum from 40 to 115 ppm has been omitted.

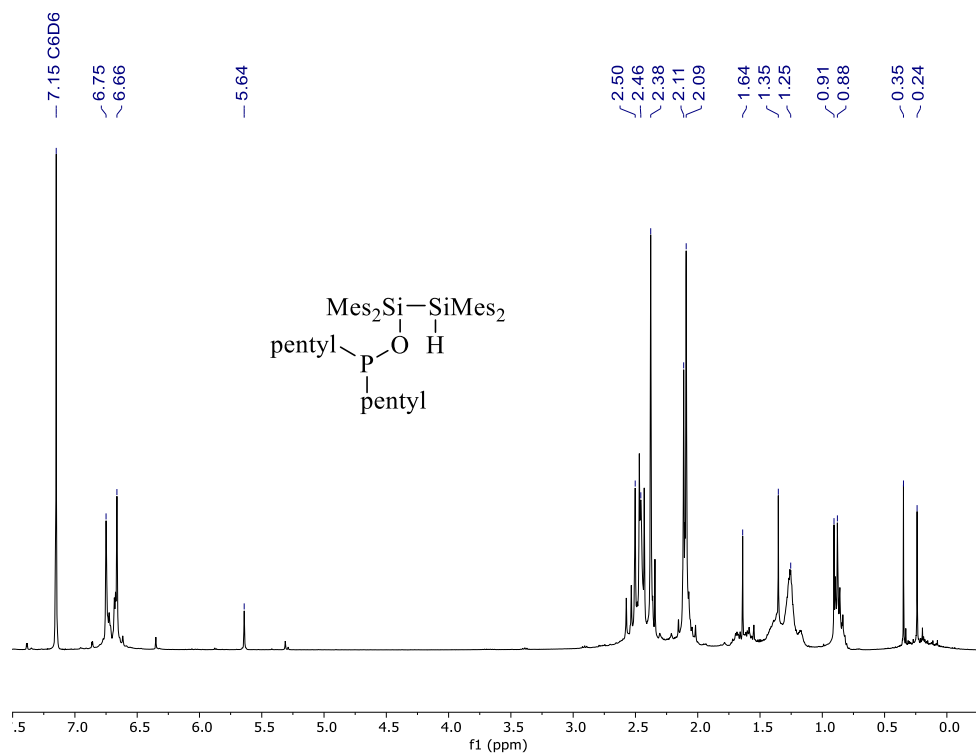


Figure A9: ¹H NMR spectrum (C₆D₆, 600 MHz) of **31**.

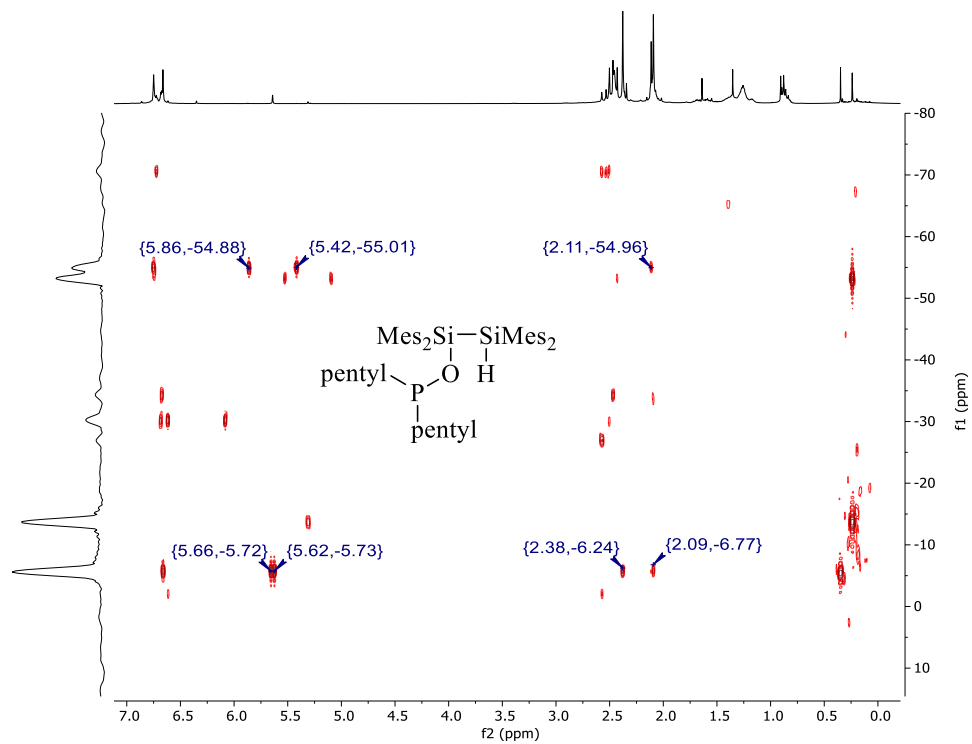


Figure A12: ^1H - ^{29}Si gHMBC NMR spectrum (C_6D_6) of **31**.

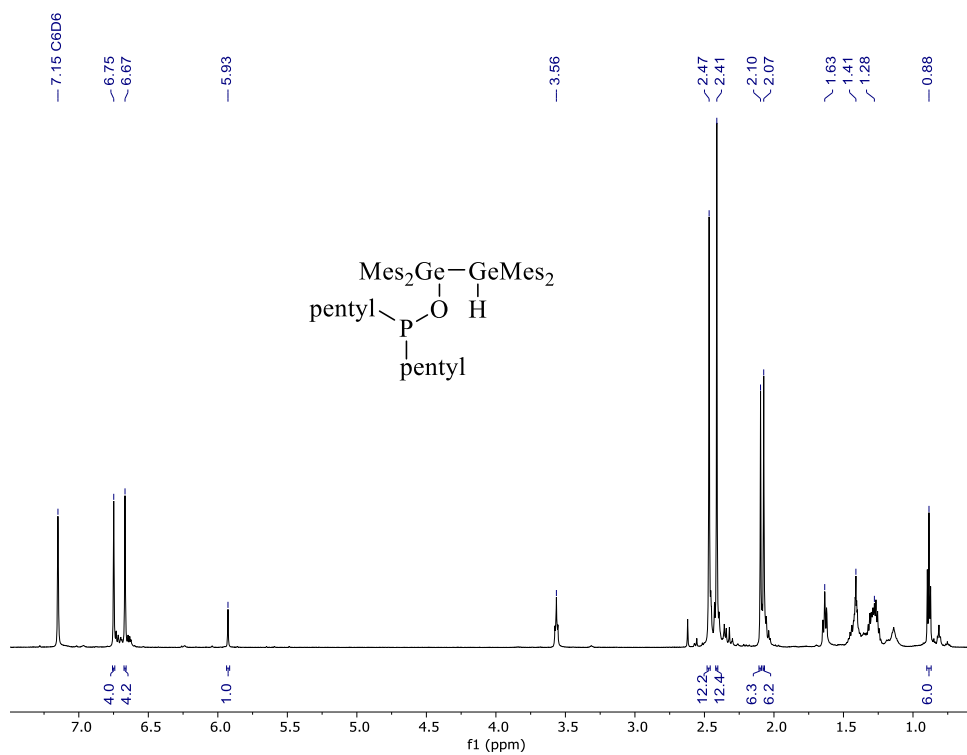


Figure A13: ^1H NMR spectrum (C_6D_6 , 600 MHz) of **32**.

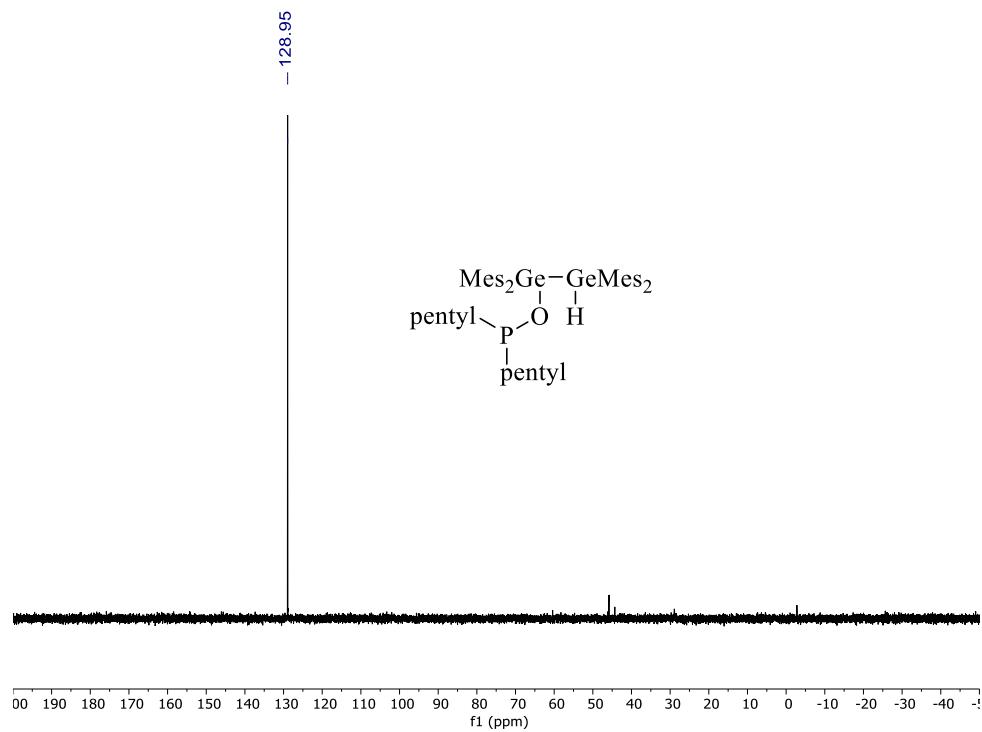


Figure A14: $^{31}\text{P}\{^1\text{H}\}$ NMR spectrum (C₆D₆, 162 MHz) of **32**.

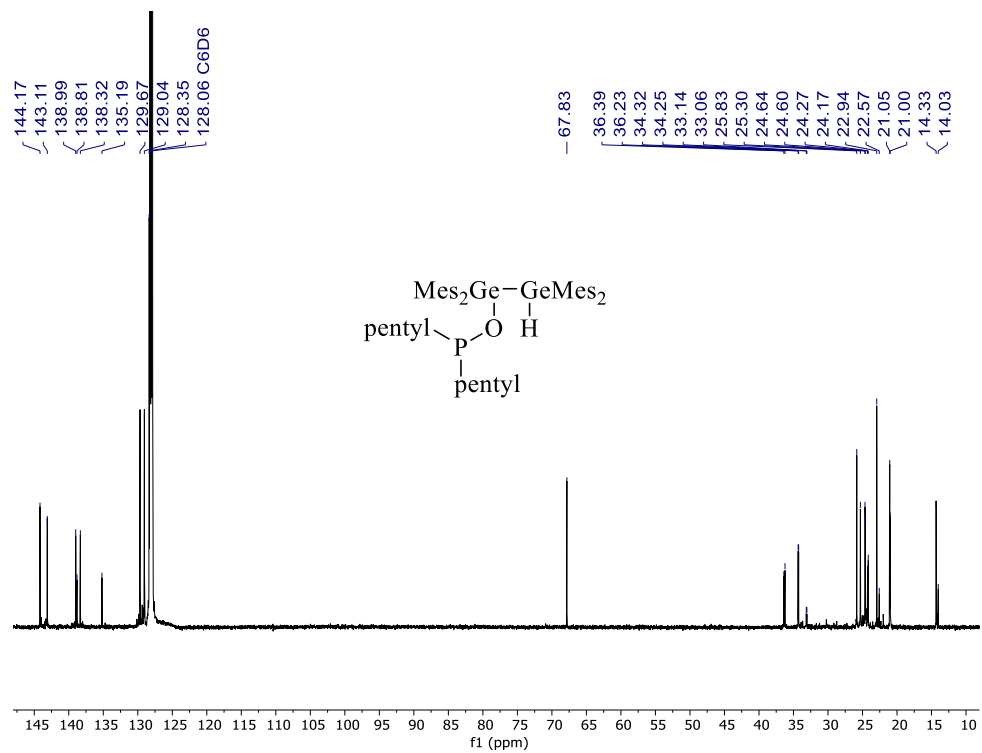


Figure A15: $^{13}\text{C}\{^1\text{H}\}$ NMR spectrum (C₆D₆, 151 MHz) of **32**.

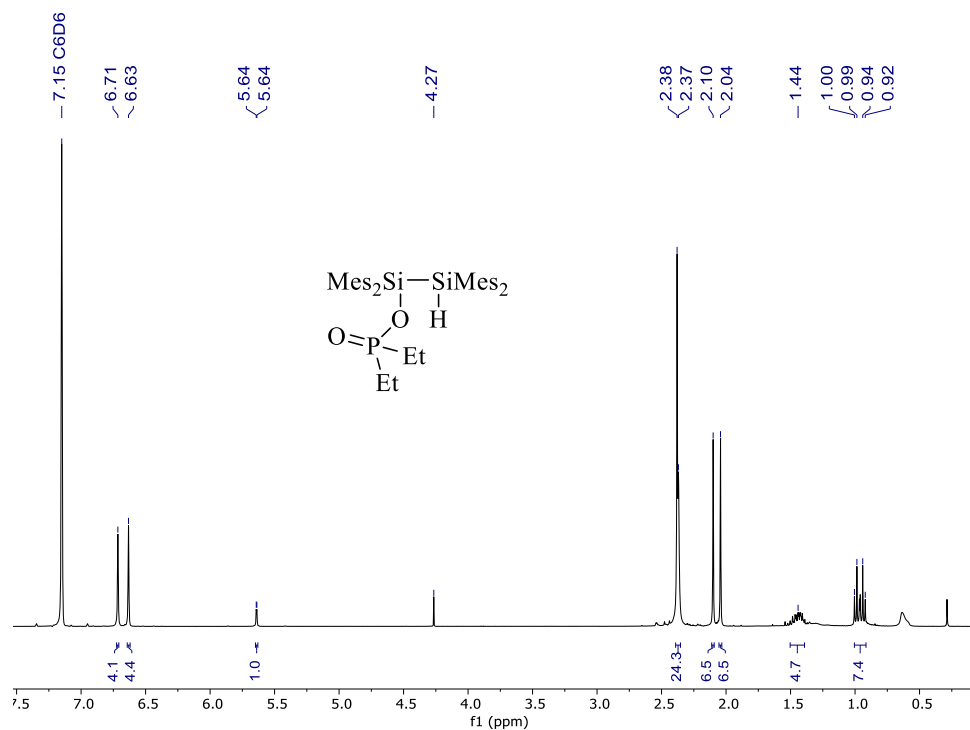


Figure A16: ¹H NMR spectrum (C₆D₆, 400 MHz) of **34**.

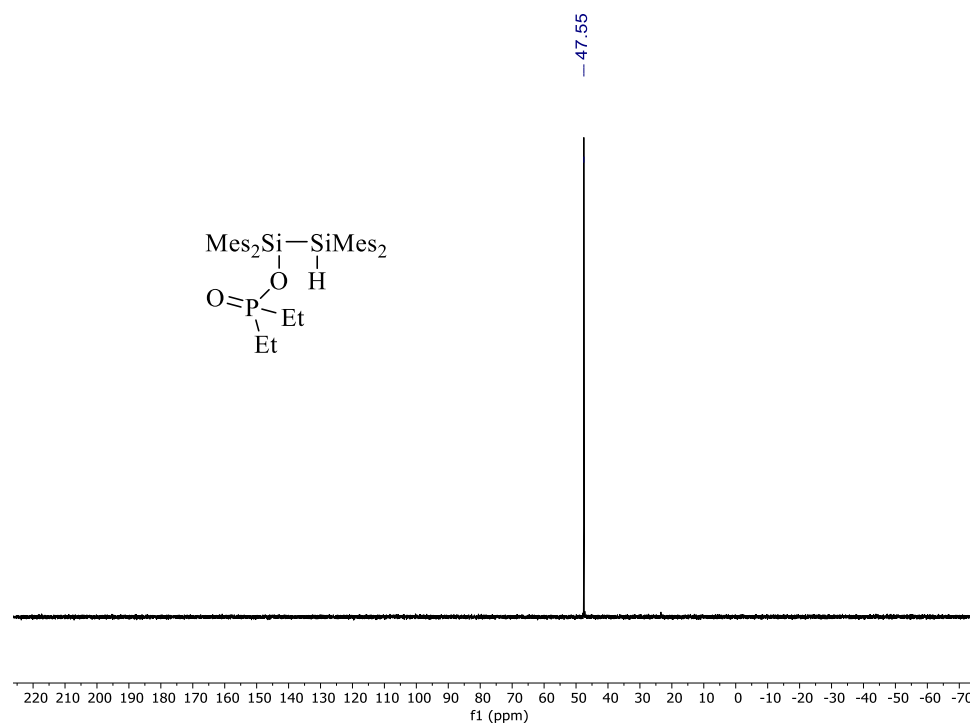


Figure A17: ³¹P{¹H} NMR spectrum (C₆D₆, 162 MHz) of **34**.

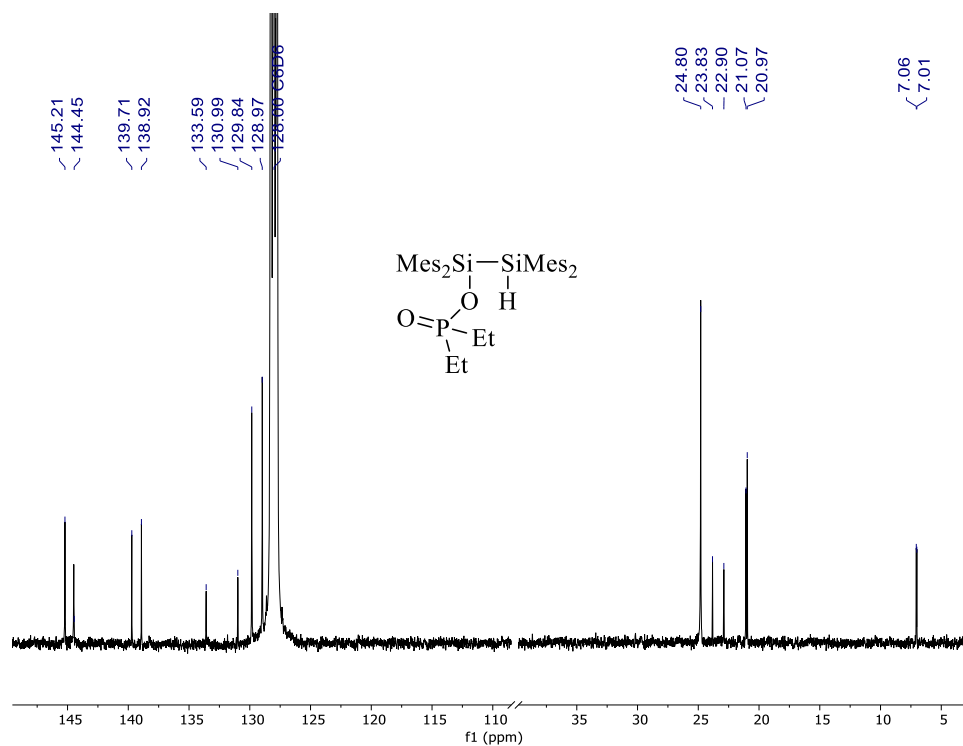


Figure A18: ¹³C{¹H} NMR spectrum (C₆D₆, 101 MHz) of **34**. The region of the spectrum from 35 to 110 ppm has been omitted.

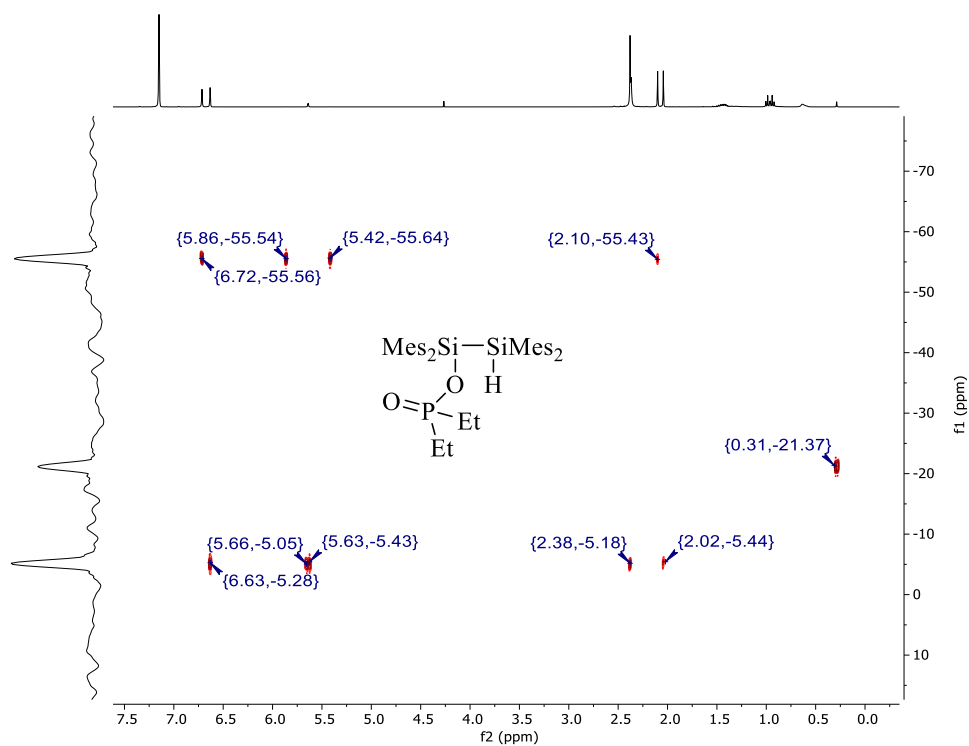


Figure A19: ¹H-²⁹Si gHMBC NMR spectrum (C₆D₆) of **34**.

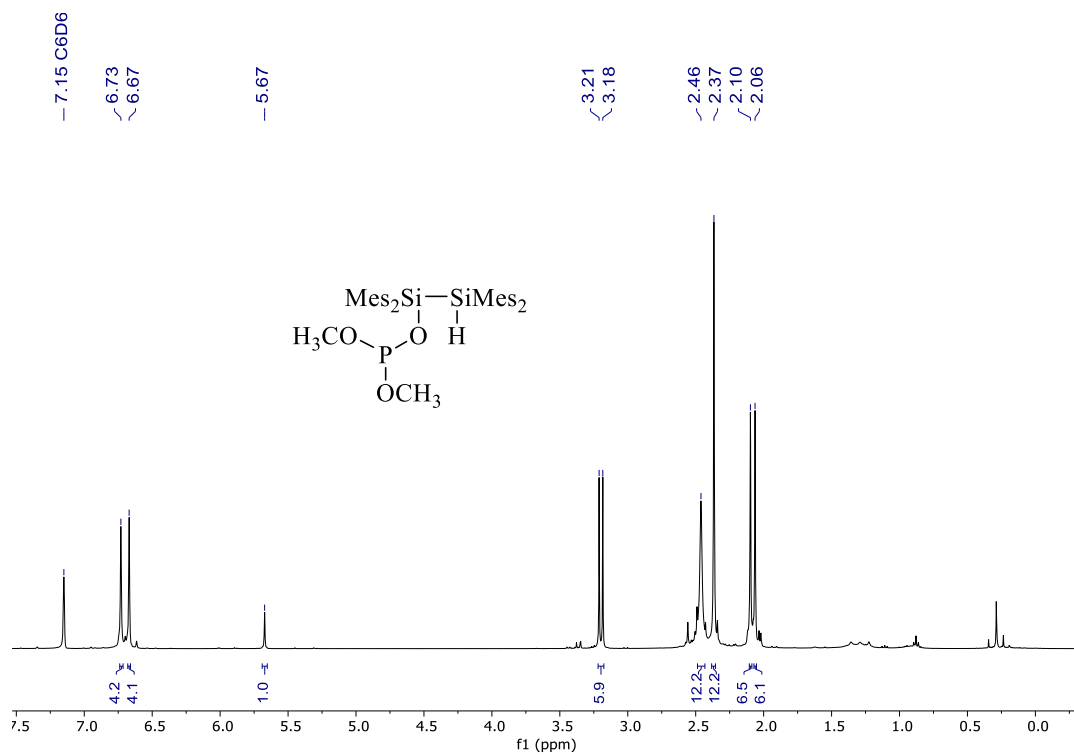


Figure A20: ¹H NMR spectrum (C₆D₆, 600 MHz) of **35**.

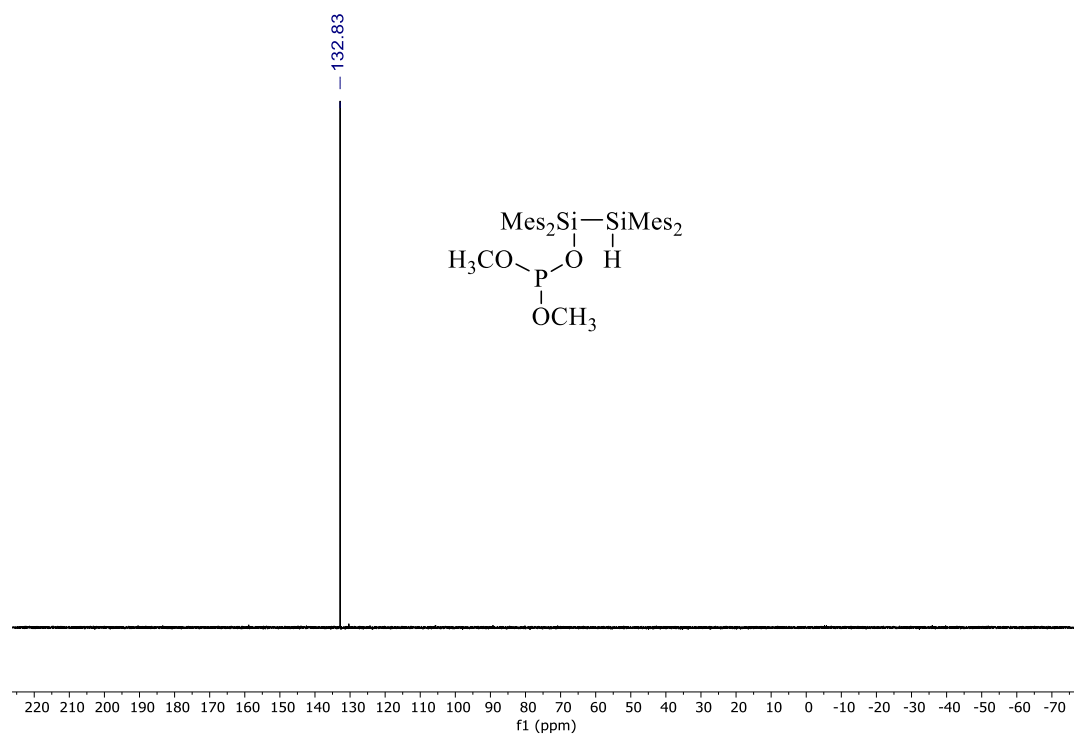


Figure A21: ³¹P{¹H} NMR spectrum (C₆D₆, 162 MHz) of **35**.

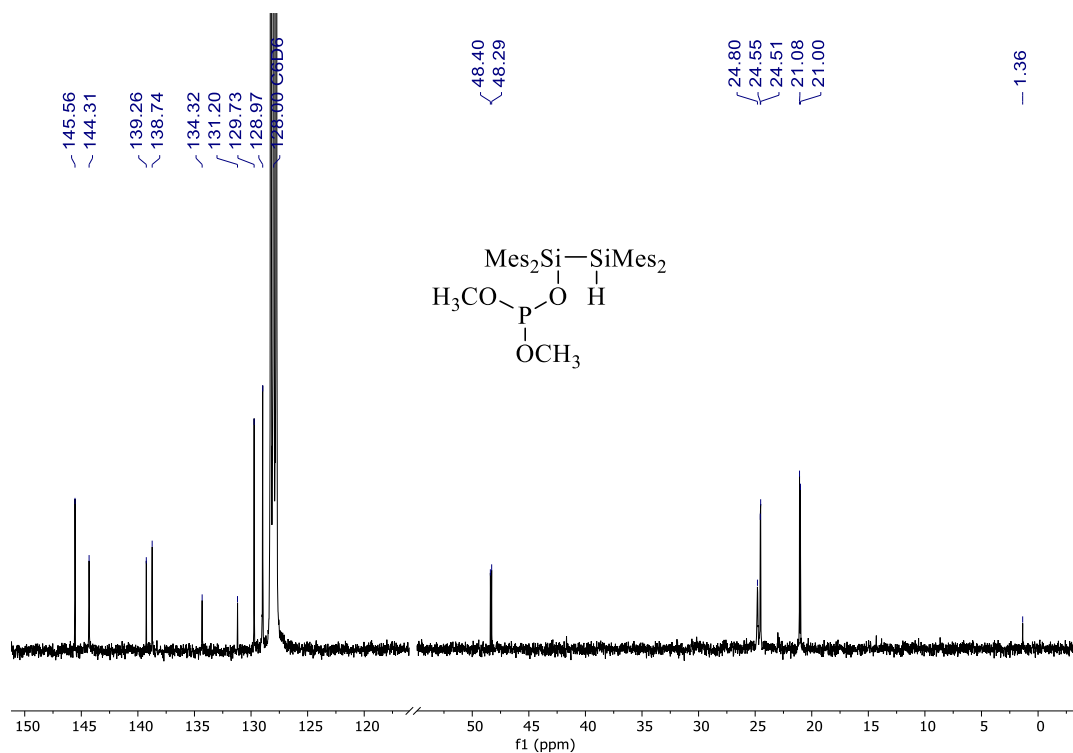


Figure A22: $^{13}\text{C}\{^1\text{H}\}$ NMR spectrum (C_6D_6 , 101 MHz) of **35**. The region of the spectrum from 50 to 120 ppm has been omitted.

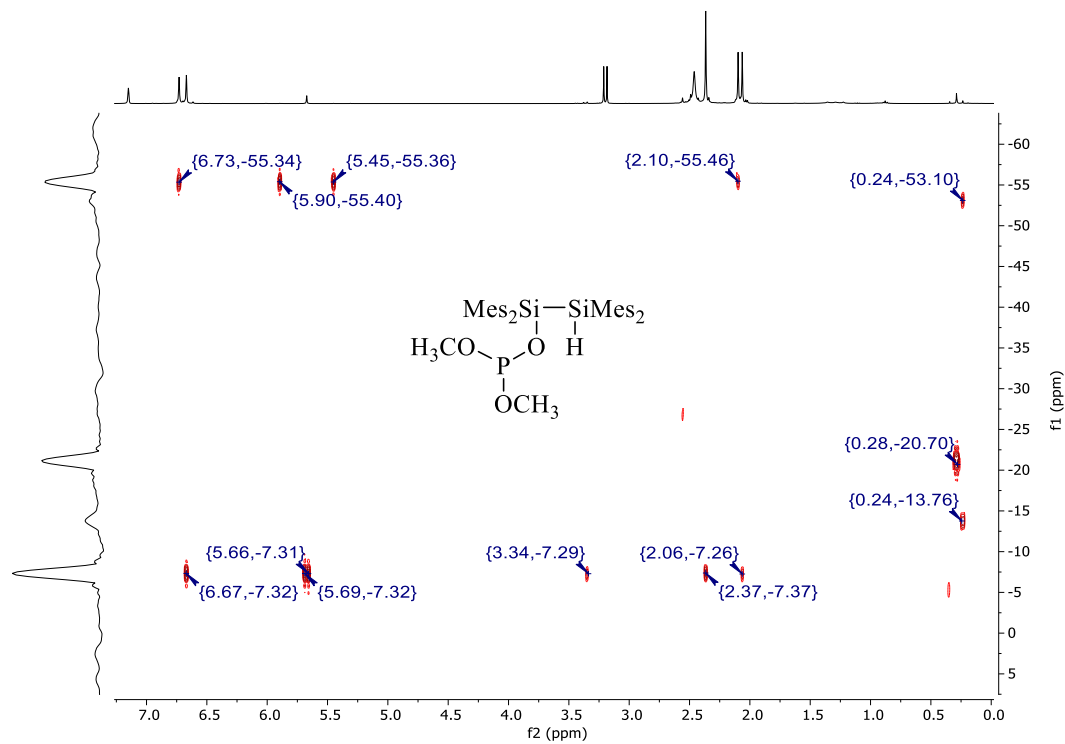


Figure A23: ^1H - ^{29}Si gHMBC NMR spectrum (C_6D_6) of **35**.

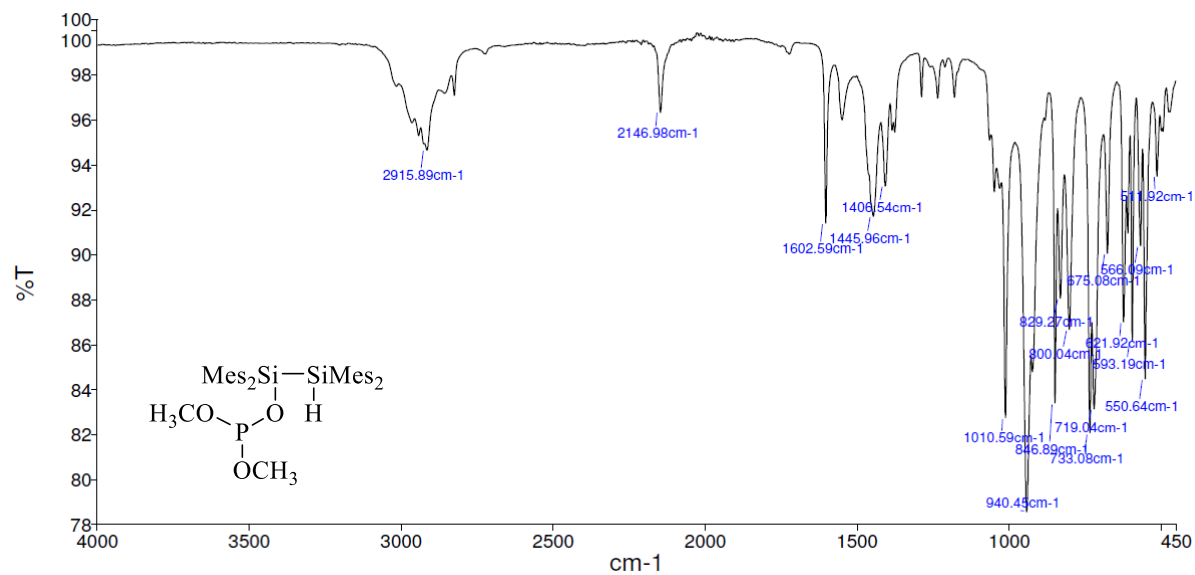


Figure A24: ATR-IR spectrum of **35**.

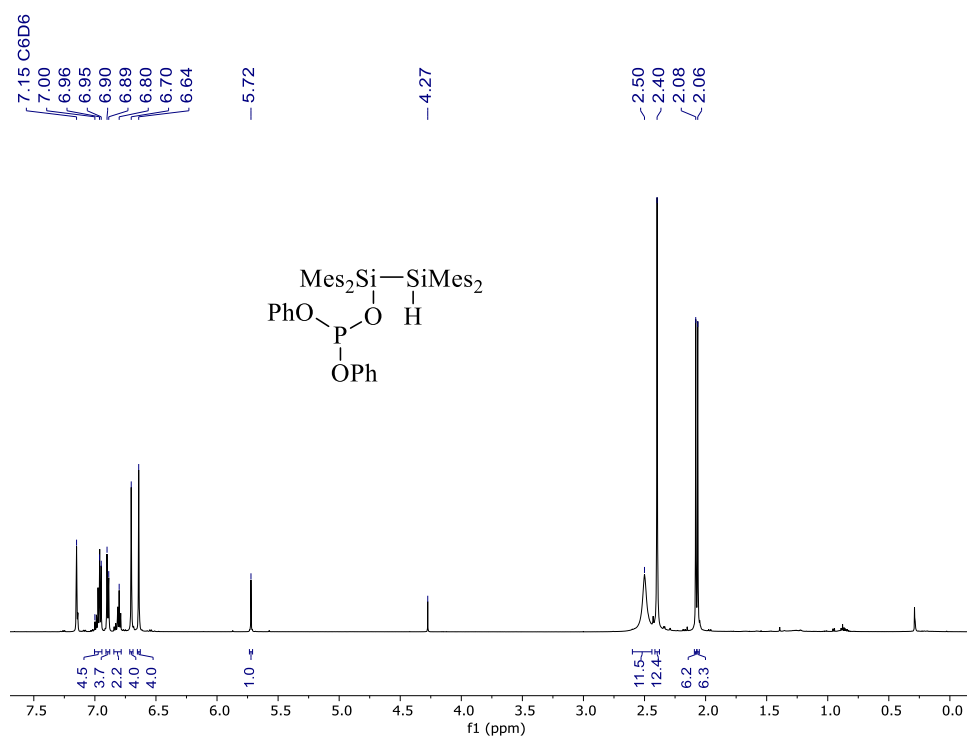


Figure A25: ^1H NMR spectrum (C₆D₆, 600 MHz) of **36**.

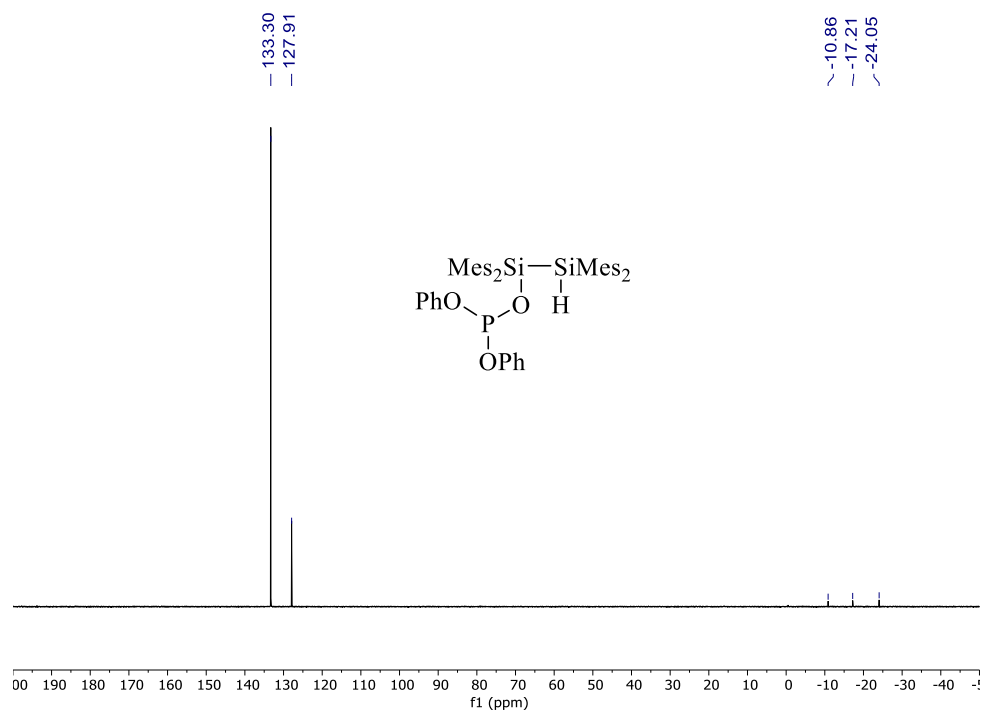


Figure A26: $^{31}\text{P}\{^1\text{H}\}$ NMR spectrum (C₆D₆, 243 MHz) of **36**.

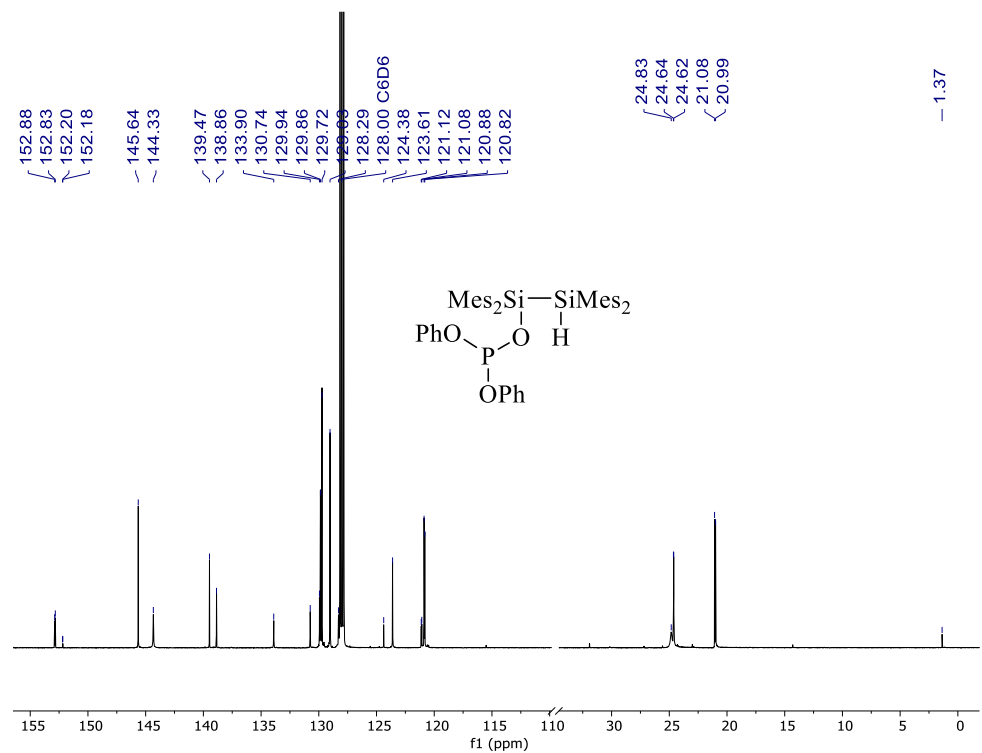


Figure A27: $^{13}\text{C}\{^1\text{H}\}$ NMR spectrum (C₆D₆, 151 MHz) of **36**. The region of the spectrum from 30 to 115 ppm has been omitted.

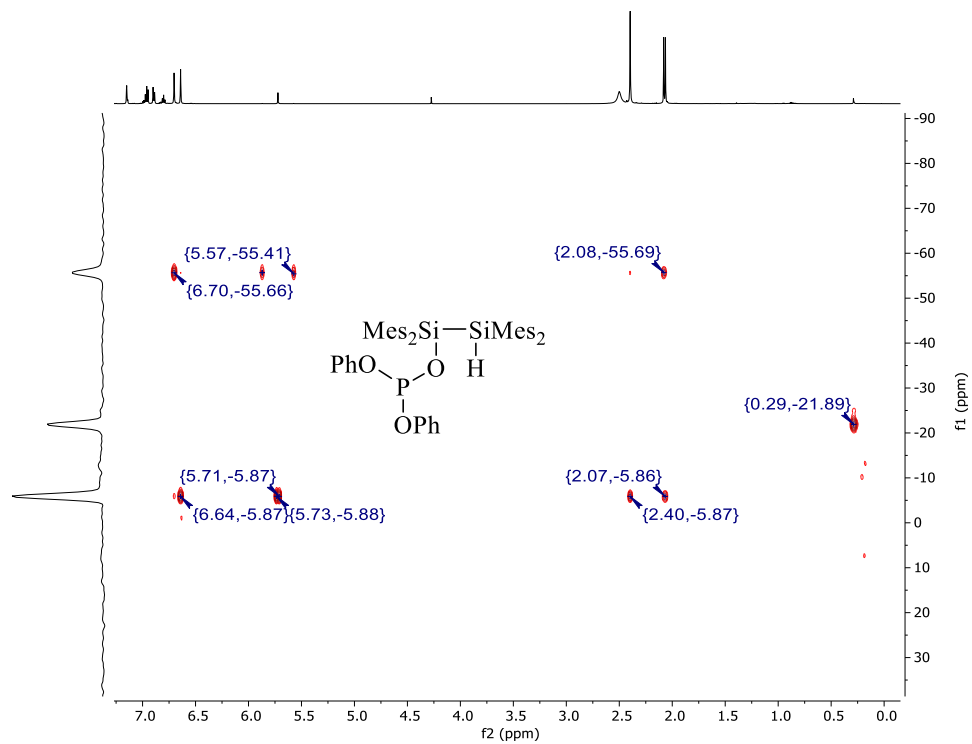


Figure A28: ^1H - ^{29}Si gHMBC NMR spectrum (C_6D_6) of **36**.

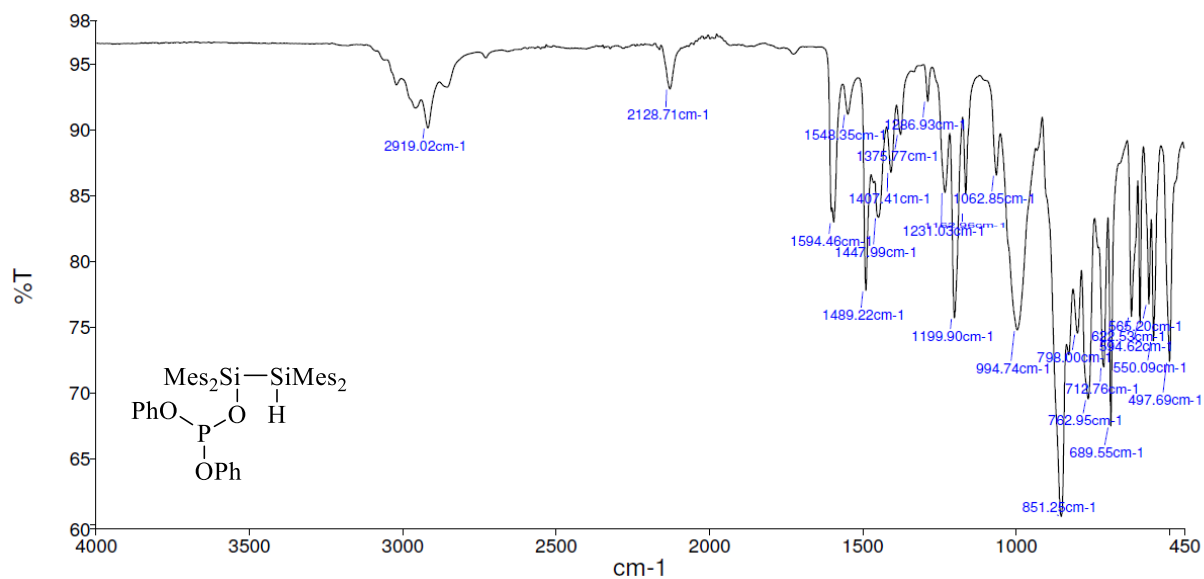


Figure A29: ATR-IR spectrum of **36**.

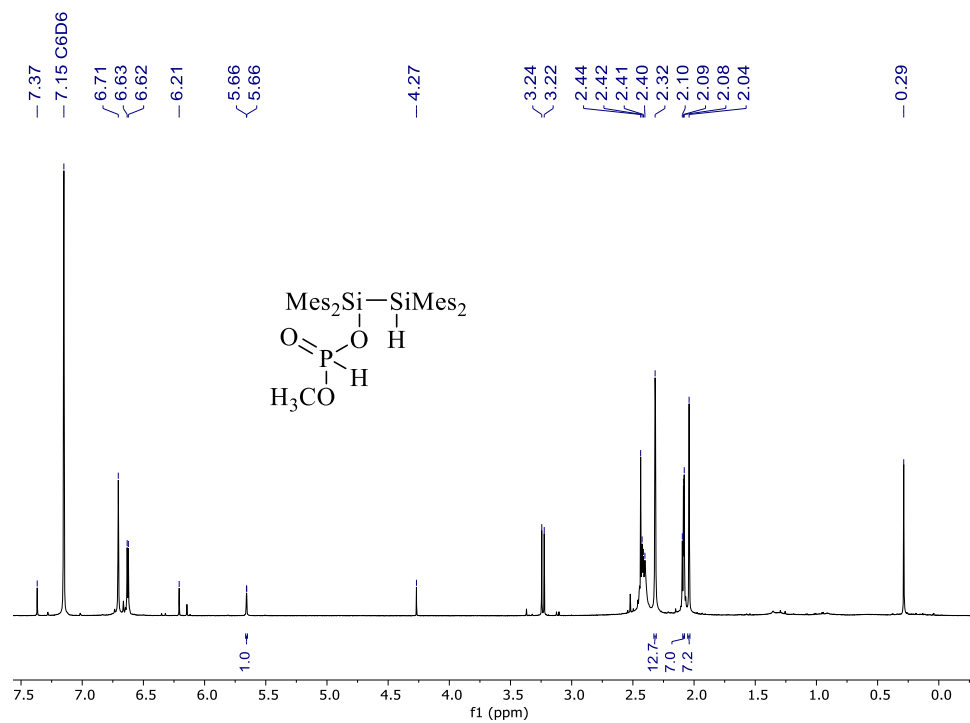


Figure A30: ¹H NMR spectrum (C₆D₆, 600 MHz) of **41**.

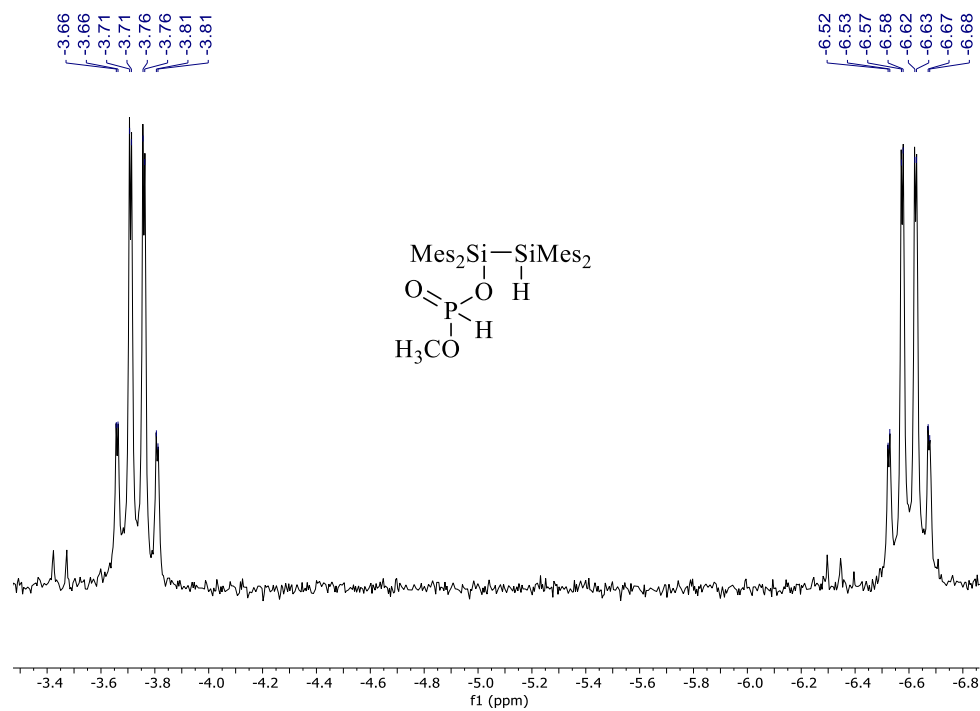


Figure A31: ³¹P NMR spectrum (C₆D₆, 243 MHz) of **41**.

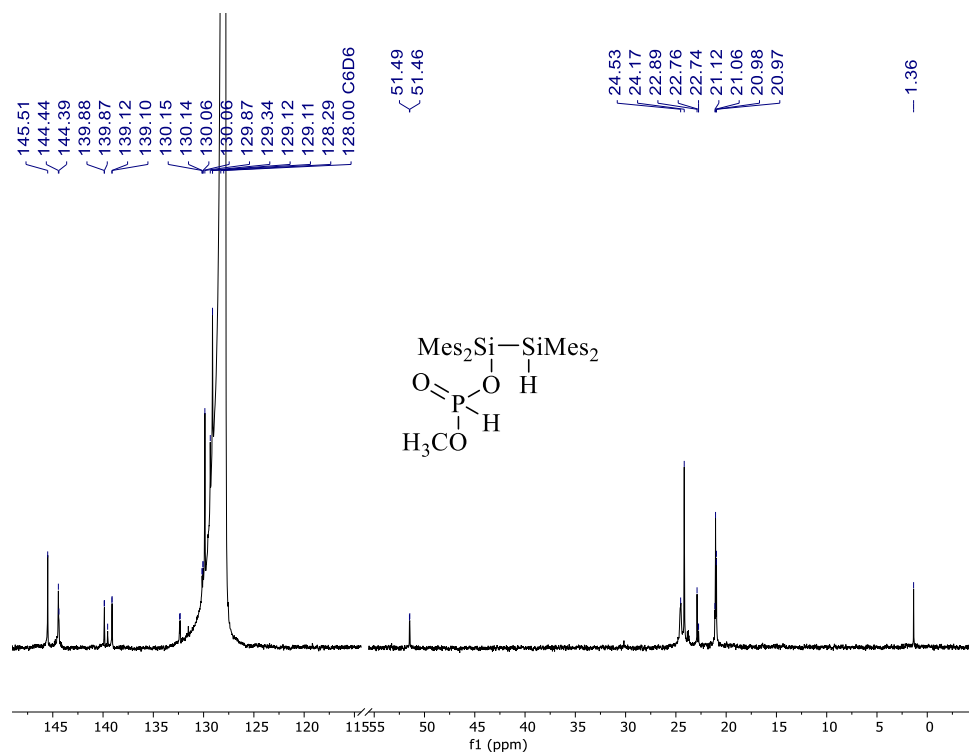


Figure A32: $^{13}\text{C}\{^1\text{H}\}$ NMR spectrum (C_6D_6 , 151 MHz) of **41**. The region of the spectrum from 55 to 115 ppm has been omitted.

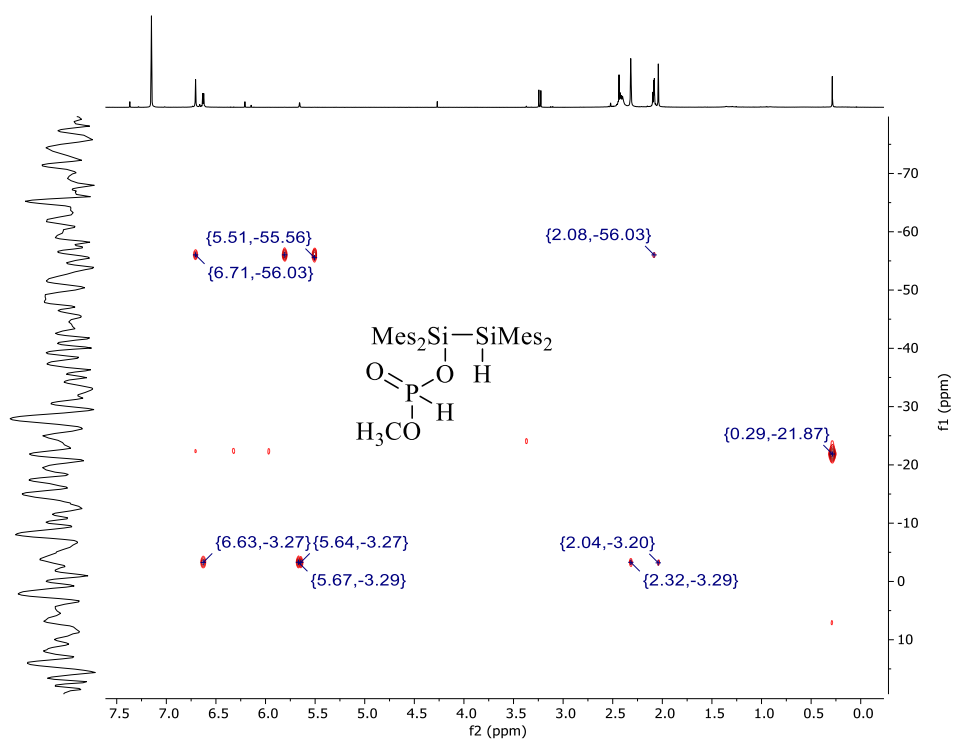


Figure A33: ^1H - ^{29}Si gHMBC NMR spectrum (C_6D_6) of **41**.

Appendix B: X-ray Crystallography Data

Appendix B1: X-ray crystallography data for **34**.

Experimental for **C₄₀H₅₅O₂PSi₂ (n19016)**

Data Collection and Processing. The sample (n19016) was submitted by Maissa Belcina of the Baines research group at the University of Western Ontario. The sample was mounted on a MiTeGen polyimide micromount with a small amount of Paratone N oil. All X-ray measurements were made on a Bruker-Nonius KappaCCD Apex2 diffractometer at a temperature of 123 K. The unit cell dimensions were determined from a symmetry constrained fit of 7915 reflections with $7.08^\circ < 2\theta < 134.7^\circ$. The data collection strategy was a number of ω and ϕ scans which collected data up to 135.51° (2θ). The frame integration was performed using SAINT.¹ The resulting raw data was scaled and absorption corrected using a multi-scan averaging of symmetry equivalent data using SADABS.²

Structure Solution and Refinement. The structure was solved by using a dual space methodology using the SHELXT program.³ All non-hydrogen atoms were obtained from the initial solution. The carbon bound hydrogen atoms were introduced at idealized positions and were allowed to ride on their parent atoms. The position of the hydrogen atom bound to the Si atom was obtained from a difference Fourier map and was allowed to refine isotropically. The structural model was fit to the data using full matrix least-squares based on F^2 . The calculated structure factors included corrections for anomalous dispersion from the usual tabulation. The structure was refined using the SHELXL program from the SHELX suite of crystallographic software.⁴ Graphic plots were produced using the Mercury program suite.⁵ Additional information and other relevant literature references can be found in the reference section of this website (<http://xray.chem.uwo.ca>).

¹ Bruker-AXS, SAINT version 2013.8, **2013**, Bruker-AXS, Madison, WI 53711, USA

² Bruker-AXS, SADABS version 2012.1, **2012**, Bruker-AXS, Madison, WI 53711, USA

³ Sheldrick, G. M., *Acta Cryst.* **2015**, *A71*, 3-8

⁴ Sheldrick, G. M., *Acta Cryst.* **2015**, *C71*, 3-8

⁵ Gabe, E. J.; Le Page, Y.; Charland, J. P.; Lee, F. L. and White, P. S. *J. Appl. Cryst.* **1989**, *22*, 384-387

Table 1. Summary of Crystal Data for *n19016*

Formula	C ₄₀ H ₅₅ O ₂ PSi ₂
Formula Weight (g/mol)	654.99
Crystal Dimensions (mm)	0.390 × 0.234 × 0.072
Crystal Color and Habit	colourless prism
Crystal System	monoclinic
Space Group	P 2 ₁ /n
Temperature, K	123
<i>a</i> , Å	11.421(2)
<i>b</i> , Å	20.397(4)
<i>c</i> , Å	16.635(3)
α, °	90
β, °	108.314(8)
γ, °	90
<i>V</i> , Å ³	3678.9(13)
Number of reflections to determine final unit cell	7915
Min and Max 2θ for cell determination, °	7.08, 134.7
<i>Z</i>	4
F(000)	1416
ρ (g/cm)	1.183
λ, Å, (CuKα)	1.54178
μ, (cm ⁻¹)	1.529

Diffractometer Type	Bruker-Nonius KappaCCD Apex2
Scan Type(s)	phi and omega scans
Max 2θ for data collection, °	135.51
Measured fraction of data	0.979
Number of reflections measured	33307
Unique reflections measured	6519
R _{merge}	0.0702
Number of reflections included in refinement	6519
Cut off Threshold Expression	I > 2sigma(I)
Structure refined using	full matrix least-squares using F ²
Weighting Scheme	w=1/[sigma ² (Fo ²)+(0.0628P) ² +1.14 35P] where P=(Fo ² +2Fc ²)/3
Number of parameters in least-squares	424
R ₁	0.0458
ωR ₂	0.1108
R ₁ (all data)	0.0692
ωR ₂ (all data)	0.1234
GOF	1.017
Maximum shift/error	0.001
Min & Max peak heights on final ΔF Map (e ⁻ /Å)	-0.341, 0.303

Where:

$$R_1 = \sum (|F_o| - |F_c|) / \sum F_o$$

$$\omega R_2 = [\sum (\omega (F_o^2 - F_c^2)^2) / \sum (\omega F_o^4)]^{1/2}$$

$$\text{GOF} = [\sum (F_o^2 - F_c^2)^2 / (\text{No. of reflns.} - \text{No. of params.})]^{1/2}$$

Appendix B2: X-ray crystallography data for 35.

Experimental for C₃₈H₅₁O₃PSi₂ (b19206)

Data Collection and Processing. The sample (b19206) was submitted by Maissa of the Baines research group at the University of Western Ontario. The sample was mounted on a MiTeGen polyimide micromount with a small amount of Paratone N oil. All X-ray measurements were made on a Bruker Kappa Axis Apex2 diffractometer at a temperature of 110 K. The unit cell dimensions were determined from a symmetry constrained fit of 9860 reflections with $5.46^\circ < 2\theta < 61.94^\circ$. The data collection strategy was a number of ω and ϕ scans which collected data up to 63.316° (2θ). The frame integration was performed using SAINT.⁶ The resulting raw data was scaled and absorption corrected using a multi-scan averaging of symmetry equivalent data using SADABS.⁷

Structure Solution and Refinement. The structure was solved by using a dual space methodology using the SHELXT program.⁸ All non-hydrogen atoms were obtained from the initial solution. The hydrogen atoms were introduced at idealized positions and were treated in a mixed fashion. The structural model was fit to the data using full matrix least-squares based on F^2 . The calculated structure factors included corrections for anomalous dispersion from the usual tabulation. The structure was refined using the SHELXL program from the SHELXTL suite of crystallographic software.⁹ Graphic plots were produced using the Mercury program suite.¹⁰ Additional information and other relevant literature references can be found in the reference section of this website (<http://xray.chem.uwo.ca>).

⁶ Bruker-AXS, SAINT version 2013.8, **2013**, Bruker-AXS, Madison, WI 53711, USA

⁷ Bruker-AXS, SADABS version 2012.1, **2012**, Bruker-AXS, Madison, WI 53711, USA

⁸ Sheldrick, G. M., *Acta Cryst.* **2015**, *A71*, 3-8

⁹ Sheldrick, G. M., *Acta Cryst.* **2015**, *C71*, 3-8

¹⁰ Gabe, E. J.; Le Page, Y.; Charland, J. P.; Lee, F. L. and White, P. S. *J. Appl. Cryst.* **1989**, *22*, 384-387

Table 1. Summary of Crystal Data for *b19206*

Formula	C ₃₈ H ₅₁ O ₃ PSi ₂
Formula Weight (<i>g/mol</i>)	642.93
Crystal Dimensions (<i>mm</i>)	0.289 × 0.189 × 0.098
Crystal Color and Habit	colourless prism
Crystal System	monoclinic
Space Group	P 2 ₁ /c
Temperature, K	110
<i>a</i> , Å	11.509(3)
<i>b</i> , Å	21.803(5)
<i>c</i> , Å	14.804(4)
α , °	90
β , °	106.380(9)
γ , °	90
<i>V</i> , Å ³	3563.8(16)
Number of reflections to determine final unit cell	9860
Min and Max 2 θ for cell determination, °	5.46, 61.94
<i>Z</i>	4
F(000)	1384
ρ (<i>g/cm</i>)	1.198
λ , Å, (MoK α)	0.71073
μ , (<i>cm</i> ⁻¹)	0.179

Diffractometer Type	Bruker Kappa Axis Apex2
Scan Type(s)	phi and omega scans
Max 2θ for data collection, °	63.316
Measured fraction of data	0.999
Number of reflections measured	179963
Unique reflections measured	11977
R _{merge}	0.0553
Number of reflections included in refinement	11977
Cut off Threshold Expression	I > 2sigma(I)
Structure refined using	full matrix least-squares using F ²
Weighting Scheme	w=1/[sigma ² (Fo ²)+(0.0586P) ² +1.71 70P] where P=(Fo ² +2Fc ²)/3
Number of parameters in least-squares	447
R ₁	0.0438
ωR ₂	0.1124
R ₁ (all data)	0.0662
ωR ₂ (all data)	0.1255
GOF	1.037
Maximum shift/error	0.001
Min & Max peak heights on final ΔF Map (e ⁻ /Å)	-0.568, 0.597

Where:

$$R_1 = \sum (|F_o| - |F_c|) / \sum F_o$$

$$\omega R_2 = [\sum (\omega(F_o^2 - F_c^2)^2) / \sum (\omega F_o^4)]^{1/2}$$

$$\text{GOF} = [\sum (\omega(F_o^2 - F_c^2)^2) / (\text{No. of reflns.} - \text{No. of params.})]^{1/2}$$

Curriculum Vitae

Education

B.Sc. Honors Chemistry
The University of Western Ontario
2013 – 2017
4491 Supervisor: Dr. Kim Baines

Presentations

“Addition of Phosphorus Oxides to Ditetrelenes” Maissa Belcina, Bahareh Farhadpour, Nada Y. Tashkandi, and Kim M. Baines*, CSC 2018

Related Experience

Research Assistant
Baines Group
May 2017 – August 2017

Graduate Teaching Assistant
2017 – 2019

Courses: Chemistry 2213 (Organic Chemistry for Life Sciences), Chemistry 2223 (Organic Chemistry of Biological Molecules), Chemistry 3373 (Organic Chemistry III: Reactions and Strategies for Synthesis)

Course Grades

9503R (Advanced NMR Spectroscopy I) – 83
9507Q (Advanced Chemical Communications) – 90
9521S (Catalysis) – 87
9603S (Advanced NMR Spectroscopy II) – 87
9657 (Seminar) – PASS